THE ROLE OF ICAM-1 IN MYOCARDIAL DYSFUNCTION DURING SEPSIS AND ISCHEMIA-REPERFUSION INJURY

by

EHSAN YOUSEFZADEH-DAVANI

M.D., Isfahan University of Medical Sciences, 1993
M.Sc., The University of British Columbia, 2002

A THESIS SUBMITTED IN PARTIAL FULFILMENT OF
THE REQUIREMENTS FOR THE DEGREE OF

DOCTOR OF PHILOSOPHY

in

THE FACULTY OF GRADUATE STUDIES

(Experimental Medicine)

THE UNIVERSITY OF BRITISH COLUMBIA

July 2005

The role of ICAM-1 in myocardial dysfunction during sepsis and ischemia-reperfusion injury

Abstract

Intramyocardial inflammation occurs in various types of cardiovascular diseases including ischemia-reperfusion, myocarditis, during orthotopic heart transplant rejection, and during sepsis-induced myocardial dysfunction. Intramyocardial inflammation results in increased expression of ICAM-1 on cardiac tissue. ICAM-1 can interact with its ligands including CD11/CD14 receptors on inflammatory cells, and fibrinogen leading to activation of intracellular signaling cascades. To test this hypothesis that ICAM-1 activation on cardiac tissue can trigger signaling which leads to decreased cardiac contractility we used three different in vitro (cardiomyocytes, polymorphonuclear leukocytes (PMN) and fibrinogen co-culture), in vivo (cardiac contractility measurement using micro-catheter) and ex vivo (reperfusion of isolated heart) methods. Cardiomyocyte ICAM-1 binding by activated PMN, by activated and killed PMNs, and by ICAM-1 cross-linking antibodies decreased cardiomyocytes contractility. In vivo, inducing severe cardiac inflammation by LPS injection decreases cardiac contractility by $58 \pm 4\%$ (using end systolic elastance) and increases ICAM-1 expression on cardiac tissue by 2.35 fold compared to control. Morphometery of cardiac vessels indicated increased intravascular PMNs after LPS injection but the number of interstitial PMNs were not different compared to control excluding the role of PMN adhesion in ICAM-1 activation in sepsis. This led to the next hypothesis that fibrinogen can interact with ICAM-1 after LPS injection. Immunohistochemistry staining indicates increased interstitial fibrinogen infiltration six hours after LPS injection supporting the interaction of ICAM-1 and

fibrinogen during sepsis. Incubation of cardiomyocytes with fibrinogen decreased cardiomyocytes contractility. This effect of fibrinogen was abolished in the presence of anti ICAM-1 antibody. Treatment of isolated heart with IGF-1 decreases ICAM-1 expression by 2 fold ($p < 0.01$), increases cardiac contractility and heart rate, and decreases CPK during reperfusion compared to TNFα. We conclude that PMN and fibrinogen interact with cardiomyocytes ICAM-1. Fibrinogen infiltrates into the myocardial interstitial space during sepsis and decreases cardiac contractility through adhesion to ICAM-1 receptor on the cardiomyocyte membrane. IGF-1 can be used as a therapeutic intervention to decrease ICAM-1 expression thereby protecting the heart from further injury during cardiac inflammation.

Tables of contents

List of tables

List of figures

List of Symbols and Abbreviations

AHA	American Heart association
ARDS	Acute respiratory distress syndrome
ASPG	Accessory subunit of the murine mitochondrial DNA polymerase γ
ATP	Adenosine triphosphate
BSA	Bovine serum albumin
C57B6	C57 black 6 mice
Ca^{2+}	Calcium ion
CABG	Coronary artery bypass grafting
cGMP	Cyclic guanosine monophosphate
COX	Cytochrome oxidase subunit 1
CPK	Creatine phosphokinase
CVD	Cardiovascular diseases
CY	Cyclophosphamide
DAB	Diaminobenzidine tetrahydrochloride
DAG	Diacylglycerol
DHPR	Dihydropyridine calcium receptors
DNA	Diamino nucleotide acid
DP	Systolic – diastolic pressure
dP/dt	Alteration of pressure in time
ECG	Electrocardiogram
Ees	End systolic elastance
EF	Ejection fraction
E_{max}	Maximum elastance
EPO	Erythropoietin
FAK	Focal adhesion kinase
Fib/Nuc	Fibrinogen to nuclear staining ration
GCSF	Granulocyte colony stimulating factor
GFR	Glomerular filtration rate
GH	Growth hormone
H & E	Hematoxylin and eosin
H+/M-	ICAM-1 competent heart/ICAM-1 knock out bone marrow derived cells
HIF-1α	Hypoxia inducible factor-1
HR	Heart rate
HRP	Horse radish peroxidase
HUVEC	Human umbilical vascular endothelia cell
ICAM-1	Intercellular adhesion molecule-1
ICU	Intensive care unit
IGF-1	Insulin-like growth factor-1
IHC	Immunohistochemistry
IL-1β	Interleukin-1 beta
IL-6	Interleukin-6
IP3R	Inositol triphosphate receptors
KO	Knock-out

LPS	Polymorphonuclear leukocytes
LV	Left ventricle
LVEDP	Left ventricular end-diastolic pressure
LVEDV	Left ventricular end-diastolic volume
LVESV	Left ventricular end-systolic volume
MHC	Major histocompatibility complex
Mit	Mitochondrial
MK	Modified Kreb's Henseleit working solution
NCX	Sodium-calcium exchange channels
NFκB	Nuclear factor kappa-B
NK	Sodium-potassium channels
NO	Nitrite oxide
NOS	Nitrite oxide synthesize
NS	Non significant
PKC	Protein kinase C
PTA	Percutaneous transluminal angioplasty
PV	Pressure-volume
RNA	Ribonucleotide acid
ROS	Reactive oxygen species
RV	Right ventricle
RyR	Ryanodine receptor
SR	Sarcoplasmic reticulum
SV	Stroke volume
TNFα	Tumor necrosis factor-alpha
VCAM-1	Vascular cellular adhesion molecule-1
VEGF	Vascular endothelial growth factor
VW	Ventricular work
vWf	von-Willebrand factor
Who	World health organization

Acknowledgement

This thesis is the result of the extensive effort of some of my best friends that I have ever had. I personally believe without their cooperation I could not have finished these projects.

I first thank Maryam, my wife, for her patience, encouragement, and support while I was working on these projects.

I thank Yingjing Wang who worked with me for the last five years. His patience and skills in animal surgeries and procedures made these investigations possible. My friends and colleagues, Teresa Wood, Treena McDonald, Shelly Dai, Amrite Samra, Kathy Grek, and Gurpreet Singhera were involved in different parts of this work. I have been trained by them and I always appreciate their cooperation. Dr. Thoma Kareko came as a postdoc in our laboratory. He dedicated his time to support others including me with his knowledge in physics and math. I always remember his extensive work on image deconvolution. I thank Dr. Ryon Bateman, and Hon Leong for their work on confocal microscopy.

I thank Drs. Chan Hang Lee and Casey Van Breeman for cooperation in calcium influx measurement in their laboratory. I also thank Dr. Helen Cote, Zebrina Brumme and Dr. Richard Harrigan for using their method (mitochondrial/nuclear DNA) in chapter 5.

My deep appreciation to Drs. James Hogg, Peter Pare, Bruce McManus, Mike Allard, David Walker, Stephan Van Eeden, Blair Walker, Tom Podor, David Granville, and Bob Schellenberg and all people at iCAPTURE center for their valuable suggestions. I would like to thank research students, Shane Olaleye, May Tee, Karen Reevere, and Alan Ng. My special thanks to Anna Meredith and Edmond Chau for their great works.

I thank Dr. Delbert Dorscheid, my co-supervisor, who has been supporting me since he came to our laboratory. He gave a great opportunity to his graduate students to train summer research students in our laboratory. He also created a free and friendly space in his research laboratory for everyone which, I think, is the most important part of the research environment that can create trust and future cooperation. He was leading the ischemia reperfusion projects and his critical suggestions and comments were essential parts of the other projects in this thesis.

I thank Dr. Keith Walley, my supervisor, for his persistent work, knowledge and involvement in the preparation of this thesis. His tremendous work on this projects resulted in supporting fund from CIHR. I always appreciate his great support especially in the first two years of my work at iCAPTURE center.

My sincere appreciation to CIHR, and Heart and stroke foundation for supporting grant to these projects. I also thank UBC department of medicine, American Lung Association, CFIC and CIHR for supporting travel funds to present my data.

Co-Authorship

Chapter 2 of this thesis was published as a manuscript in American Journal of Physiology. The authors are; Ehsan Y Davani, Delbert R Dorscheid, Chan Han Lee, Casey Van Breeman, and Keith R Walley. Dr. Chan Han Lee and Casey van Breeman were involved in Ca2+ measurement. Dr. Dorscheid partially supervised this project and Dr. Keith Walley supervised and leaded this project.

Chapter 3 is in submission. Authors are Ehsan Davani, Delbert Dorscheid, Yingjing Wang, Anna Meredith, Edmond Chau, Gurpreet Singhera and Keith Walley. Yingjing Wang performed most of the animal surgeries. Anna Meredith worked on the immunohistochemistry and morphometery of the hearts slides. Gurpreet Singhera was responsible for some of the data collection and protein assays. Dr. Keith Walley was leading this project.

In chapter 4, I have done immunohistochemistry, Immunoflurescent studies, confocal microscopy and mice studies based on the generated hypothesis from my previous works. I supervised Edmond Chau during his two months summer research studentship. Edmond Chau's tremendous work during this period resulted in important observations. He has done all of cardiomyocytes co-culture experiments in this chapter. Dr. Ryon Batemen has performed co-localization study of this chapter.

Chapter 5 is the results of cooperation of Dr. Gurpreet Singhera, who measured the CPK level and Shane Olaleye who did some ex-vivo experiments during his summer research studentship. Drs. Helen Cote, Richard Harrigan, and Zebrina Brumme performed the mitochondrial/nuclear DNA ratio. Dr. Delbert Dorscheid supervised and led this project.

To

Dr. James Hogg, who dedicated his life time to improve
and to support research in medicine.

Chapter-1: Overview

1.1   Sepsis and myocardial ischemia are important health problems.

The heart contracts continuously to prepare and facilitate life for other organs. It has been named the center of love, and of hate. Ancient Egyptian physicians believed that heart could speak to other parts of the body since they heard the sound of pulsation (Ebner Papyrus) and assumed the heart was the center of management for other organs. The heart beats 2.5 billion times during an average life of 70 years. It supplies energy for all organs and when it dies none of the other organs can survive. During past centuries cardiovascular diseases have been progressively affecting human life, especially in western countries. It has been estimated that cardiovascular diseases (CVD) will be the most common human health problem until 2020 (AHA).

Sepsis and myocardial infarction are important health problems. Cardiovascular diseases are one of the most common problems in health care in our new world, resulting in more than 17,000,000 death annully worldwide (www.who.int). Each year millions of people die because of myocardial infarction. Many of these patients need cardiac transplantation, cardiac bypass, and invasive therapeutic interventions, with their consequent side effects and disabilities, direct either because of procedures or indirect because of using various types of drugs. CVD are the leading causes of mortality in North America resulting in the death of more than 432,000 males and 499,000 females annually (AHA). The majority of these deaths are a result of coronary vascular atherosclerosis and myocardial infarction. It has been estimated that CVD drains more that 329.2 billion dollars annually in North

America. Tissue damage due to myocardial infarction involves the innate immune system triggering the responses of defensive cells and proteins against the infarcted myocardium, thereby inducing further damage to the remaining non-infarcted myocardium.

Sepsis also involves the innate immune system in our body. It is a severe inflammatory response of the body against bacterial and other infectious pathogens. Sepsis syndrome occurs as a result of primary infection and also as one of the consequences for trauma and post surgery patients. It is the leading cause of death in non-coronary ICUs. Sepsis affects more than 750,000 people annually in North America and results in 215,000 deaths. The average health care cost of a septic patient is about $22,000 in North America and results in more than $18 billion of expense annually [1]. Most septic patients die of severe hypotension and myocardial depression, leading to multiple organ hypoperfusion and dysfunction [2]. Although the reported number of cases of sepsis is about 1,800,000 per year worldwide [3], it has been estimated that the actual number of reported and non-reported cases of sepsis could be around 18,000,000 per year worldwide, based on an observed incidence of 3 cases per 1000 patients. Given the 30% mortality rate, this would mean that sepsis is the leading cause of death worldwide. Epidemiological investigations of sepsis have defined a numbers of issues, including an increasing incidence of sepsis, and the lack of a unique definition to diagnose sepsis syndrome which results in high numbers of non-registered cases worldwide. According to recent clinical investigations, the stability of hemodynamic state is one of the most important factors required to survive from sepsis [4].

This thesis is focused on one of the intracellular mechanisms of myocardial dysfunction during sepsis and ischemia-reperfusion injury. Here I explain the importance of cardiac contractility in various diseases including sepsis.

1.2 The importance of cardiac physiology in cardiovascular diseases

1.2.1 Cardiac function

The main cellular component of the heart is the cardiomyocyte. It is the contractile part and forms the majority of heart mass and volume. A cardiomyocytes in vivo is approximately 20 μm wide, 100 μm long and 5 to 7 μm thick. The contractile component of each cardiomyocyte is a sarcomere with a length of 2.5 to 3 μm. The sarcomere is connected to the cardiomyocyte membrane (sarcolemma) through cytoplasmic cytoskeletal proteins, mainly microfilaments (actin) and intermediate filaments [5]. Each sarcomere has longitudinal networks of actin and myosin filaments with a specific arrangement. The contractile force is the product of interaction and sliding of sarcomeric actin filaments and myosin heads on each other. Each sarcomere is connected to the neighboring sarcomere through accumulation of α-actinin protein in a special area called the Z line which is visible by light microscopy. Light microscopy of the sarcomere shows light areas on either sides of Z lines, named I bands. I bands are fractions of sarcomeric actin filaments, tropomyosin and troponin proteins. Thick filaments (myosin) are interspersed among sarcomeric actin filaments (A band). They are divided in two sections in the middle by the H band. The H band is also divided in two parts by the M line. Various proteins are located in the M line including myomesin and creatine phosphokinase (CPK). CPK is an enzyme with various isotypes that maintains enough adenosine triphosphate (ATP) for muscular contraction. CPK is released into the plasma during muscular injury and death, and it is used as a diagnostic test to measure muscular or myocardial injury. Thick filaments are also connected to the Z lines and each other by titin and myomesin respectively.

Cardiomyocyte membrane is invaginated into the cytoplasm creating transverse tubules (T tubules). Many types of ion channels are located on the T tubule including dihydropyridine calcium receptors (DHPR), sodium-calcium exchange channels (NCX) and sodium-potassium channels (NK). Other important micro-organelles in cardiomyocytes are mitochondria and the sarcoplasmic reticulum (SR). Mitochondria are important organelles because they are the main source of energy production and occupying 40% of the total volume of each cardiomyocyte. SR is important due to its role as the source of Ca^{2+} (100 μmol/L).

1.2.2 Ca^{2+} receptor and excitation-contraction coupling

Voltage dependent channels control cardiomyocyte sarcoplasmic Ca^{2+} concentration. The most acceptable theory for Ca^{2+} influx into the cardiomyocyte is Ca^{2+} induced Ca^{2+} release. The two major types of voltage sensitive Ca^{2+} channels are L and T type channels on the cardiomyocyte membrane [6,7]. T type channels have a negligible role in regulating the Ca^{2+} gradient in cardiomyocytes. The L type Ca^{2+} channel is also called the DHPR receptor. Alteration in Ca^{2+} influx is the basic pathophysiological cause of cardiac arrhythmia and contractility dysfunction. Resting intracellular Ca^{2+} concentration is less than 0.1 μmol/L. Depolarization of the membrane activates DHPR and induces Ca^{2+} entry resulting in an increase in the Ca^{2+} concentration around ryanodine receptors (RyR) [8]. This event changes the protein configuration of the RyR receptor in 2 to 3 milliseconds and triggers Ca^{2+} release from the SR. This alteration in turn changes the intracellular Ca^{2+} concentration to 10 to 12 μmol/L. The raise in sarcoplasmic Ca^{2+} concentration

changes the DHPR receptor structure and negatively influences Ca^{2+} entry so that the speed of Ca^{2+} entry is reduced by 50% [6].

Alteration in intracellular Ca^{2+} concentration during the cardiac excitation contraction period is mainly regulated by RyR and inositol triphosphate receptors (IP3R) on the SR [9]. It has been shown that IP3 receptors are involved in Ca^{2+} release from the SR in heart failure. It is worth noting that the IP3 receptors can be activated by endothelin-1, angiotensin, and α-adrenergic stimulation [10,11]. RyR receptors control Ca^{2+} release, and interestingly, the tertiary structures of RyR receptors are also controlled by Ca^{2+} concentration. T tubules in cardiomyocytes and skeletal muscle have special localization close to the SR projection (terminal cisterna). The space between T tubules and the terminal cisterna is about 10 to 20 nm and called the couplon space. This space is very important in maintaining the juxtaposition between RyR on the terminal cisterna and DHPR on T tubules. DHPR in the T tubule contains four similar proteins, and in skeletal muscle it is aligned with one RyR on the SR [6,12]. In cardiomyocytes one DHPR is aligned with 5 to 10 RyRs. This position ensures the opening of all RyR in one couplon space at once [13]. It is worth noting that in skeletal muscle most RyR isoforms are type 1 (RyR1) while in cardiomyocytes the majority is type 2 isoform (RyR2). The head of RyR is a large protein which is located in the couplon space. The function of RyR is dependent on the activation of voltage-dependent Ca^{2+} receptors or DHPRs [14]. Depolarization of T tubules leads to changes in tertiary structure of DHPRs and results in the opening of DHPR channels. During cardiac excitation-contraction, thousands of Ca^{2+} sparks synchronize in time along the membrane [6]. Entry of 2 to 4 Ca^{2+} ions is sufficient to

activate the RyR channel and the whole couplon space [15]. Each Ca^{2+} spark is the function of a cluster of 6 to 20 activated RyR receptors increasing the Ca^{2+} influx. If these sparks are not synchronized in time, it causes wave shape propagation and non-harmonic sarcomere contraction leading to a reduction of cardiomyocyte contractility. Release of Ca^{2+} in the cytosol removes the inhibition of the actin myosin interaction [14]. This is the predominant position for cardiomyocytes at rest. The binding of four Ca^{2+} ions to troponin, located on the actin filament, changes the conformation of troponin, removes tropomyosin from the contractile part of myosin and exposes the binding site of myosin to actin. Using ATP, the cross-bridge between actin and myosin creates tension along the sarcomeric structure, generating enough force to fold the membrane and other organelles in the cardiomyocyte during contraction. The next step is dissociation of actin from myosin which requires ATP [13]. The ability of the sarcomere to generate force decreases when sarcomeric length reaches 2 to 2.2 μm. Ca^{2+} decay occurs during this time by activation of NCX, Ca^{2+} pumps on the membrane, SR and mitochondria [6]. The sum of the force of all the cardiomyocytes contracting generates enough force for ventricular contraction. Any type of influx alteration can change cardiomyocyte contraction.

Alteration in Ca^{2+} sparks, juxtaposition of RyR and DHPR receptors, and propagation of Ca^{2+} ions can be the source of cardiac dysfunction. These above mechanisms have been postulated to describe myocardial dysfunction in sepsis and ischemia reperfusion injury.

1.2.3 Cardiodynamics

The heart is the organ responsible for pumping blood into the conductive system, arteries and capillaries. Veins are the reservoirs of blood. The right ventricle (RV) is responsible for pumping non-oxygenated blood into the lungs. The left ventricle (LV) is the main pump in normal physiologic circulation and it distributes nutrients and oxygen to all organs. Thus the LV is responsible for maintaining systemic blood pressure.

The power of the LV pump is directly related to its cone shape structure and the volume of blood which can be pumped out of the left ventricle. Since during LV (cone shape) contraction the LV height is almost constant, the LV ejects blood by reducing its volume through a reduction in radius. Since volume is directly related to the squared radius of LV (r^2), the ejection of blood is directly related to r^2 of LV. LV output is an important factor in measuring workload of the left ventricle and maintaining systemic blood pressure in normal range. LV output is related to heart rate (HR) and the volume of ejected blood in each beat (stroke volume, SV). Thus the LV output = SV $\cdot$ HR.

The cardiac cycle starts by atrial contraction, a function that is especially important when the heart beats faster than normal. In fact 75% of the left ventricular blood volume comes from the pre-atrial contraction and atrial contraction is just responsible for the ejection of the remaining blood volume. However when heart beats faster, the diastolic phase decreases and atrial contraction plays its major function. The volume at the end of the diastolic phase is called the left ventricular end-diastolic volume (LVEDV) and in turn it makes a pressure gradient which is called the left ventricular end-diastolic pressure

(LVEDP). Ventricular contraction starts at the end of diastole. First it increases the intraventricular chamber pressure without changing the intraventricular volume, which is called isovolumic contraction. When left ventricular pressure reaches the pressure of the aorta, it causes opening of the aortic valve so that the blood is pushed by left ventricle contraction into the aorta until the end of contraction. The diastolic phase starts by closure of the aortic valve and relaxation of the left ventricle causing isovolumic relaxation. This cycle repeats in each beat. The plot between LV pressure and volume in each cardiac cycle generates a loop. Obtaining of number of loops with different LV volumes generates a tremendous amount of information about the function of LV (refer to Figure 3.1). The pressure-volume (PV) loops of LV contractility provide various types of cardiac parameters including end systolic elastance (Ees), maximum elastance (E_{max}) and ventricular work (VW). Ees and E_{max} are from the slope of the end systolic PV loops and they are load independent cardiac parameters. VW is reflected by the size of the above loops and it is proportional to the pressure and stroke volume. The ventricular work also reflects oxygen consumption by ventricular muscles and vice versa because VW is related to ventricular wall tension.

Normal LV output is around 5 liters per minute in humans. The LV output is not independent from RV and it is also related to the RV output. This phenomenon has been named Frank-Starling mechanism. According to Frank-Starling mechanism the energy produced by LV is a function of length of muscle fibers in LV, considering the radius of LV is adjusted by length of muscle. In fact the length of muscle fibers determines the preload. The maximal volume of LV is achieved at the end-diastolic time point exactly

before LV contraction when the muscle fibers have the highest normal length. This volume is called LV end diastolic volume (LVEDV). In humans LVEDV is about 120 to 140 mL. The tension and length of muscle fibers is also related to the LV end-diastolic pressure (LVEDP) because LVEDP is proportional to LVEDV. The LVEDP in human is around 12-14 mmHg. Thus an increase in LVEDV or LVEDP mirrors increment in LV preload which is related to RV function. Frank-Starling's law explains the balance between RV and LV function.

An increase in muscle fiber length in LV (preload) up to the optimal point (before disruption) induces more probability of cross bridging of actin and myosin in sarcomeric structure of LV muscle fibers because of an increase in tension. The more interaction between actin and myosin enhances the force of cardiomyocyte contraction. Eventually this results in increased in LV contraction and depletion of blood to the aorta so that the ventricular volume reaches the minimum level which is called left ventricular end-systolic volume (LVESV). The fraction of the blood that has been pushed into the aorta is called ejection fraction (EF%) which is stroke volume divided by LVEDV. It is practically important to measure changes in ventricular pressure and volume that can be used as a source of information about ventricular function. According to the Laplace law ventricular wall tension is directly related to pressure and radius of the left ventricle and inversely related to thickness of the left ventricle.

Left ventricular contractility is not only affected by preload but it is also influenced by afterload or the resistance of the blood vessels. The LV contractility is related to both LV

force generation and the velocity of contraction. The velocity of LV contraction is affected by afterload. In any type of muscle contraction the velocity of contraction is inversely related to the force development. Hence in muscular contraction both force generation and velocity of shortening are important factors. LV shortening velocity is not affected by any changes in preload parameters such as venous pressure, LVEDP and LVEDV. This notes the importance of other cardiac parameters including alteration of pressure in time (dP/dt).

This section explained that LV contractility is not only depends on the cardiomyocyte contractility and interaction between myosin and actin filaments but also is affected by external parameters including the preload and afterload which are also the results of contractility. The cardiomyocyte shortening is the main source of force generation of the LV. However LV force generation is under the influence of the other hydrodynamic parameters such as systemic or pulmonary blood pressure, and the volume of the blood in the venous lake. Heart function is also influenced by other organ functions such as liver, kidney and gastrointestinal systems thereby looking at the function of the heart in a patient should always be accompanied with consideration of other external factors.

1.3   *Myocardial dysfunction in sepsis and ischemia reperfusion injury*

Myocardial dysfunction is an important feature of sepsis and cardiac ischemia-reperfusion injury. It is one of the most common causes of death in septic patients [16]. In fact during severe sepsis and septic shock, and in the presence of refractory hypotension, the only compensation to maintain sufficient blood flow in the vital organs is left ventricular contractility. Animal and human studies have shown early myocardial dysfunction during sepsis [17]. Myocardial dysfunction during sepsis is biventricular and biphasic. It occurs within day 2 to 4 of early presentation of sepsis and returns to normal within 7 to 10 days in survivors [18].

Hypotension is the main characteristic of septic shock. Regardless of the cause of hypotension in septic shock, the mean arterial pressure is decreased because of reduction in vascular tone. This also increases the importance of cardiac output in saving organs from severe hypoperfusion. It has been shown that infusion of endotoxin in healthy individuals induced vasodilation follow by high cardiac output both of which are characteristic of sepsis [19]. During sepsis, the higher cardiac output results from a combination of tachycardia and the reduction in vascular resistance. Tachycardia is a cardiac reflexive defense for coping with hypotension, however the response of the heart rate to the degree of hypotension in sepsis is not as beneficial as in other types of hypotensive crisis such as in severe bleeding [20]. In septic patients, continuous inflammatory processes cause fever, diarrhea, perspiration and edema, leading to a reduction in fluid and preload. The reduction in cardiac preload causes decreased LVEDV and eventually falling cardiac output.

It is important to note that cardiac output is not predictive of the severity of sepsis. In fact most of patients who survive during and after the recovery phase have lower cardiac output than non-survivors [21]. It is only at the late stage of septic shock (near death), that non-survivors have very low cardiac output. Global circulation and the blood flow of different organs can change during sepsis [18].

Visceral blood flow is different in septic patients. Several studies have shown an increase in hepatic blood flow in the hyperdynamic phase of sepsis compared to controls [22,23]. Fong et al. have shown that low dose injections of endotoxin in normal individuals increases splanchnic blood flow and oxygen uptake, probably because of an increase in protein synthesis and gluconeogensis in the acute phase response of the liver [23]. The splanchnic oxygen extraction ratio is also higher than the systemic one, possibly because of increased oxygen demands. Another study has shown a reduction in gastric mucosal pH indicating existence of hypoperfusion and ischemia [24]. In fact one of the speculated mechanisms of endotoxemia and sepsis syndrome in critically ill patients was intestinal ischemia and translocation of bacterial endotoxin into the blood stream through the injured epithelium. This mechanism has been excluded in human septic shock.

Renal blood flow increases during the early phase of sepsis. However renal blood flow usually declines during the course of sepsis leading to decreased glomerular filtration rate (GFR), and in severe cases results in renal failure. Most of the time septic patients present with oliguria, and diminished creatinine clearance [25].

Cerebral blood flow is preserved during sepsis indicating normal global flow for the brain, however it does not exclude regional ischemia, especially because most septic patients have symptoms of brain involvement such as lethargy and stupor [26-28]. Furthermore it is not clear if the reduction in brain activity is because of reduced oxygen uptake or supply.

Various studies have shown different conclusions on skeletal muscle perfusion during sepsis. Early studies indicated a higher fraction of cardiac output goes into the skeletal muscle while Neviere et al. have shown that skeletal muscle blood flow was decreased during severe sepsis [29]. Administration of endotoxin to normal individuals did not change lower limb blood flow and animal studies have also indicated conflicting results.

Many different mechanisms have been considered to explain the pathogenesis of myocardial dysfunction during sepsis [16]. One of the manifestations of myocardial dysfunction in sepsis is pre-terminal or end stage fall in cardiac output and EF%. During sepsis and in the presence of normal pulmonary capillary wedge pressure (an indicator of left ventricular preload), left ventricular stroke volume decreases even in resuscitated patients [30]. It has been shown that the ratio of left ventricular stroke work and pulmonary capillary wedge pressure is decreased during sepsis and septic shock, indicating disturbance of left ventricular performance [30]. Raper et al. have shown that the slope of LV stroke work against LVEDV is significantly lower compared to other types of hypotension [31]. Injection of LPS in normal individuals depressed the above parameter [32]. One of the best characteristic parameters for measuring LV contractility during sepsis is

the slope of left ventricular end systolic pressure volume relation which is also called end-systolic elastance (Ees). Similarly the maximal elastance (E_{max}) of the left ventricle provides another index of the LV contractility. Ees and E_{max} describe cardiac contractility without consideration of left ventricular loading. It has been shown that even in the early phase of sepsis and in the absence of shock, Ees and E_{max} can change [33,34]. Animal studies have also confirmed the efficiency of E_{max} in predicting cardiac performance during sepsis.

One of the postulated mechanisms of myocardial dysfunction during sepsis is global ischemia because of the presence of severe hypotension and presumably a reduction in coronary blood flow, which finally results in decreased EF%. However several studies have shown different changes in EF% during sepsis and septic shock [16,18,35-37]. In fact most non-survivors of sepsis have a higher left ventricular EF% than survivors. It is also important to note that EF% is affected by vessels wall resistance or afterload. EF% is a load dependent cardiac parameter and this has been confirmed by several studies that explained different changes in left ventricular EF% of septic patients [38]. According to the Frank-Starling Law the rise in left ventricular EF% can be accomplished by increased LVEDV. Several studies confirmed the increase in LV compliance during sepsis [32] however there is good evidence of the opposite result, showing no difference in EF% between survivors and non-survivors of patients with ARDS, though ventricular compliances in survivors was higher than non-survivors [39]. Based on previous studies LVEDV can differ from the high volumes seen in the early phase of sepsis to the very low volumes that has been documented in the end-stage of septic shock [18,40,41]. Moreover

it can also differ based on previous heart function and the nature of cardiovascular tissue. Taken together, it seems that LVEDV and EF% are not good indicators of depressed cardiac function during sepsis and septic shock, though they may change in a manner consistent with myocardial depression in some patients.

Another speculation of myocardial dysfunction in sepsis is right ventricle stress. It has been shown that pulmonary arterial blood pressure was increased during sepsis because of the presence of various types of mediators, leading to a fall in right ventricular contractility and a rise in right ventricle volume, especially in volume resuscitated patients [42]. The high volume of the right ventricle shifts the interventricular septum to the left side and in turn reduces left ventricular motion [43]. However further studies using angiography excluded the above claim and indicated that right ventricular depression results from left ventricular dysfunction [44].

Other studies have suggested that the left ventricular depression during sepsis occurs because of a lack of response to endogenous inotropics substances such as cathecholamines. Low adernergic responses may be one of the reasons for lower cardiac output in septic patients [45]. Defects in cAMP production and downstream signals of β-receptors have also been suggested [46]. It has been shown that the high activity of inhibitory G protein in septic patients is involved in the mechanism of hypotension and low cardiac output [47,48].

Disturbed coronary circulation has been suspected in septic patients and it raises many questions in describing ventricular dysfunction in sepsis. Coronary blood flow in septic patients is higher compared to controls, both in survivors and non-survivors [49]. Cunnion et al. have explained that the cardiac dysfunction in humans with severe septic shock is independent of myocardial blood flow and metabolism in most patients [50]. During septic shock myocardial blood flow is preserved or even increased in experimental animals [51]. Cunnion et al. concluded that coronary sinus blood flow is higher in most patients with septic shock compared to normal subjects, especially in non-survivors. [50] Bloos and Herbertson groups have shown that the septic heart has a higher global perfusion compared to controls. The above observations can be explained by vasodilative mechanisms such as NO production in the septic heart [51,52]. Dhainaut's study revealed that global ischemia is not responsible for the cardiac dysfunction in septic shock because there is no change in net lactate production and low lactate extraction by myocardium in the septic heart. However this does not exclude possible focal ischemia in the septic heart. They concluded that myocardial contractility depression is independent from blood flow and metabolic changes. In fact myocardial blood flow is often preserved in patients with septic shock [53]. The septic heart is overperfused, however, oxygen extraction is less than in normal subjects [52].

In the normal heart, coronary blood flow is highly different in myocardial regions over time and space. In fact even in the normal myocardium, blood flow is heterogenous because of differences in myocardial segmental force. This is directly related to the local force of contraction that is cardiomyocyte shortening force. This mechanism seems to be

necessary to adjust the demand and supply in various regions of the heart. This means that the septum of LV (highly active) has higher blood flow compared to the basal part of LV (less active) at the same time point [53].

It has been suggested that the differences in regional blood flow may be higher in septic heart and may affect the corresponding regional supply. Although workload and demands for one specific region of the heart in septic shock may be lower than in a normal heart because of the lower afterload (lower resistance), the septic heart does not have sufficient supply because of increased heterogeneity of blood flow resulting in focal ischemia [51,54,55].

On the other hand, during sepsis and septic shock, oxygen metabolism is changed and the relation between oxygen delivery and uptake is interrupted. In normal individuals the critical oxygen delivery level is about 400 mL/min/m^2 of body surface with almost 100 mL/min/m^2 of oxygen uptake. During sepsis these levels are changed to significantly higher oxygen delivery (about 700-800 mL/min/m^2) because of impaired oxygen extraction, and higher oxygen uptake because of increased demand [39]. In fact it has been suggested that the circulatory changes during septic shock are associated with impaired oxygen extraction, indicating that abnormal circulation rather than changes in cellular metabolism that causes impaired oxygen uptake [39]. However there is still debate about the impact of impaired oxygen extraction versus defects in sufficient oxygen supply [35].

The endothelium functions as the first barrier for separating the vascular space from surrounding tissues. Endothelial damage and leakage has been mentioned as a reason for myocardial edema in septic shock that leads to leakage of coronary capillaries and finally vascular compression, suggesting more defects in the supply/demand of the heart during sepsis [56]. On the other hand endothelial dysfunction may occur because of intravascular coagulation or NO production [57].

Other factors may be involved in the mechanism of myocardial depression including a hypercoagulative state, microembolisms, contractile-metabolic mismatch, and ion channel defects [37,56,58].

One of the most important components of the inflammatory response is the function of leukocytes. Our laboratory has shown the direct effects of inflammatory cells (macrophages and neutrophils) on the contractility of the cultured cardiomyoctes [59,60]. Botha et al. have shown that leukopenia is a sign of progression of the inflammatory response and shock, to multi-organ dysfunction in septic and traumatic patients, suggesting neutrophil involvement [61]. Chiba's group studied the effect of leukocyte depletion on patient survival after cardiopulmnary bypass. They found that depletion of leukocytes and platelets protects cardiac function after cardiopulmonary bypass [62]. This may suggest that leukocytes, especially neutrophils, play important roles in cardiac dysfunction during systemic inflammatory responses syndrome. Based on these observations, different anti PMN receptors blocking antibodies have been used. Study of the lung has shown that PMN number is significantly higher in the right atrium compared

to the left atrium of septic patients after cardiopulmonary bypass. Although leukocytes can infiltrate into the tissue in various types of inflammation including ischemia-reperfusion injury, there is no strong evidence for the presence of leukocytes in the myocardium of non-survivors of sepsis. However it has been documented that during sepsis, neutrophils and inflammatory cells release significant amount of toxic substances including oxygen free radicals and elastase [63-65].

Cytokines have always been suspected in many types of inflammatory responses. TNFα [66], IL-1β, and IL-6 are the major cytokines affecting myocardial contractility [67]. Although there is some strong evidence about the cardiac depressive effects of the above cytokines, some investigators did not find independent effects of the cytokines in vitro [59,60]. The idea that TNFα and other cytokines are not specifically important in septic patients was strengthened by the failure of a clinical trial of anti-cytokines therapies [68]. Instead it is believed that these cytokines are very important in the presence of inflammatory cells which then exaggerate inflammatory responses [69].

Nitrite oxide (NO) is another factor that has been postulated to contribute to myocardial depression during sepsis [70]. Arginine is converted to NO under the effect of various types of NOS. NO increases cGMP concentration leading to modulation of contraction and finally more relaxation [71]. It is worth noting that inhibition of NOS in a selective or non-selective way did not improve cardiac dysfunction [72-75], however other investigations demonstrated the protective effects of NO inhibition with various methods [76,77].

Metabolic acidosis almost always accompanies sepsis, leading to increased potassium channel activation at the vascular level and vasodilation [78]. In cardiomyocytes acidosis interferes with intracellular Ca^{2+} concentration and the interaction between actin and myosin [79]. Reduction in intracellular pH first increases ionized Ca^{2+} concentration in the sarcolemma, however the total stored Ca^{2+} concentration decreases over time. This may also affect cardiomyocyte metabolism and finally contraction.

Hormonal alteration is one of the characteristic changes in sepsis. Growth hormone (GH) fluctuates in the first week of the sepsis state [80]. It has been shown that the serum insulin growth factor-1 (IGF-1) level is significantly lower in septic patients [81]. The plasma insulin level is initially low however this level tends to increase rapidly after 24 hours [82,83]. There is strong evidence of benefit of IGF-1 injection in various types of injury [84-86]. IGF-1 is involved in different pathways including anti-apoptotic signaling through the protection of mitochondria [87].

Erythropoietin (EPO) secretion is also affected by sepsis. It has been shown that the level of EPO is significantly lower in critically ill patients and/or the response of target cells to EPO is impaired in septic patients [88]. Recent studies on the effect of EPO in various models showed novel protective effects of EPO against cellular injury including anti-apoptotic and anti-oxidant effects. Interestingly recent clinical data have shown negative results to blood transfusion in critically ill patients and conversely beneficial results after EPO injection, suggesting a more protective effect of EPO in those patients [89].

Although coronary blood flow is higher in septic patients, there is some evidence that may confirm the existence of focal ischemia in the cardiac tissue of these patients. However this theory needs to be investigated using new techniques. Furthermore ischemia, especially in cardiac tissue, is accompanied by a number of symptoms and signs including electrocardiogram (ECG) changes, alteration in ischemic area motion, arrhythmia and permanent sequelaes. Conversely in septic patients there is no strong evidence of such changes. The most common alteration in ECG of septic patients is supraventricular tachycardia which itself could be contradict the above theory. Autopsies of septic patients have shown evidence of necrosis only in those patients who had myocardial infarction during sepsis syndrome, probably because of reflex tachycardia [90]. Although most septic patients have myocardial dysfunction, there is no evidence of myocardial necrosis in the majority of these cases [90]. Additionally myocardial depression during sepsis is a reversible event. The myocardium regains its normal contractility by the end of 14 days in survivors [1].

However we cannot ignore the possibility of a type of ischemia that is not severe enough to induce myocardial sequelaes. This could be explained by stunned myocardium which can be seen in brief myocardial ischemia and more importantly it is also a reversible event which occurs in the prone regions of the injured myocardium after ischemia. Myocardial stunning occurs in the surrounding viable tissue around necrotic parts after myocardial infarction, cardiopulmonary bypass, and exercise induced ischemia. It is demonstrated by a persistent defect in regional myocardial motion even in the presence of normal blood flow. Within a few days to several weeks the stunned myocardium assumes

its normal function which was demonstrated by positron emission tomography scanning in the above patients [91].

Myocardial ischemia contributes to the pathophysiology of many different types of conditions in cardiovascular diseases including angina, infarction, cardiovascular surgery, angioplasty, transplantation, shock and sepsis. It was described as the imbalance between myocardial oxygen supply and demand. The duration of ischemia is also an important factor in the myocardial survival rate [92]. While prolonged ischemia is seriously harmful for the affected myocardium [93] brief periods of ischemia could result in different pathogenesis which also affects cardiac function in a reversible manner [91]. These reversible phenomena can be generated by the reperfusion of acutely ischemic myocardium and chronic myocardial ischemia. The two types of reversible myocardial injury are myocardial stunning and hibernation. Myocardial stunning is characterized by persistent and reversible systolic and diastolic depression of myocardial wall motion which is affected by previous ischemia, reperfusion or both injuries. The section of ischemic hearts which is affected by the above mechanisms is viable and it is capable of restoring its function gradually (days to weeks). The main mechanisms of myocardial stunning are not clear yet, however ROS formation, alteration in calcium homeostasis and low responds of contractile apparatus to calcium have been considered as the major mechanisms [91,94]. Hibernating myocardium is similar to stunned myocardium with the exception that recovery occurs after removal of the causes of ischemia. The blood flow in hibernating myocardium is adequate to maintain its basic function and viability of at risk cardiomyocytes, however it is not sufficient to maintain optimal ventricular contractility

[91]. Myocardial dysfunction in the hibernated or stunned myocardium responds to β-stimulators. The function of stunned myocardium improves over time, whereas hibernating myocardium needs revascularization to recover function. This reversible myocardial dysfunction in ischemia-reperfusion injury is very similar to that of sepsis. In fact we can see these phenomena even during prolonged exercise and in the absence of coronary occlusion [95]. There are two major hypothesis to explain this type of myocardial dysfunction: first the role of oxygen radicals [93] and secondly Ca^{2+} involvement [96].

Non-reversible myocardial ischemia results in cellular changes from metabolism to contraction. It changes oxidation phosphorylation and results in less ATP and creatinine phosphate production [93]. ATP is the main source of energy for activation of ATP dependent ion channels and actin-myosin interaction. The lack of channel activity during prolonged myocardial ischemia results in accumulation of intracellular Ca^{2+} ions and an increase in cellular osmolar pressure which results in higher intracellular water, higher membranous tension, and finally cardimyocyte sacomeric fragility [97].

Reactive oxygen species (ROS) are the products of the prolonged myocardial ischemia. They are also the main causes of progression of injury started by ischemia. During ischemia because of the failure in oxidation phosphorylation, ADP cannot be converted to ATP [98]. In fact it progresses to more dissociation of Phosphorus from ADP and creation of AMP which results in higher catabolism of adenosine nucleotides and accumulation of hypoxanthine. On the other hand because of ischemia, hypoxanthine dehydrogenase, an important enzyme which is responsible for converting hypoxanthine

to xanthine and finally uric acid, is changed to hypoxanthine oxidase leading to excessive production of ROS [99]. Other potential sources of ROS are semi-ubiquinone of mitochondria, cytochrome C450, cycloxygenase and NADPH oxidases [100]. NO can also be a source of ROS formation when eNOS is not working properly under the influence of hypoxia. Oxygen free radicals interact with NO to create peroxynitrate, one of the most harmful ROS in cardiomyocyte physiology [93].

It has been shown that ROS can initiate cell signaling cascades via changes in regulatory proteins. Accumulation of ROS in Escherichia Coli changes the thiol group (H-S group) of regulatory proteins into the disulfide (S-S) leading to signal transduction of the membrane and activation of various types of transcription factors such as superoxide dismutase, catalase and glutathione reductase [101]. The role of ROS has been investigated extensively during the last 5 years in various types of cells. The results suggest that ROS can initiates some signals including activation of receptor tyrosine kinases, insulin receptors, increased intracellular Ca^{2+} concentration, JNK and P38 MAPK pathways stimulation, and activation of NFκB and PKC-α [101].

Defects in ATP production also affect sodium-potassium channels, resulting in higher concentrations of Na^+ and Ca^{2+} ions. Lack of energy changes the oxidation phosphorylation pathway to glycolysis and production of acid. The depressed intracellular pH leads to an increase in ionized Ca^{2+} concentration and eventually a reduction in Ca^{2+} storage [102].

Collectively, the defect in ATP production during myocardial ischemia increases cytoskeletal fragility, accelerates intracellular edema, changes membrane electro-potential and intracellular Ca^{2+} concentration, and produces ROS which then promote further injury to cardiomyocytes during reperfusion [103]. However all of the above alterations may be a signaling mechanism to save the myocardium from further injury by reducing cardiac contractility and demands. Indeed if ischemia is severe enough, the cardiomyocyte goes into a rapid process of death such as apoptosis and or necrosis.

Reperfusion, although necessary to restore blood flow into the myocardium and to save myocardium from severe ischemia, is another type of damage to the cardiac tissue. Many mechanisms are involved in reperfusion injury. Accelerated ROS formation that was started during ischemia leads to persistent damage to the coronary endothelial layer and cardiomyocyte membrane, action potential prolongation, early membrane depolarization and contractility failure. These events finally result in activation of NFκB transcription factor and translocation of this factor into the nucleus, followed by expression of different inflammatory proteins and cytokines including IL-6, IL-8, TNFα, tissue factors, iNOS [104] and adhesion molecules such as selectins, VCAM-1 and ICAM-1 [103].

A rapid rise in intracellular Ca^{2+}, higher numbers of open L-type channels or dihydropyridine receptors (DHPR), free release of Ca^{2+} from ryanodine receptors (RyRs), membrane leakage to Ca^{2+} and failure to clear Ca^{2+} from intracellular space are all suggested mechanisms for further cardiac injury during the reperfusion period [103]. It is important to note that during reperfusion white blood cells, especially polymorphonuclear

cells (PMN), support further injury by releasing free radicals, proteolytic enzymes, superoxide anions and hypochlorus acid into the injured area [61,105]. Complement cascades also exaggerate reperfusion injury by activation of classic or alternative pathways to create a membrane attack complex. This process is continued by opsonization of target cells with iC3b and the chemo-attractive effect of C3a and C5a. Interstitial edema during reperfusion rapidly progresses because of the leaky endothelial layer causing lymphatic drainage failure and vicious cycle of edema [92,106].

Taken together, during reperfusion fast recovery of extracellular osmolarity is achieved while intracellular osomolarity is still higher than normal because of deficiencies in ion channel function suggesting increased cellular swelling and cellular vulnerability.

Also cytoskeletal filaments are fragile because of the existence of intracellular ROS formation and low pH, while extracellular pH returns to normal faster indicating fast re-energization in the presence of high intracellular Ca^{2+} levels and membrane fragility that is also a cause of hypercontracture and disruption of sarcolema [92,106].

There are different theories and results explaining myocardial dysfunction during sepsis and ischemia reperfusion injury. There is one common belief that, myocardial dysfunction during these events is an inflammatory response which has intracellular consequences.

1.4 Molecular mechanism of cardiac inflammation

1.4.1 ICAM-1 interaction initiates intracellular signaling

Regardless of the causes of inflammation in cardiac tissue, including endothelial cells or cardiomyocytes, the final pathway is the activation of intracellular signaling. These intracellular signaling pathways can be initiated by ROS formation (ischemia), LPS or toll like receptor activation on inflammatory cells, and triggered cytokines production (sepsis). They induce production of transcription factors such as NFκB and or HIF-1α. These transcription factors are translocated into the nucleus and activate specific genes including adhesion molecule such as selectin, VCAM-1 and ICAM-1 on the endothelial cells. Additionally they can directly activate translation of different inflammatory proteins (Figure 1.1).

The cardiomyocyte has various types of adhesion receptors including ICAM-1. ICAM-1 (CD-54), a 76-114 kDa glycoprotein, is expressed in both normal and activated cardiomyocytes [59,60,107]. It is a member of the immunoglobulin gene superfamily, which includes other adhesion molecules such as ICAM-2, ICAM-3, VCAM-1, PECAM-1, neural crest adhesion molecule-1 (NCAM-1) and myelin adhesion glycoprotein [108]. ICAM-1 and ICAM-2 are constitutively expressed on endothelial cells. Cytokines and LPS treatments increase endothelial ICAM-1 expression while the level of ICAM-2 is not changed after endothelial cells activation [109,110].

ICAM-1 contains five extracellular Immunoglobulin domains, a transmembrane domain, and a short cytoplasmic tail at its C terminal end. A soluble form of ICAM-1 (s ICAM-1) has been found in normal human plasma at levels of 100-200 ng/mL [111-114]. It is speculated that the levels of sICAM-1 is under the control of matrix metalloproteinases (MMP) and higher levels of sICAM-1 modulate inflammatory responses [115,116]. The sICAM-1 level increases markedly in many inflammatory reactions including atherosclerosis, ischemia reperfusion injury, transplant rejection and chronic inflammatory diseases [109,117,118]. Lower levels of ICAM-1 expression on tumor cells is associated with increased metastasis and invasiveness of cancerous cells [119]. ICAM-1 is a ligand for β_2-integrins on leukocytes. This interaction between ICAM-1 and β_2-integrins (LFA-1) was prevented using an anti-ICAM-1 monclonal antibody as reported by Dustin et al. [120]. ICAM-1 is widely distributed in different cells including endothelial cells [121], fibroblasts, dendritic cells, keratinocytes [122], mesenchymal cells, monocytes, lymphocytes, epithelial cells [123], smooth muscle cells [117] and cardiomyocytes [59,60].

Expression of ICAM-1 on non-hematopoietic cells is low, but surface expression is markedly up-regulated by various types of inflammatory mediators including LPS, IL-1β, TNFα, and IFNγ [60,110,124,125]. Cytokines can increase ICAM-1 production after 2-4 hours and maximal production occurs 18 to 24 hours after stimulation. Upregulation of ICAM-1 by cytokines or LPS also facilitates neutrophil binding and migration through a cultured endothelial cell monolayer in vitro, a process involving the interaction of ICAM-1 with LFA-1 (CD11a/CD18) and Mac-1 (CD11b/CD18). Immunofluorescence studies have shown a punctuated distribution of ICAM-1 on endothelial cells and cardiomyocytes

[60,110]. Localized distribution of ICAM-1 may facilitate its interaction with LFA-1 and Mac-1 [126]. ICAM-1 on the cell surface presents as a homodimer, which may facilitate high-affinity binding to LFA-1 [126-128]. ICAM-1 can interact with various ligands including fibrinogen [129], Rhinoviruses [125], Coxsackie viruses [130,131], and Plasmodium falciparum [132].

The relation between adhesion molecules such as Mac-1 and LFA-1 has been shown by Smith and Lo in different studies. They have shown that the adhesion of PMN to ICAM-1 on stimulated endothelial cells is largely Mac-1 dependent but in the un-stimulated cell it is exclusively dependent on LFA-1 [127,128]. The above interaction can be inhibited using an anti-ICAM-1 antibody, however only some kinds of ICAM-1 antibodies inhibited the interaction between ICAM-1 and integrin receptors on leukocyte membranes.

The extracellular domains of ICAM-1 are important for interaction with their ligands. This part is highly glycosylated indicating high solubility of ICAM-1. A flexible hinge between domains 2 and 3 creates a good position for domains 1 and 2 to interact with their ligands [133]. The binding site for LFA-1 on the extracellular domains of ICAM-1 is on the edge of domain 1 and at the center of C and D strands.

Maximal production of ICAM-1 is reached within 18 to 24 hours and its expression is maintained about 48 hours after first activation. However the level of ICAM-1 expression can be high as long as the inflammatory process is active or around ten days after initiation of inflammation on coronary endothelial cells as reported by Bevilacqua and his

colleagues [110]. LFA-1 (CD11a/18) binds to the first and second domains and Mac-1 (CD11b/18) binds to the third domain of ICAM-1.

Fibrinogen is also an important ligand for ICAM-1 [134,135]. It is a 340 kDa plasma protein involved in inflammation and the coagulation cascade. It has been shown that fibrinogen can facilitate the interaction of vascular endothelium and leukocytes [136]. The fibrinogen molecule (composed of three α, β, and γ chains) has three domains, a central E domain and two lateral D domains. Fibrinogen can infiltrate into the tissue during inflammation, ischemia, trauma and cancer. The association of fibrinogen with a higher risk of myocardial infarction and atherosclerosis has been reported in several studies [137]. The presence of thrombin affects peptides A and B of the central part of the α and β chains resulting in dissociation of the above two peptides from the related chains, polymerization of fibrin molecules together and formation of fibrin networks [138]. Plasmin cleaves fibrin networks and separates the two D domains from the central E domain resulting in formation of fragment D and E in the serum. Fragment D contains α, β and γ chains [139]. It has been shown that amino acid sequence of 117-133 of the γ chain is the location for adhesion to the first domain of ICAM-1. Hence both fibrinogen and fragment D can attach to ICAM-1 [139,140].

Fibrinogen can increase endothelial leakiness and enhance angiogenesis on endothelial cells [141-143]. It is able to attach to ICAM-1 through its 117-133 amino acid sequence located on its γ chain [134,135]. There is controversy about the location of fibrinogen adhesion on ICAM-1. It seems that aspartic acid and proline residues and amino acid 8-

21 of domain-1 of ICAM-1 are very important for the above interaction. However those amino acids are not on the 8-21 amino acid sequence of ICAM-1, which were previously shown to be important for the above interaction [144]. Upregulation of ICAM-1 in cardiovascular diseases is also accompanied by high expression of fibrinogen and vice versa [145,146]. Fibrinogen and ICAM-1 interaction promotes platelet and leukocyte adhesion on endothelial cells [147]. It has been shown that fibrinogen deposition on endothelial cells was significantly reduced using ICAM-1 knock out mice in a model of intestinal ischemia reperfusion injury [148]. Hicks et al. have shown that fibrinogen deposition on endothelial cells induced vasodilation, however when they increased fibrinogen concentration this effect was converted to vasoconstriction [149]. Fibrinogen deposition upregulated ICAM-1 expression through activation of NFκβ and IL-8 production [146,150].

The short intracellular domain of ICAM-1 is an important part for initiation of signals. Conformational change in tertiary structure of the ICAM-1 molecule induces phosphorylation of different amino acids including tyrosine residues leading to activation or inactivation of other downstream signals. It is evident that the cortical cytoskeleton is an important regulator for the above function. Carpen et al. have shown that a specific region of ICAM-1, 478-505-peptide, interacted with alpha-actinin in chinese ovary hamortoma cells [151]. This region is close to the cell membrane spanning region and contains several positively charged residues, and appears to mediate a charged interaction with alpha-actinin, which is not highly dependent on the order of the residues. They also showed that ICAM-1 activation is through homo-oligomerization. This needs a substrate

from PI pathway (PIP2) to promote conformational change in tertiary structures of intracellular domain of ICAM-1 [151]. In another study, Vogetseder and his colleagues have shown that the intracellular domain of ICAM-1 is associated with actin filaments in endothelial cells [152]. Cross-linking of ICAM-1 on synovial cells induced IL-1β transcription and AP-1 activation. ICAM-1 functions not only as a glue for integrin binding, but also as a transducer for AP-1 activation signals that are important for IL-1β gene transcription [153]. ICAM-1 cross-linking initiated production of oxidative metabolites and oxygen free radicals on monocytes [154]. It has been shown that cross-linking of ICAM-1 on HUVEC cells can increase VCAM-1 expression and exacerbate the inflammatory reaction [121]. A study on brain microvascular endothelial cells reported by Durieu-Trautmann et al. has shown the tyrosine phosphorylation of the cytoskeleton-associated protein, cortactin, after ICAM-1 activation suggesting interaction of ICAM-1 with cytoskeletal proteins [155]. Activation of ICAM-1 receptors on Burkitt cell lymphoma increased Ca^{2+} concentration [156]. Etienne et al. have also found that ICAM-1 cross-linking on brain endothelial cells participated in cellular shape changes and gene regulation [157].

Interaction between fibrinogen and ICAM-1 induces tyrosine phosphorylation at locations 474 and 485 of cortactin which is also associated with the intracellular domain of ICAM-1 [155]. The above interaction also increased phosphorylation of cortactin on endothelial cells [145,158]. Holland et al. have shown adhesion of fibrinogen on ICAM-1 phosphorylated Erk1/2 which is through the interaction of sequences 117-133 of fibrinogen and 8-21 of ICAM-1 [129,159].

ICAM-1 is not only responsible for interaction of leukocytes and proteins with the target cells, but is also involved in antigen recognition through major histocompatibility complex (MHC-II) interaction. Exogenous antigens are engulfed and processed in antigen presenting cells followed by presentation of the above antigens to the CD4 T lymphocytes. Interaction between T cell receptor complexes such as CD3, CD4/CD8 with MHC- restricted antigen presenting cells initiates intracellular signaling. ICAM-1 acts as an accessory molecule in strengthening the interaction between CD4 and MHC-II to initiate an immune response once the T cells has interacted with exogenous antigens. Hence ICAM-1 plays a major role after exogenous antigens fragments have interacted with T cell receptors.

In the next chapters I will discuss the novel finding of cardiomyocyte ICAM-1 activation in regard to cardiomyocyte contractility and finally cardiac contractility. The possible pathways which may be involved in ICAM-1 activation and intracellular signaling will be studied. The possible ligands for cardiomyocyte ICAM-1 were considered and studied in the in vitro and in vivo models in chapters 2, 3 and 4. Finally the similar ex vivo model for high expression of ICAM-1 on cardiac tissue was used to find a new therapeutic intervention to inhibit intracellular signaling.

1.5   General Hypothesis

In this thesis my general hypothesis is that the expression and activation of cardiomyocyte ICAM-1 is responsible for myocardial depression during sepsis. I also hypothesize that the expression of ICAM-1 can be modulated by intervention in intracellular signaling cascade of ICAM-1 for example PI3K pathways (Figure 1.2).

In order to test this hypothesis, in an in vitro model I first show that cardiomyocyte ICAM-1 expression increases after cytokine treatment and activation of ICAM-1 by adherent PMN and cross-linking of ICAM-1 decreases cardiomyocyte contractility. Using an in vivo model I then show that the absence of ICAM-1 on cardiac tissue is protective against the effect of LPS on cardiac contractility. I also investigate the presence of inflammatory cell in the cardiac tissue after LPS injection.

Next I show that the interaction of ICAM-1 with fibrinogen results in a decrease in cardiomyocyte contractility and fibrinogen can infiltrate into the cardiac tissue after LPS injection thereby fibrinogen can trigger cardiomyocyte ICAM-1 activation.

Using an ex vivo model of myocardial ischemia reperfusion injury, I show that ischemia-reperfusion injury is associated with high expression of ICAM-1. I also show that IGF-1 therapeutic intervention can prevent ICAM-1 expression during reperfusion period resulting in better cardiac function and less cardiac injury. This latter effect of IGF-1 is partly because of less ICAM-1 expression on cardiac tissue.

1.6   Conclusions

The final conclusions of this thesis are;

1- Cardiomyocyte ICAM-1 activation decreases cardiomyocyte contractility.

2- Cross-linking of ICAM-1 or adhesion of PMN activates ICAM-1.

3- ICAM-1 activation is associated with cortical cytoskeletal assembly and disruption of cortical actin filaments inhibits this effect of ICAM-1 on the cardiomyocyte contractility.

4- ICAM-1 activation alters intracellular Ca^{2+} propagation.

5- The lack of ICAM-1 on cardiac tissue is protective against the effect of LPS.

6- Fibrinogen adhesion to ICAM-1 can activate this receptor and decrease cardiomyocyte contractility.

7- Ischemia reperfusion injury is associated with an increase in cardiac ICAM-1 expression. IGF-1 prevents the membranous presentation of ICAM-1 thereby protects cardiac tissue from further injury.
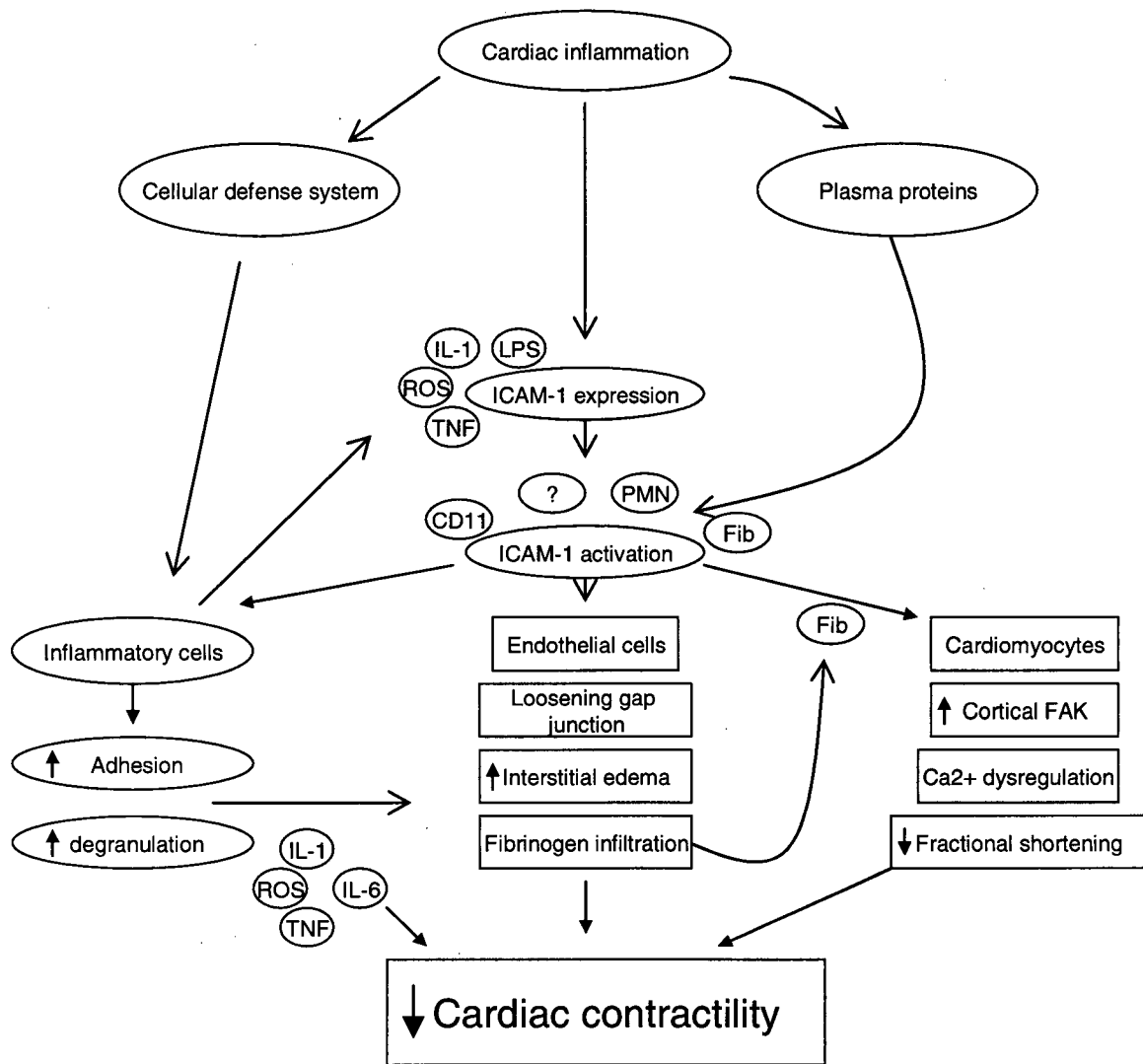
Figure 1.1　　Schematic pathways involved in cardiac inflammation.
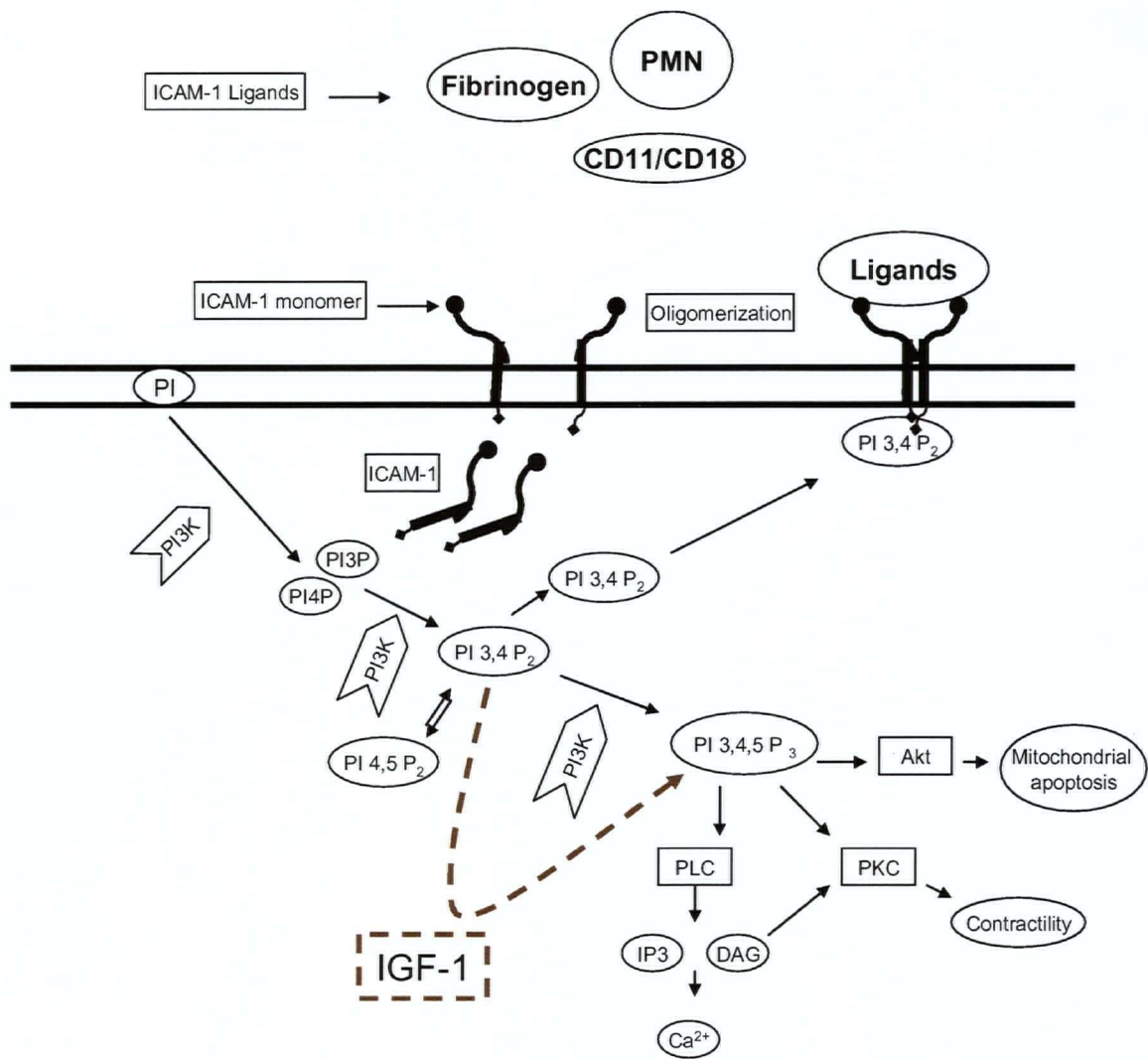
Figure 1.2   Schematic pathways involved in ICAM-1 presentation and activation and the possible

effect of IGF-1 on ICAM-1 expression.

Chapter-2

Novel regulatory mechanism of cardiomyocyte contractility involving ICAM-1 and the cytoskeleton

[1]2.1 Abstract

ICAM-1 mediates interaction of cardiomyocytes with the extracellular matrix and leukocytes, and may play a role in altering contractility. To investigate this possibility rat ventricular cardiomyocytes were activated using TNFα, IL-1β or LPS, washed, co-cultured with quiescent rat polymorphonuclear leukocytes (PMN) for 4 hours, and electrically stimulated to determine fractional shortening. PMN co-cultured with activated cardiomyocytes reduced control fractional shortening of 20.5±0.7% by -2.8±0.3% per adherent PMN ($p<0.001$). Fixing PMN with paraformaldehyde or gluteraldehyde did not prevent PMN-mediated decreases in cardiomyocyte fractional shortening. However, PMN adherence and decreased fractional shortening were prevented by anti-ICAM-1 and anti-CD18 antibodies. Reduced fractional shortening was reproduced in the absence of PMN by ICAM-1 binding using cross-linking antibodies (reduced by 36±3% from control, $p<0.01$). Immunofluorescent staining demonstrated increased cortical cytoskeleton-associated FAK expression following ICAM-1 cross-linking, suggesting involvement of the actin cytoskeleton. Indeed, disruption of F-actin filament assembly using cytochalasin D or latrunculin A did not prevent PMN adherence but prevented decreased fractional shortening. Inhibiting the cytoskeleton-associated Rho kinase pathway using HA-1077 prevented ICAM-1 mediated decreases in cardiomyocyte contractility, further suggesting a central role of the actin cytoskeleton.

Importantly, ICAM-1 cross-linking did not alter the total intracellular Ca^{2+} transient during cardiomyocyte contraction but greatly increased heterogeneity of intracellular Ca^{2+} release. Thus, we have identified a novel regulatory mechanism of cardiomyocyte contractility involving the actin cytoskeleton as a central regulator of the normally highly coordinated pattern of sarcoplamic Ca^{2+} release. Cardiomyocyte ICAM-1 binding, by PMN or other ligands, induces decreased cardiomyocyte contractilty via this pathway.

Key words: ICAM-1, Intracellular signaling, FAK, Rho, Calcium.

2.2   Introduction

Intramyocardial inflammation, for example following ischemia-reperfusion, in inflammatory cardiomyopathy, during orthotopic heart transplant rejection, and during sepsis-induced myocardial dysfunction, results in increased expression of ICAM-1 on cardiomyocytes [92,160-162] and accumulation of intramyocardial leukocytes [92,160-162]. Adhesion of polymorphonuclear leukocytes (PMN) or macrophages to cardiomyocytes is mediated in part by binding to ICAM-1 on cardiomyocytes. If PMNs are highly activated they kill cardiomyocytes within minutes by release of reactive oxygen intermediates [100,163,164]. However, ICAM-1 mediated adhesion of relatively quiescent macrophage/monocytes to cardiomyocytes causes a reduction in contractiltiy without cardiomyocyte killing [59] and a recent report implicates ICAM-1 in mediating reduced cardiomyocyte contractility independent of PMN accumulation [160].

ICAM-1 is fundamentally important in linking extracellular mechanical signals to regulation of intracellular processes [123,151]. ICAM-1 is closely associated with the actin cytoskeleton [123,165] and ICAM-1 binding increases linkage between the cell surface ICAM-1 receptor and the cytoskeleton [152,166]. Whether the cytoskeleton plays a role in modulating cardiomyocyte contractility is unknown and potential signaling pathways and mechanisms involved have not been identified. Accordingly, we postulated that ICAM-1 and the cardiomyocyte cytoskeleton may be involved in a novel pathway leading to cardiomyocyte contractile dysfunction. While many mediators (e.g., cytokines, leukocytes, reactive oxygen intermediates, NO) [167-169] and pathways (e.g., apoptosis, adrenergic signaling) [16,18,45,46,69,170] are involved in myocardial dysfunction during

intramyocardial inflammation, here we focus on the potential role of ICAM-1 binding and its relationship to the cardiomyocyte cytoskeleton.

2.3   Materials and Methods

This study was approved by the University of British Columbia Animal Care Committee and adheres to Canadian and National Institutes of Health guidelines for animal experimentation.

2.3.1   Isolation of rat ventricular myocytes: Male Sprague-Dawley rats (250-300 g) were anesthetized using 3% halothane and the heart was excised and mounted on a modified Langendorff apparatus and perfused with oxygenated (95% O_2, 5% CO_2) HEPES-Joklik modified MEM buffer (Gibco BRL, Grand Island, NY) at 37°C for 2 minutes. Then the perfusate was changed to 30 mL recirculating calcium free MEM containing 236 U/mL collagenase (Worthington Biochemical, Freehold, NJ). At 15 and 20 minutes, the calcium concentration was increased, stepwise to 0.025 and 0.075 mmol/L. After 30-40 minutes the ventricles were removed from the perfusion system and gently teased apart and agitated for 2-3 minutes at 37°C. The tissue and dispersed cells in solution were then filtered through a 200 μm nylon mesh. The cells were then washed three times at 37°C in MEM containing increasing Ca^{2+} concentrations (200 μM, 500 μM and 1 μM), allowing the cells to settle by gravity for 10 minutes between each wash. Cells were resuspended in 37°C HEPES-modified M199 buffer (Gibco BRL) with 1% BSA. The cells were diluted to a final concentration of 50,000 cells/mL, 100 μL loaded into each well of 96 well plates, and incubated at 37°C in 95% O_2, 5% CO_2. At 90 minutes, the medium was changed to fresh M199 with BSA and the cardiomyocytes were incubated for 24 hours to allow them to become relatively quiescent. After 24 hours cells

43

were considered viable if they demonstrated a characteristic rod shape without cytoplasmic blebbing. This morphometric assessment of viability was confirmed in a subset of experiments with trypan blue exclusion. We have found that the fraction of viable cardiomyocytes is always greater than 85%.

2.3.2 Cardiomyocyte ICAM-1 protein expression: We and others have shown that activation of cardiomyocytes by inflammatory cytokines increases cardiomyocyte expression of ICAM-1 [59,160,171]. To confirm this we measured ICAM-1 protein expression on cardiomyocytes incubated with TNFα (20 ng/mL) for 4 hours and then fixed using paraformaldehyde 3% for 30 minutes. Cardiomyocytes were incubated with mouse anti-rat ICAM-1 antibody (1A29, BD Pharmingen) 10 µg/mL for 3 hours, washed, and incubated with a fluorescent secondary anti-mouse antibody (Alexa-Fluor 488, 1/500, Molecular Probe, Eugene, OR) for 3 hours and imaged using confocal microscopy (LEICA DIMRE2, Exton, PA). The mean of intensity / pixel of each cardiomyocyte was measured using Image Pro-Plus {Cybernetics, 1998}.

2.3.3 Cardiomyocyte ICAM-1 mRNA expression: Cardiomyocytes (5×10^5) were cultured in 60 mL laminin coated dishes and incubated with or without TNFα. Cells were then lysed and frozen at -70°C. RNA was extracted using standard technique of Qiagen RNA kit (Qiagen Inc. Mississauga, ON, Canada): 1 µL eluted RNA was added to 999 µL of 0.1M NaOH solution in diethyl pyrocarbonate-water; 3 µg of RNA were taken as constant template for RT cycle to make cDNA; 2 µL of cDNA were made from total RNA and used as template to amplify rat ICAM-1 and rat GAPDH using the following

primer sequence: 5' AGG TCA GGG GTG TCG AGC (forward ICAM-1 primer) and 5'

CAA GGA GAT CAC ATT CAC GG (reverse ICAM-1 primer). The PCR conditions for

Perkin Elmer 9700 model were 95°C for 15 minutes (Qiagen Taq Polymerase enzyme

Activation), denaturing at 94°C for 30 seconds, annealing at 55°C for 30 seconds and

extension at 72°C for 1 min. The whole cycle was repeated 40 times. PCR products were

separated on 3% agarose gel stained with ethedium bromide and visualized using Eagle

eye UC scanner. The ratio of ICAM-1 signal was normalized to GAPDH signal for each

time point sample. The final results of TNFα treated cardiomyocytes were compared to

controls.

2.3.4 Measurement of cardiomyocyte fractional shortening:

Fifteen minutes before

measuring fractional shortening 2 μL of 0.5% trypsin was added to each well.

Preliminary experiments demonstrated that this concentration of trypsin did not alter cell

viability and cleaved greater than 95% of the adherent cardiomyocytes from their

attachments to the bottom of the well. Specially designed platinum electrodes were then

lowered in each well in the 96-well plate, and the cardiomyocytes were electrically

stimulated (Grass S48 stimulator, West Warwick, RI; 45V, 2.2 ms duration, 25-Ω

resistance) while being recorded by video-microscopy (Sony SLV-760HF) at 400X

magnification. This electrical stimulus was chosen from preliminary threshold

experiments, as two times the minimum electrical stimulus required to maximally

contracting the cardiomyocytes. Still frames of systolic and diastolic cardiomyocytes

were captured using Scion Image PC (Scion, Frederick, MD) and cardiomyocyte

fractional shortening was calculated as the difference between diastolic and systolic length divided by diastolic length.

2.3.5   Isolation of peripheral blood PMN: Male Sprague-Dawley rats (250-300 g) were anesthetized as above and, via cardiac puncture, 8 mL of blood was drawn into a syringe containing 2 mL anticoagulant citrate dextrose solution (Baxter, Deerfield, IL). Leukocyte rich plasma was obtained from the blood using dextran sedimentation. Red blood cells were lysed using sterile water and PMN were purified using Histopaque 1077 (Sigma-Aldrich Canada, Oakville, ON) to remove the remaining erythrocytes and mononuclear cells. Purified PMN were resuspended in M199 and used immediately. In further experiments PMN were fixed by incubation in paraformaldehyde 3% for 15 minutes or, alternatively, by incubation in glutaraldehyde 0.025 % for 30 minutes.

2.3.6   CD11b expression on PMN: To confirm that this very low concentration of gluteraldehyde preserves the extracellular domains of PMN CD11b [172] freshly isolated PMN and gluteraldehyde-fixed PMN were incubated with mouse anti-rat CD11b R-PE conjugated antibody (Biosource, Camarillo, CA) or non-specific mouse antibody (IgG negative control, Biosource) 30 μL/mL for 30 minutes. Cells were washed with PBS, fixed with paraformaldehyde 3%, and read using a flow cytometer (EPICS XL-MCL, Beckman Coulter, Miami, FL).

2.3.7   Co-culture of PMN and cardiomyocytes: After 24 hours of cardiomyocyte incubation 50,000 freshly isolated PMN were added to each well of cardiomyocytes

(ratio of 10 PMN per cardiomyocyte) in the 96 well laminin-coated plates for co-culture experiments. During off-line analysis of captured video sequences, we viewed all cardiomyocytes throughout a contraction. To be counted as adherent, PMN had to move with the contracting cardiomyocyte and maintain a contact relative location on the cardiomyocyte membrane during contraction.

2.3.8 ICAM-1 cross-linking: Following previously reported methods of cross-linking ICAM-1 and initiating intracellular signaling [153,173,174], we incubated cardiomyocytes with mouse anti-rat ICAM-1 1 µg/mL or control mouse non-specific IgG 1 µg/mL (Dako, Carpinteria, CA) for one hour. Cells were washed and then incubated with goat anti-mouse IgG 10 µg/mL (Transduction Laboratories, San Jose, CA) for 4 hours to cross-link the bound anti-ICAM-1.

2.3.9 Immunoflurescent imaging of Focal Adhesion Kinase (FAK): Cardiomyocytes were cultured on 8 well laminin coated slides (LAB-TEK, Naperville, IL). After 24 hours, ICAM-1 on cardiomyocytes was cross-linked as above. Cells were fixed and permeabilized with paraformaldehyde 3% for 20 minutes and Triton X-100 0.5 % for 5 minutes in Microtubule Stabilizing Buffer (MES 0.1 M, EGTA 2mM, $MgCl_2$ 2mM, and 4% polyethylene glycol 8000, Sigma-Aldrich). After blocking with PBS + 0.5% BSA for 60 minutes, rabbit anti-FAK 40 µg/ml (UBI, Lake Placid, NY) was added and incubated overnight at 4°C. After washing, Alexa fluor 488 labeled secondary goat anti-rabbit 10 µg/mL (Molecular Probes, Eugene, OR) was added for 45 minutes at room temperature.

Images were captured using a Noran Oz laser scanning confocal microscope with a high power objective lens (Nikon, Plan Fluor, 100X oil, NA: 1.30) and slit width of 10 µm. For visualizing the Alexa 488-labelled specimens, the sample was illuminated using 488 nm light from an Argon-Krypton laser. A high-gain photomultiplier tube collected the emission after it had passed through a 525/52 nm band pass filter. All parameters (laser intensity, gain, etc.) were left unchanged during the experiment and were set so that the level of photo-bleaching was negligible.

To obtain high resolution images within the cortical cytoplasm, multiple images were acquired along the Z-axis at 0.5 µm steps. Z-stack images were deconvolved using XCOSM [175] and a reconstructed image 2 µm from the top surface of each cardiomyocyte was evaluated. Fluorescence intensity of FAK staining was then measured as mentioned.

2.3.10 Cardiomyocyte Ca^{2+} transient: Cardiomyocytes (10^4) were cultured in each well of 8 well laminin coated slides. After ICAM-1 cross-linking or control, cardiomyocytes were incubated with 2 µM Fluo-4 (F14201, Lot 28A2-5, Molecular Probes) for 10 minutes, washed 3 times, and electrically stimulated as above. One hundred and fifty time series images were captured at 33 millisecond intervals during cardiomyocyte contraction using laser scanning confocal microscopy. To quantify coordination of simultaneity of intracellular Ca^{2+} release, three regions of interest were selected at the center and at each end of each cardiomyocyte. The mean intensity/pixel in each region of interest was measured from the beginning of contraction to the end of relaxation in each cardiomyocyte. The relative dispersion between the three regions of

interest was used to quantify heterogeneity. The time integral of Ca^{2+} intensity curve was used to quantify total Ca^{2+} release.

2.3.11 Data analysis: We tested for differences in fractional shortening and number of adherent PMN between control and treated groups of cardiomyocytes using ANOVA, choosing $p < 0.05$ as significant. When a significant difference was found we identified specific differences between groups using a sequentially rejective Bonferroni test procedure. Data are expressed as means $\pm$ standard error throughout.

2.4 Results

2.4.1 Uniform co-culture conditions: We conducted preliminary experiments to establish uniform co-culture conditions for the experiments in this study. Preliminary experiments demonstrated that, after 24 hours incubation, cardiomyocyte fractional shortening was 20.5±0.7 % (n=36). In the absence of PMN, fractional shortening did not significantly change following activation of quiescent cardiomyocytes using a 2 hour incubation with TNFα 20 ng/mL (BD Pharmingen, San Jose, CA) (91.3±4% of control, p=NS), interleukin IL-1β 20 ng/mL (Sigma-Aldrich) (91.1±6% of control, p=NS), or lipopolysaccharide 10 μg/mL (Sigma-Aldrich) (86.5±5% of control, p=NS). One hour after TNFα activation, the ratio of cardiomyocyte ICAM-1 to GAPDH mRNA increased from 0.091±0.08 to 0.361± 0.10. Similarly, following TNFα activation, ICAM-1 protein expression significantly increased (Figure 2.1).

When non-activated cardiomyocytes were co-cultured with freshly isolated PMN for 4 hours, fractional shortening did not change (20.7±1.2 %, n=36) (Figure 2.2A). However, TNFα-activated cardiomyocytes in co-culture with freshly isolated PMN did decrease fractional shortening. Based on the percentage of cardiomyocytes with normal morphology, the number of PMN adherent to each cardiomyocyte, and maximal contractile dysfunction (Figure 2.2) all subsequent experiments were conducted following a 4-hour co-incubation of TNFα-activated cardiomyocytes and freshly isolated PMN.

ICAM-1 protein expression of control and activated cardiomyocytes
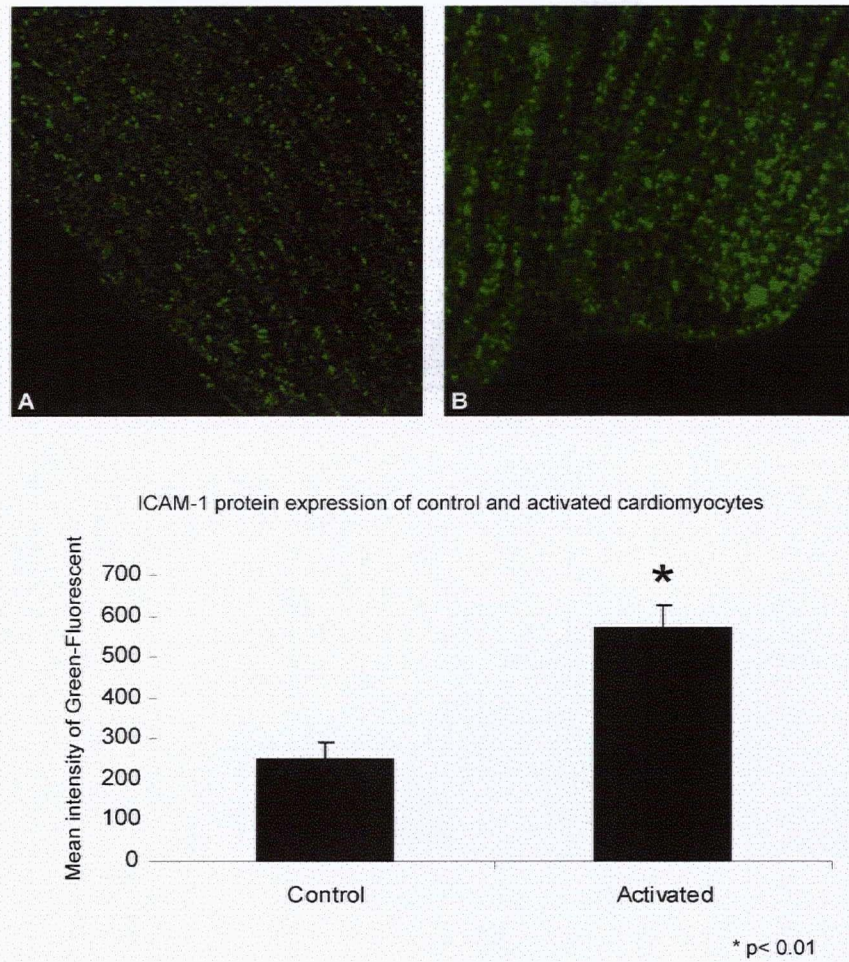
Figure 2.1   ICAM-1 protein expression on cardiomyocytes increases 4 hours after activation with TNFα (B) compared to non-activated controls (A), which was significantly different (*, p<0.01) (bottom panel).
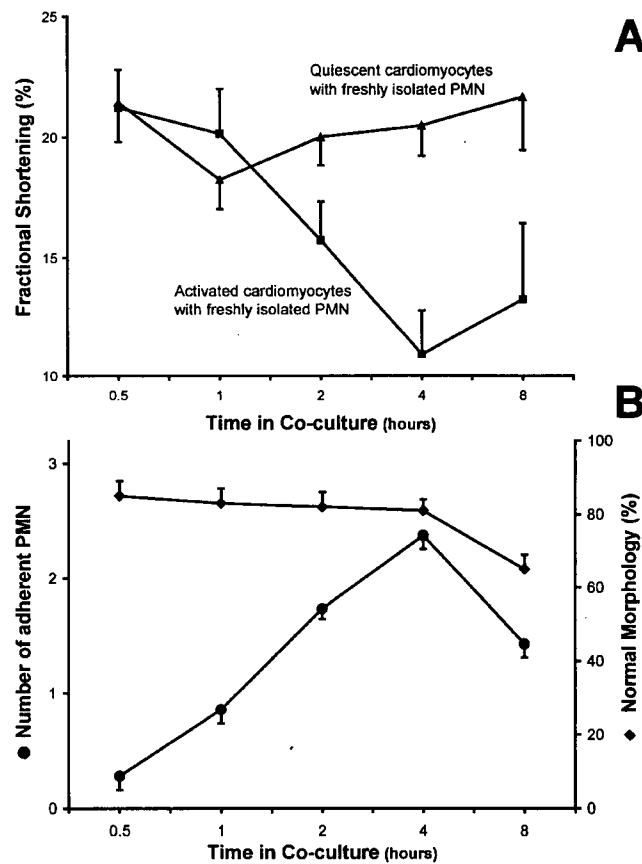
Figure 2.2   Preliminary experiments were used to determine the conditions for all further experiments. Panel A shows that PMN in co-culture with quiescent cardiomyocytes (Triangle) did not alter fractional shortening while PMN in co-culture with activated cardiomyocytes (which induces cardiomyocyte ICAM-1 expression) significantly reduces fractional shortening by 4 hours of co-culture (Squares). Panel B shows that the number of PMN adherent to activated cardiomyocytes increases to a maximum at 4 hours and cardiomyocyte viability remains high until 4 hours in co-culture. Based on these results further experimental measurements used PMN in co-culture with TNFα-activated cardiomyocytes for 4 hours.

2.4.2 Adherent PMN reduce cardiomyocyte fractional shortening: When activated cardiomyocytes were co-cultured with freshly isolated PMN, fractional shortening decreased significantly in TNFα (-34.2±5%, $p<0.001$), IL-1β (-48.6±3.2%, $p<0.001$) and LPS (-23.1±3.9%, $p<0.001$) treated cardiomyocytes. Average PMN adhesion increased from 1.1±0.2 PMN per cardiomyocyte in the non-activated cardiomyocytes to 2.7±0.2, 1.4±0.1, 1.9±0.2, in the TNFα, IL-1β, and LPS treated cardiomyocytes respectively ($p<0.05$ for each). Fractional shortening of cardiomyocytes in co-culture with PMN decreased by -2.8±0.3% per adherent PMN ($p<0.001$) (Figure 2.3A).

Adherent PMN may have contributed to decreased cardiomyocyte contractility simply by release of reactive oxygen intermediates or other mediators in close proximity to the cardiomyocyte [164]. Alternatively, adhesion itself may have contributed. To help distinguish between these two possibilities we fixed PMN before co-culture. First, PMN were fixed with paraformaldehyde 3% for 15 minutes. After washing five times, fixed PMN were co-cultured with cardiomyocytes. Paraformaldehyde-fixed PMN decreased fractional shortening by 27±2% compared to control ($p<0.05$), which is comparable to the effect of freshly isolated PMN. Gluteraldehyde-fixed PMN similarly decreased cardiomyocyte fractional shortening by 25±4% ($p<0.05$) compared to control. The relationship between the number of adherent PMN versus decrease in fractional shortening was preserved (Figure 2.3B) suggesting that this effect was due to adhesion of PMN to cardiomyocytes. To exclude the possibility that gluteraldehyde fixation may have   prevented   binding   by   altering   the
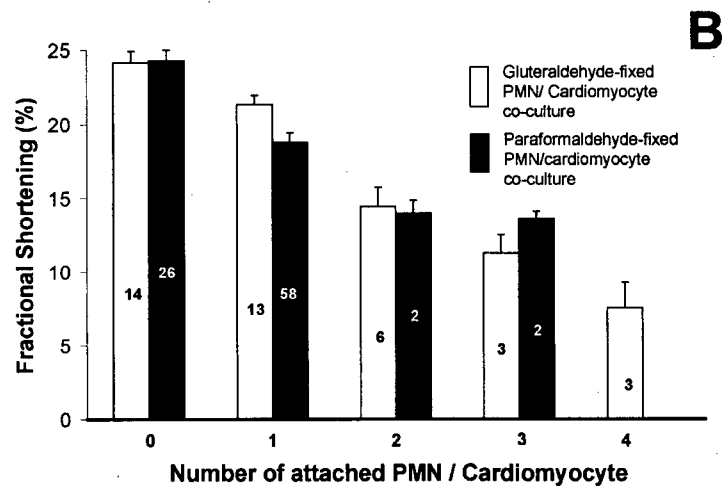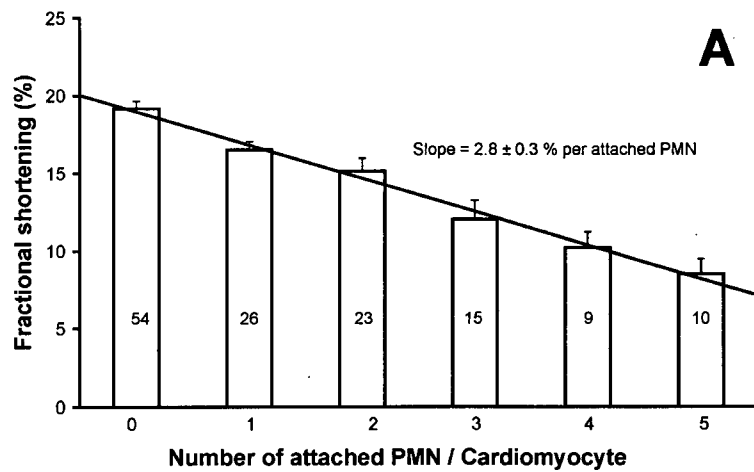
Figure 2.3   Panel A illustrates that fractional shortening of cardiomyocytes decreased as the number of attached PMN per cardiomyocyte increased. Panel B illustrates that this same effect was present even when PMN were first killed and fixed using either gluteraldehyde or paraformaldehyde. These results implicate PMN-cardiomyocyte binding as a key step in mediating decreased cardiomyocyte fractional shortening. Numbers within columns indicate the number of cardiomyocytes measured.

extracellular domain of CD11b on PMN we used a low concentration of glutaraldehyde

and confirmed unchanged CD11b expression on PMN using flow cytometry (Figure 2.4).
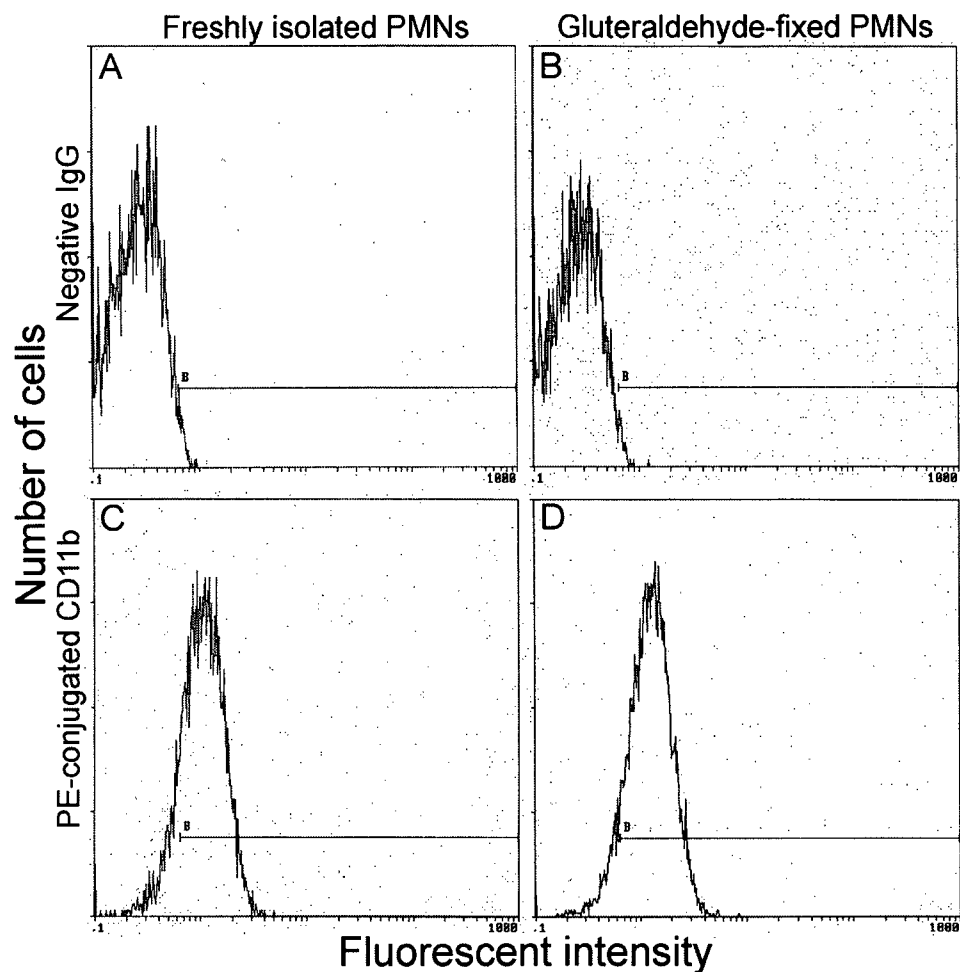
Figure 2.4   Flow cytometery of freshly isolated (left hand panels) and gluteraldehyde-fixed (right hand panels) PMN is shown. Panel A shows results for freshly isolated PMN (identified from side scatter – back scatter plots) incubated with non-specific IgG. Panel C shows results for freshly isolated PMN, incubated with antibody to CD11b. Increased fluorescent intensity specific for CD11b is seen. Panel B shows results for gluteraldehyde-fixed PMN incubated with non-specific IgG. In comparison panel D demonstrates the same increase in fluorescent intensity specific for CD11b as seen with freshly isolated PMN (panel C).

2.4.3 ICAM-1 binding mediates decreased cardiomyocyte contractility: Antibody to ICAM-1 and antibody to CD-18 (Pharminogen), to block this important PMN-expressed ligand of ICAM-1, prevented the PMN-induced decrease in cardiomyocyte fractional shortening (Figure 2.5A). The average number of PMN adherent to each TNFα–activated cardiomyocyte was also reduced by antibody to ICAM-1 and antibody to CD-18 (control 2.7±0.2, antibody to ICAM-1 1.2±1.0, antibody to CD-18 1.1±1.0 adherent PMN per cardiomyocyte). Thus, the contractile effect of PMN binding involves binding to cardiomyocyte ICAM-1.

To demonstrate that PMN binding, and the decrease in contractility, in co-culture with gluteraldehyde-fixed PMN were still ICAM-1 - dependent, we repeated these experiments with and without antibody to ICAM-1. The number of adherent gluteraldehyde-fixed PMN was reduced from 1.8 ± 0.2 to 0.58 ± 0.1 by antibody to ICAM-1 and the decrease in fractional shortening was prevented (fractional shortening in the presence of PMN without anti-ICAM-1 16.8 ± 1.1%, with anti-ICAM-1 22.0 ± 1.1%, p<0.05).

To determine whether ICAM-1 binding itself can cause decreased contractility we used cross-linking antibodies to ICAM-1, in the absence of PMN. ICAM-1 cross-linking decreased fractional shortening by 36±3% compared to control groups at 4 hours (Figure 2.5B). In contrast, replacement of anti-ICAM-1 antibodies with nonspecific IgG, followed by addition of cross-linking antibodies, did not change fractional shortening compared to control.

A

Fractional Shortening (%)

| Non-activated cardiomyocytes | Non-activated cardiomyocyte-PMN co-culture | TNF-activated cardiomyocyte-PMN co-culture | anti-ICAM-1 + TNF-activated cardiomyocyte-PMN co-culture | anti-CD-18 + TNF-activated cardiomyocyte-PMN co-culture |

(bars labelled 36, 36, 36 (*), 24, 8)

B

Fractional Shortening (%)

| Control | IgG Control | ICAM-1 cross-linked | ICAM-1 cross-linked + Cytochalasin D | ICAM-1 cross-linked + Latrunculin A |

(bars labelled 46, 18, 37 (*), 11, 37)

Figure 2.5   Panel A shows that the decrease in cardiomyocyte fractional shortening in the TNF-activated cardiomyocyte-PMN co-culture group (*, $p<0.05$) was prevented by either antibody to ICAM-1 or antibody to its important ligand, CD18. Panel B demonstrates that, even in the absence of PMN, ICAM-1 cross-linking reduces cardiomyocyte fractional shortening (*, $p<0.05$). This effect is prevented by disruption of the actin cytoskeleton, either by cytochalasin D or latrunculin A.

2.4.4   ICAM-1 cross-linking alters the cortical cytoskeleton: ICAM-1 is connected to cytoskeletal proteins [123,151,152,165]. To test for involvement of the cortical cytoskeleton following ICAM-1 cross-linking we examined the distribution of the actin cytoskeleton-associated protein FAK within cardiomyocytes. Immunofluorescent imaging of FAK at 2 μm below the cardiomyocyte surface demonstrated increased cytoskeleton-associated FAK staining in ICAM-1 cross-linked cardiomyocytes compared to controls (Figure 2.6).

2.4.5   Functional role of the cardiomyocyte actin cytoskeleton: To test the hypothesis that the actin cytoskeleton is involved in signaling pathways that lead to decreased cardiomyocyte contractility induced by ICAM-1 binding, we preincubated cardiomyocytes with cytochalasin D 10 μM, an actin depolymerizing agent, for 2 hours. Control cardiomyocyte fractional shortening was not altered by this concentration of cytochalasin D (106±10% of control fractional shortening, n=39 vs. n=60 controls) confirming previous observations that these concentrations of cytochalasin D did not have a measurable effect on the function of sarcomeric F-actin [176]. Cytochalasin D prevented the decrease in cardiomyocyte contractility due to ICAM-1 cross-linking (Figure 2.5B). We repeated these experiments, disrupting the actin cytoskeleton in an independent way using Latrunculin A (Calbiochem, San Diego, CA) 10 μM, an agent that sequesters monomeric actin and inhibits elongation of actin filaments [177,178]. Latrunculin A by itself did not significantly alter cardiomyocyte fractional shortening (111±10% of control fractional shortening, n=29 vs n=22 controls). Again, latrunculin A prevented the decrease in cardiomyocyte contractility due to ICAM-1 cross-linking (Figure 2.5B).

Similarly, in experiments of PMN co-cultured with activated cardiomyocytes, cytochalasin D and latrunculin A prevented the PMN-induced decrease in cardiomyocyte fractional shortening (control 20.5±0.6%, cardiomyocyte-PMN co-culture 13.6±0.8%, cytochalasin D 17.5±1.2% and latrunculin A 19.9±2.7%) but did not alter the number of PMN adherent to cardiomyocytes (1.6±0.4, 1.8±0.5, and 1.3±0.8 in control, Cytochalasin D, and Latrunculin A respectively).

Control cardiomyocyte

ICAM-1 cross-linked cardiomyocyte
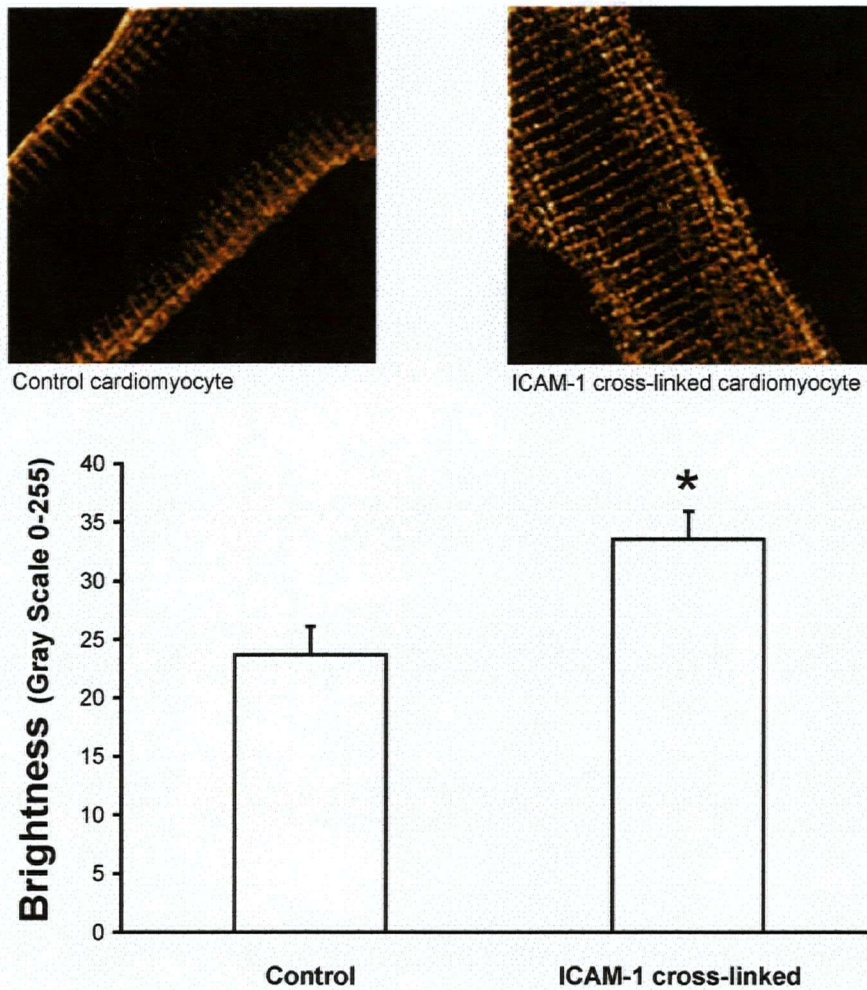
Figure 2.6   Top panels show example FAK staining in control (top left hand panel) and ICAM-1 cross-linked cardiomyocytes (top right hand panel). The bottom panel shows average results for all cardiomyocytes (n=64 for each group from 6 experiments) indicating that ICAM-1 cross-linking increases FAK expression associated with the cortical actin cytoskeleton 2 μm below the cardiomyocyte surface (*, $p < 0.05$).

2.4.6 Possible downstream signaling pathways: Rho family proteins (small G proteins) are associated with the actin cytoskeleton and regulate both cytoskeletal reorganization and gene expression. To investigate the role of these pathways we used Fusadil (HA-1077, Sigma-Aldrich), an inhibitor of Rho-kinase, in ICAM-1 cross-linked cardiomyocytes. HA-1077 50 μM completely prevented ICAM-1 binding-induced decreases in cardiomyocyte fractional shortening (Figure 2.7) suggesting that this actin cytoskeleton-associated signaling pathway mediates ICAM-1 binding-induced decreases in cardiomyocyte fractional shortening.

FAK activation leads to activation a series of proteins and pathways, including MAPK pathways in other cell lines [179]. To investigate the role of these pathways on contractility of ICAM-1 cross-linked cardiomyocytes, we treated ICAM-1 cross-linked cardiomyocytes with the ERK1/2 inhibitor, PD98059 10 μM (New England BioLabs Ltd. Mississauga, OA, Canada) 20 μM. ERK1/2 inhibition had no effect on the ICAM-1-induced decreases in cardiomyocyte fractional shortening (Figure 2.7) suggesting that this signaling pathway was not directly involved.
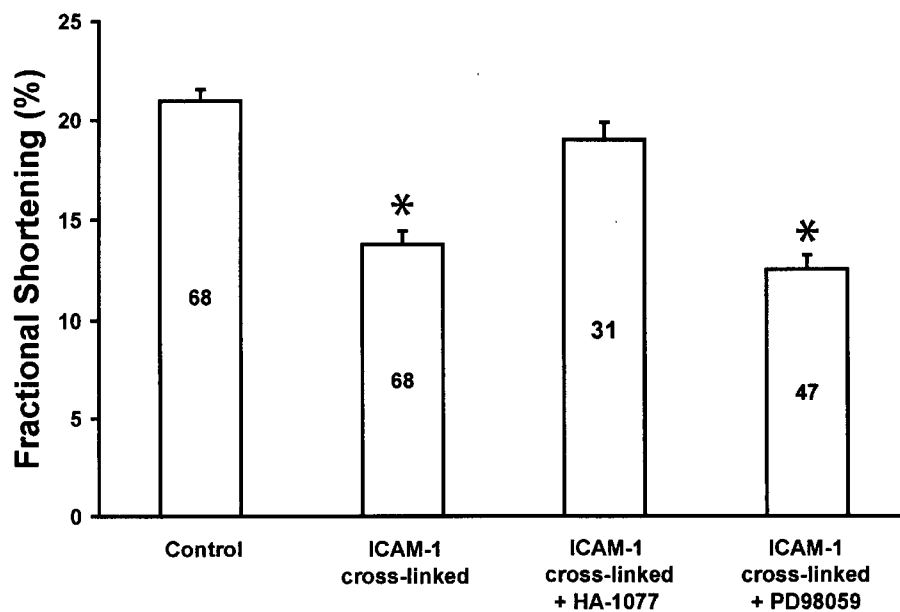
Figure 2.7   The effect of ICAM-1 cross-linking on fractional shortening (*, p<0.05 compared to Control) is prevented by the Rho A inhibitor (HA-1077) but not by the MAPK inhibitor (PD98059).

2.4.7 ICAM-1 activation changes the pattern of Ca^{2+} release: To better understand how ICAM-1 binding could alter contractility we measured the cardiomyocyte intracellular calcium transient. ICAM-1 cross-linking changed the pattern of Ca^{2+} release in contracting cardiomyocytes. Ca^{2+} release changed from homogenous and synchronized in control cardiomyocytes to a focal starting point propagating wave in ICAM-1 cross-linked cardiomyocytes (Figure 2.8). The focal starting point propagating wave occurred in 86±3% of ICAM-1 cross-linked cardiomyocytes compared to 31±7% of control cardiomyocytes ($p<0.05$). As a result, ICAM-1 cross-linking increased the duration of the Ca^{2+} transient (Figure 2.8A). The slope over the most linear middle 50% of the decay curve was decreased to $1.53 \pm 0.14 \times 10^{-4}$ in ICAM-1 cross-linked cardiomyocytes from $2.94 \pm 0.24 \times 10^{-4}$ in control cardiomyocytes ($p<0.0001$). Heterogeneity of Ca^{2+} release increased in the ICAM-1 cross-linked group as indicated by an increase in relative dispersion in ICAM-1 cross-linked cardiomyocytes (Figure 2.8B). Total Ca^{2+} release (integral of Ca^{2+} release in Figure 2.8A) did not differ significantly in ICAM-1 cross-linked cardiomyocytes versus controls.

2.5 Discussion

The key finding of this study is that ICAM-1 binding decreases cardiomyocyte contractility. ICAM-1 binding by freshly isolated PMN, by PMN fixed in either paraformaldehyde or gluteraldehyde, and ICAM-1 binding using cross-linking antibodies, all caused a significant decrease in cardiomyocyte contractility. The actin cytoskeleton plays a central role. Evidence for this includes increased immunofluorescent staining of cortical actin cytoskeleton - associated FAK (2 μm below the cell surface) after ICAM-1 cross-linking. The decrease in cardiomyocyte contractility due to ICAM-1 cross-linking could be prevented by cytochalasin D and, using an alternative strategy, by latrunculin A. Furthermore, inhibition of the cytoskeleton - associated Rho kinase pathway also prevented decreased contractility due to ICAM-1 cross-linking. The ultimate mechanism of loss of contractility due to ICAM-1 binding appears to be loss of the normal coordination of intracellular Ca^{2+} release. Even though total intracellular Ca^{2+} release during a single contraction did not change significantly, the release did not occur in the normal coordinated manner throughout the entire cell over a short period of time, so that fractional shortening decreased.

ICAM-1 expression on activated cardiomyocytes [107,180,181] plays an important role in ICAM-1 - CD18 dependent adhesion of PMN to cardiomyocytes [107,164,171]. In a whole animal model, antibody to CD18 protects against myocardial damage and dysfunction following ischemia-reperfusion [127,182] and reduces PMN adherence within the heart. ICAM-1 and CD18 deficient mice demonstrate a marked
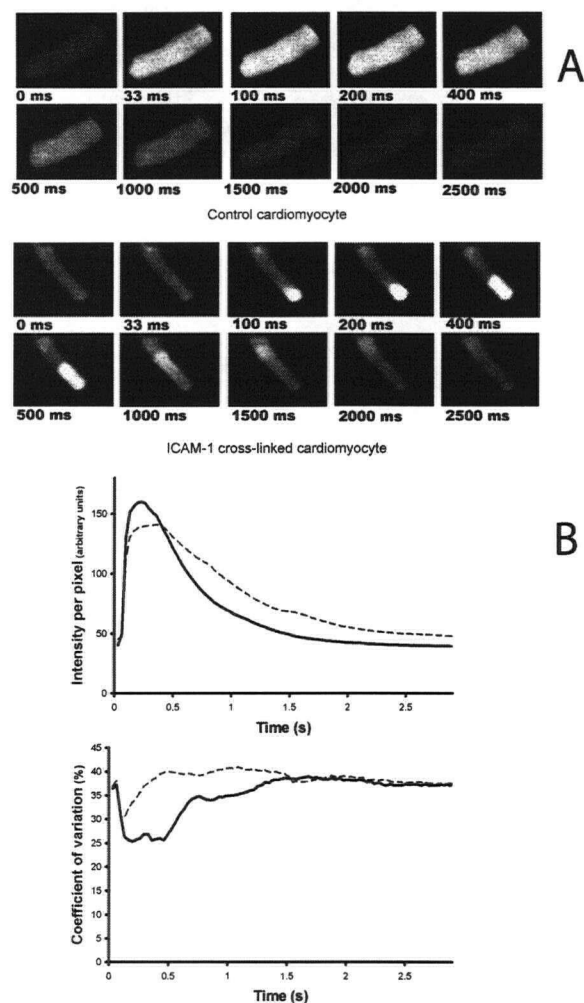
Figure 2.8   The top panels illustrate in typical examples that Ca^{2+} release and reuptake in control cardiomyocytes is rapid whereas Ca^{2+} release in ICAM-1 cross-linked cardiomyocytes is much slower, with the appearance of a wave of Ca^{2+} release moving along the length of the cardiomyocyte. Average results for all cardiomyocytes are shown in the bottom panel for control cardiomyocytes (n=37, solid line) and for ICAM-1 cross-linked cardiomyocytes (n=67, dashed line) demonstrating increased dispersion, or heterogeneity, of calcium release in ICAM-1 cross-linked cardiomyocytes. The coefficient of variation is particularly increased in ICAM-1 cross-linked cardiomyocytes for the first 1.5 seconds after cardiomyocyte electrical stimulation.

reduction in PMN accumulation and myocardial necrosis after acute ischemia-reperfusion [183]. Activated PMN in vitro can cause dysfunction and kill cardiomyocytes within minutes via production of reactive oxygen intermediates [163,164]. However, this short time course and the cardiomyocyte necrosis caused by highly activated PMN are not fully consistent with in vivo observations of the prolonged time course of ischemia/reperfusion-induced myocardial stunning [103,184] and of sepsis [38,55,66,185]. It is useful to note that PMN adhesion to human umbilical vein endothelial cells following anoxia/reoxygenation demonstrate both early effects (minutes) mediated by reactive oxygen intermediates and late effects (hours) involving other pathways [186] including the actin cytoskeleton [187]. In these cells PMN-induced cytoskeletal changes are inhibited by antibodies to ICAM-1 [173]. Thus, our results are consistent with, and extend, previous studies.

This novel mechanism of decreased cardiomyocyte contractility implicates the cytoskeleton in maintaining normal coordination of intracellular Ca^{2+} release and, hence, normal contractility. Ca^{2+}-induced Ca^{2+} release from the sarcoplasmic reticulum triggered by Ca^{2+} influx via dihydropyridine receptors is the main regulator of cardiomyocyte contractility [188,189]. The novel finding that impaired coordination of Ca^{2+}-induced Ca^{2+} release is an additional mechanism regulating cardiomyocyte contractility may have broad implications in myocardial processes involving inflammation and up-regulation of ICAM-1 expression on cardiomyocytes. It may play a role in disease processes which involve leukocyte infiltration in the heart including ischemia reperfusion, inflammatory cardiomyopathy, and septic myocardial dysfunction.

Furthermore, disease and repair processes that alter extracellular matrix constituents so that increased ICAM binding occurs, may also be implicated. For example, changing extracellular matrix composition and ICAM-1 expression also occur during normal embryogenesis [190,191].

PMN and macrophages have previously been shown to bind ICAM-1 expressed on cardiomyocytes [59,107,164]. In many of the studies of the interaction between highly activated PMN and cardiomyocytes, ICAM-1 mediates binding and activated neutrophils cause cardiomyocyte cell death by release of reactive oxygen intermediates. The effect of non-activated neutrophils and ICAM-1 binding by itself has not previously been examined. However, Simms et al. [59] reported that ICAM-1 mediated the effects of macrophage/monocyte binding on decreased cardiomyocyte contractility. Recently, Raeburn, et al. [160] report that ICAM-1 and VCAM-1 mediate endotoxemic myocardial dysfunction independent of neutrophil accumulation in the myocardium. While the earlier results implicate ICAM-1 largely as a mediator of tethering of cytotoxic neutrophils to cardiomyocytes [107,164], these recent studies [59,160] suggest a potential alternative role for ICAM-1 binding.

Our current results identify and illuminate this potential alternative role. Binding of freshly isolated PMN to cardiomyocytes causes a decrease in contractility without cardiomyocyte cell death, presumably because the PMN are not highly activated and releasing reactive oxygen intermediates and other damaging mediators. To confirm this, and to exclude the possibility that PMN release damaging mediators as a result of PMN

activation during the isolation procedure, we repeated these experiments in both paraformaldehyde and gluteraldehyde - fixed PMN. Surprisingly, even when PMN are killed and fixed in two different ways, to prevent further activation and release of mediators, PMN still cause a dose-dependent decrease in cardiomyocyte contractility (Figure 2.3). The importance of ICAM-1 binding by itself in causing decreased contractility was then confirmed in a leukocyte-free condition where ICAM-1 cross-linking antibodies were applied - which results in a decrease in cardiomyocyte contractility.

This decrease in contractility clearly involves the cortical actin cytoskeleton. First, utilizing 3D reconstruction techniques to examine the cortical region of cardiomyocytes, we found that cytoskeletal-associated FAK expression increases following ICAM-1 binding. Furthermore, inhibition of normal cytoskeletal function using either cytochalsin D or latrunculin A prevented ICAM-1 binding-induced decreases in cardiomyocyte contractility. Finally, inhibition of the actin cytoskeleton-associated Rho kinase signaling pathway also prevented ICAM-1 binding induced decrease in contractility.

We found that the decrease in contractility was due to loss of simultaneity of intracellular Ca^{2+} release. One key coordinating mechanism of Ca^{2+}-induced Ca^{2+} release is colocalization of dihydropyridine receptors on external or T-tubule sarcolemma with ryanodine receptors on the sarcoplasmic reticulum [192]. This geometric arrangement is instrumental in allowing the relatively small intracellular Ca^{2+} flux introduced via dihydropyridine receptors to trigger Ca^{2+}-induced Ca^{2+} release by ryanodine receptors.

We postulate that disruption of this coordinating mechanism would result in increased heterogeneity of Ca^{2+} release by the sarcoplasmic reticulum. That is, if dihydropyridine receptors do not cause coordinated induction of Ca^{2+}-induced Ca^{2+} release by ryanodine receptors, then simultaneous contraction throughout the cardiomyocyte would be impaired. In the absence of normal coupling, a stimulus sufficient to cause local sarcoplasmic release of Ca^{2+} would then cause further Ca^{2+}-induced Ca^{2+} release by adjacent sarcoplamic reticulum ryanodine receptors. If true, this would take the form of a wave of contraction travelling from the initial site along the cardiomyocyte. Indeed, this is what we observed with ICAM-1 cross-linking (Figure 2.8). Thus, we think that it is reasonable to postulate that the actin cytoskeleton plays a key role in maintaining coordination of cardiomyocyte contractility, possibly by contributing to maintainance of normal co-localization of dihydropyridine receptors and ryanodine receptors.

Identification of this novel pathway, which may contribute to myocardial dysfunction during intramyocardial inflammation (e.g., following ischemia-reperfusion, in inflammatory cardiomyopathy, during orthotopic heart transplant rejection, and during sepsis-induced myocardial dysfunction), is clearly only one of many pathways involved. Indeed, ICAM-1 binding may be a component of some of these alternative pathways such as apoptosis [193] and reactive oxygen intermediate production [194].

It is interesting to speculate when and why such a mechanistic pathway may confer an evolutionary advantage. Is this mechanism of regulation of cardiomyocyte contractility just pathological loss of normal coordination or is there some benefit? This novel

pathway would be evoked during inflammation and subsequent resolution and repair or conceivably even during embryogenesis. We speculate that it may be beneficial to down-regulate contractility for a period of time during these processes. This ICAM-1 and cytoskeleton-mediated pathway could provide this mechanism.

In summary, we have identified a novel pathway and mechanism of regulation of cardiomyocyte contractility. While we have demonstrated that this pathway plays a role in neutrophil-cardiomyocyte interaction, it may play a role in the interaction of the cardiomyocyte with other inflammatory cells and potentially even with the extracellular matrix. Thus, this novel mechanism of decreased contractility may have much broader implications.

In the next chapter I will investigate the role of ICAM-1 in an in vivo model of endotoxemia to test the importance of ICAM-1 presentation and activation in vivo. I will also investigate the presence of inflammatory cells in the septic heart to test this hypothesis that whether inflammatory cell including PMNs can infiltrate and attach to the cardiomyocyte ICAM-1 receptors using their CD11/CD18 receptors.

Chapter-3

Cardiac ICAM-1 mediates leukocyte-dependent decreased ventricular contractility in endotoxemic mice.

3.1   Abstract

Binding of ICAM-1 expressed on isolated cardiomyocytes decreases cardiomyocyte contractility by altering the intracellular Ca^{2+} transient. To test the hypothesis that signaling via ICAM-1 contributes to decreased left ventricular contractility in an in vivo model of sepsis, C57B6 wild-type mice and ICAM-1 knock out mice were treated with intraperitoneal lipopolysaccharide (LPS) then left ventricular contractility was measured 6 hours later using a volume-conductance micromanometer catheter. In C57B6 wild-type mice LPS injection significantly increased cardiac ICAM-1 expression and decreased left ventricular contractility (end-systolic elastance, Ees decreased 58 ± 4%, $p<0.05$, [dP/dt_{max}]/EDV decreased 60 ± 6%, $p<0.05$). Cyclophosphamide pretreatment to decrease leukocyte count prevented the LPS-induced decrease in contractility. In ICAM-1 knock out mice LPS did not decrease any measure of contractility. We produced chimeric mice lacking ICAM-1 expression in bone marrow-derived cells (M-) and/or lacking ICAM-1 expression in the heart and other tissues (H-). LPS did not decrease left ventricular contractility in M+/H- mice but decreased contractility in M+/H+ and M-/H+ mice to the same extent as in C57B6 wild-type mice implicating the importance of cardiac ICAM-1. We conclude that signaling via cardiac ICAM-1 is necessary to mediate leukocyte-dependent decreases of left ventricular contractility in endotoxemic mice.

3.2 Introduction:

Sepsis is responsible for more than 200,000 deaths annually in North America [1]. Myocardial dysfunction, caused by the systemic inflammatory response of sepsis, contributes to multi-organ dysfunction and death in these patients [195]. When the degree of myocardial dysfunction is substantial, cardiac output cannot be increased sufficiently to maintain an adequate systemic arterial pressure in the face of the decreased systemic vascular resistance of septic shock. Indeed high versus low cardiac output during septic shock distinguishes survivors from non-survivors [16]. Leukocytes are a component of the systemic inflammatory response of sepsis and have been implicated in contributing to myocardial dysfunction in experimental models both in vivo [65,196] and in vitro [59,60,107,197].

Leukocytes decrease isolated cardiomyocyte contractility in vitro by binding to ICAM-1 expressed on the cardiomyocytes[59,60,107] and by release of reactive oxygen intermediates from the activated leukocytes [107,163]. In addition, even non-activated leukocytes or ICAM-1 cross-linking antibodies can decrease contractility by binding ICAM-1 expressed on cardiomyocytes [59,60]. ICAM-1 binding then mediates decreased cardiomyocyte contractility by signaling via the cortical actin cytoskeleton, which leads to increased heterogeneity of intracellular Ca^{2+} release and decreased cardiomyocyte contractility [60]. Whether ICAM-1 binding plays an important role in development of myocardial dysfunction in vivo has not been demonstrated.

Accordingly, we first determined the extent of increased cardiac ICAM-1 expression using a lipopolysaccharide (LPS) injection model of systemic inflammation in mice.

Next, we tested the hypothesis that myocardial dysfunction occurs in this model and, further, we determined whether the degree of myocardial dysfunction is prevented by decreasing the peripheral blood leukocyte count. We then determined whether ICAM-1 expression is also necessary for the development of myocardial dysfunction in this model, using ICAM-1 knock-out mice. Finally, to determine if cardiac ICAM-1 expression is necessary for myocardial dysfunction (versus ICAM-1 expressed on bone marrow-derived cells), we developed chimeric mouse models lacking ICAM-1 expression in bone marrow-derived cells and/or lacking ICAM-1 expression in the heart and other tissues. We found that activation of cardiac ICAM-1 plays a key role in mediating decreased left ventricular contractility in this whole animal model of systemic inflammation.

3.3 Material and Methods

This study was approved by the University of British Columbia Animal Care Committee and adheres to Canadian and U.S.A. National Institutes of Health guidelines for animal experimentation.

3.3.1 Experimental preparation: Mice, C57B6 wild-type and C57B6/J-ICAM [tml-jcgr] knock-out (ICAM-1 knock out, Jackson Laboratory, Bar Harbor, ME) weighing 25-30 g, were given intraperitoneal injection of purified lipopolysaccharide (LPS, E. coli strain 01 II: B4, Sigma, St. Louis, MO) 40 mg/kg or the same volume of normal saline. Six hours after LPS injection, mice were anesthetized using ketamine (75 mg/kg) and xylazine (10 mg/kg); total volume 0.2 mL, injected subcutaneously. Anesthesia effectiveness was confirmed throughout the procedure. Tracheal intubation was performed through a 1 cm midline neck incision and mice were ventilated (Mouse Ventilator model 687, Harvard Instruments, Holiston, MA) at 120 breaths/min with a 200 µL tidal volume. A substernal transverse incision was made to expose the apical portion of the heart and inferior vena cava. The left ventricle was punctured using a 27 gauge needle approximately 1 mm lateral to the interventricular septum. Then a number 2 French volume-conductance micromanometer catheter (Mikro-tip SPR-838, Millar Instruments Inc., Houston, TX) was inserted into the left ventricle. Correct placement of the catheter was determined by checking pressure-volume loops for vertical isovolumic phase traces and characteristic diastolic and systolic trajectories. Pressure-volume data were recorded at steady state and the inferior vena cava was occluded for 3-5 seconds while pressure-volume data were

again recorded. The heart was excised and frozen (isopentane in liquid nitrogen) or fixed

(10% formalin) for further histopathology and morphometry measurements.
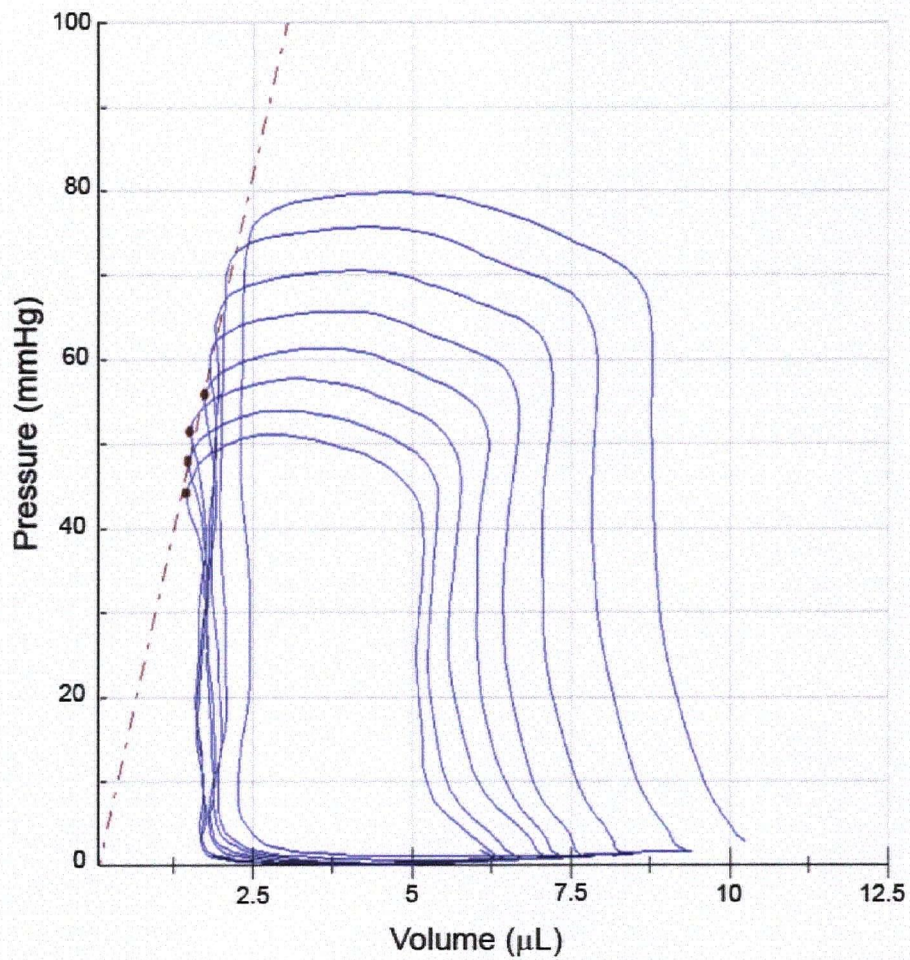
Figure 3.1   Pressure-volume measurements of multiple heart beats during a vena-caval occlusion are illustrated. A best fit line to the end-systolic points of these beats (red line) is the end-systolic pressure-volume relationship. The slope of the end-systolic pressure volume relationship is end-systolic elastance, Ees; a preload and afterload independent measure of left ventricular contractility.

3.3.2 Left ventricular contractility and cardiac function: Left ventricular contractility and other measures of ventricular function were determined from pressure-volume measurements using Pressure-Volume Analysis software (PVAN 2.9, Millar Instruments Inc., Houston, TX). Six to ten pressure-volume loops during a vena cava occlusion were sampled and used to measure end-systolic elastance (Ees), which is the slope of the end-systolic pressure-volume relationship (Figure 1). Ees is an ejection phase measure of left ventricular contractility which, among many others, is least sensitive to changes in preload and afterload [198] anticipated to occur in this model of sepsis. The volume axis intercept, Vd, was considered zero volume for the steady-state measurement of end-diastolic volume (EDV) and end-systolic volume (ESV). Pressure-volume loops measured during steady-state conditions were used to measure the maximum rate of change of intraventricular pressure during isovolumic systole divided by EDV, $[dP/dt_{max}]/EDV$, which is a sensitive isovolumic phase measure of left ventricular contractility [199]. Steady state pressure-volume loops were also used to calculate ejection fraction as the difference between EDV and ESV divided by EDV, which is a further measure of cardiac function. End-systolic pressure during steady state was used as a measure of systemic arterial pressure afterload.

3.3.3 The role of leukocytes: To determine whether leukocytes contributed to decreased left ventricular contractility and function in this animal model we increased leukocyte count by pretreating C57B6 wild-type mice with GCSF and, alternatively, we decreased leukocyte count by pretreating C57B6 wild-type mice with cyclophosphamide.

Mice were then injected with LPS and left ventricular contractility and function were measured as above and compared to C57B6 wild-type mice treated with LPS.

To increase leukocyte count, mice received GCSF (Filgrastim 300 μg/ml vial, Neupogen) 120 μg/kg subcutaneously twice daily for four days and were then rested for 3 days. This time course was determined from preliminary experiments where we measured the ratio of CD11b expression to total actin content as an indicator of bone marrow cell maturation. Compared to non-treated controls we found a significant decrease in this ratio immediately after the 4 day GCSF treatment. Following 3 days of rest, the ratio of CD11b expression to total actin content returned towards normal in the GCSF-treated mice indicating that 3 days of rest after GCSF injection was necessary to approximate normal bone marrow cell maturation.

To decrease leukocyte count, mice received cyclophosphamide (Bristol Laboratories, Montreal, Canada) 150 mg/kg intraperitoneal daily for 2 days and were then rested for 3 days. This time course was determined from preliminary experiments and the literature which indicated that the nadir of the peripheral blood leukocyte count occurred 3 days after the last cyclophosphamide injection [200-202].

To confirm the effect of GCSF and cyclophosphamide, we measured total leukocyte count and polymorphonuclear leukocyte (neutrophil) count in peripheral blood and in bone marrow using a Cell-Dyn 3700 counter (Abbott Diagnostic Division, Abbott, IL).

3.3.4 Chimeric models: We reasoned that any difference in LPS effect found in ICAM-1 knock-out mice could either be due to loss of cardiac ICAM-1 expression or due to loss of ICAM-1 expression on blood borne bone marrow-derived cells transiting the heart. To distinguish between these two possibilities, and thereby specifically implicate cardiac ICAM-1 expression, we designed three different chimeric mouse models; ICAM-1 expressed on marrow-derived cells and on heart cells (M+/H+), ICAM-1 expressed on marrow-derived cells but not on heart cells (M+/H-), and ICAM-1 not expressed on marrow-derived cells but expressed on heart cells (M-/H+).

We developed these chimeric mice as follows. To increase the number of progenitor cells in donors, C57B6 wild-type and ICAM-1 knock out mice were first pretreated with GCSF as described above. Bone marrow from femurs and tibias of 8 to 10 GCSF-treated mice (donors) was extracted and separated in PBS plus ACD 10% (C3821 Acid Citrate-Dextrose solution, Sigma), washed 4 times in PBS plus ACD and filtered. After a final wash in PBS, cells were suspended in normal saline. In this bone marrow concentrate the total leukocyte count was $12.2 \pm 1.2 \times 10^9$ /L, the fraction of granulocytes was $94.8 \pm 0.3\%$, and the fraction of lymphocytes was $3.5 \pm 0.1\%$. To suppress inflammatory cell progenitors in recipient mice, C57B6 wild-type and ICAM-1 knock out mice were first pretreated with cyclophosphamide as described above.

Bone marrow cells concentrate (300 µL) from the donor mice were injected into recipient mice through a tail vein. Bone marrow from C57B6 wild-type mice injected into C57B6 wild-type recipients gave M+/H+ chimeric mice. Bone marrow from C57B6 wild-type

mice injected into ICAM-1 knock out recipients gave M+/H- chimeric mice. Bone marrow from ICAM-1 knock out mice injected into C57B6 wild-type recipients gave M-/H+ chimeric mice. All groups of chimeric mice were then treated with LPS or saline and 6 hours later left ventricular contractility and function were measured and hearts were harvested as described above.

3.3.5 Cardiac ICAM-1 expression: To measure ICAM-1 protein expression, 10 μm thick frozen sections were prepared and fixed using 3% paraformaldehyde for 20 minutes and then incubated with Universal Blocking Agent (Dako, Carpinteria, CA) for 2-3 hours. Sections were treated with rat-anti mouse ICAM-1 antibody (1/500) (BD Pharmingen) at 4°C overnight followed by incubation with goat anti-rat fluorescently labeled antibody (1/ 1000) (Alexa-fluor 594, Molecular Probes, Eugene, OR) and Hoechst nuclear stain (1/1000) (H3570, Molecular Probes) for 3 to 4 hours at room temperature. Images were captured at 400 X using a confocal microscope (SP-2, Leica Corporation, Exton, PA). The ratio of mean intensity of ICAM-1 staining (red) to mean intensity of nuclear staining (blue) was measured (Fluocytogram, Leica Corporation, DIMRE2, Exton, PA).

3.3.6 Cardiac leukocyte infiltration: Sections (6 μm) were prepared from formalin fixed hearts and stained with hematoxylin and eosin. Images were captured at 400 X using a spot camera and measurements were made using Image-Pro Plus software (Media Cybernetic Inc., Silver Spring, MD). The number of neutrophils within coronary arteries, the number of neutrophils adherent to the endothelial surface, and the number of

neutrophils within the perivascular space (defined as an area of double the largest radius of the corresponding coronary artery) were measured.

3.3.7 Statistical analysis: We tested for differences in Ees, $[dP/dt_{max}]/EDV$, and ejection fraction between groups using analysis of variance, choosing $p<0.05$ as significant. When a significant difference was found we identified specific differences between groups using a sequentially rejective Bonferroni test procedure. Data are expressed as mean ± standard error throughout.

3.4   Results

3.4.1   Endotoxemic C57B6 wild-type mice: Immunofluorescent staining of frozen sections from LPS-treated and saline-treated C57B6 wild-type mice demonstrated that ICAM-1 expression in heart sections significantly increased 6 hours after LPS (Figure 2). The ratio of the mean intensity of ICAM-1 staining to the mean intensity of nuclear staining was greater in the LPS-treated mice (4.59 ± 0.32) than in control saline-treated mice (1.96 ± 0.16, $p < 0.001$).   The intensity of ICAM-1 staining was heterogeneously distributed within each LPS-treated mouse heart section.

We then determined whether this endotoxemic murine model of sepsis resulted in decreased left ventricular contractility and function comparable to large animal models [51,203] and human sepsis [38,195].   Six hours after LPS injection in C57B6 wild-type mice, heart rate increased by 72 ± 6% ($p < 0.01$) and end-systolic pressure decreased by 12 ± 4% compared to saline-treated controls (Table 1).   Left ventricular contractility decreased after LPS injection as indicated by a 58 ± 4% decrease in Ees ($p < 0.05$; Figure 3A) and a 60 ± 6% decrease in $[dP/dt_{max}]/EDV$.   Ejection fraction decreased by 14 ± 10% despite the decrease in end-systolic pressure (Table 1).

Table 3.1 **Hemodynamics and ventricular function measures**

	C57B6 wild-type Saline	C57B6 wild-type LPS	C57B6 GCSF Saline	C57B6 GCSF LPS	C57B6 CY Saline	C57B6 CY LPS	ICAM-1KO Saline	ICAM-1KO LPS
Number	8	8	6	8	6	6	8	8
Heart rate (bpm)	280 ± 41	481 ± 18 *	303 ± 32	450 ± 16 *	181 ± 7	347 ± 29 *	340 ± 17	388 ± 13 *
End Systolic Pressure (mmHg)	77 ± 7	68 ± 3	81 ± 6	62 ± 7	58 ± 6	76 ± 5	103 ± 15	78 ± 7
End Diastolic Pressure (mmHg)	4.7 ± 0.9	3.7 ± 0.6	5.3 ± 2.4	2.7 ± 0.7	4.6 ± 0.7	5.5 ± 0.8	3.7 ± 1.3	3.2 ± 0.4
End Systolic Volume (μL)	6.4 ± 1.1	14.5 ± 2.2 *	7.5 ± 1.3	13.9 ± 2.2 *	25.7 ± 5.5	10.4 ± 3.1	7.4 ± 1.1	9.2 ± 2.3
End Diastolic Volume (μL)	12.9 ± 2.3	24.7 ± 2.7 *	16.6 ± 2.7	20.4 ± 2.7	48 ± 7	18.2 ± 5.8	13.9 ± 1.0	15.1 ± 2.8
Ejection Fraction	48 ± 4	41 ± 5	54 ± 5	34 ± 5	46 ± 3	39 ± 7	48 ± 5	46 ± 6

C57B6 GCSF: GCSF pretreated mice.

C57B6 CY: cyclophosphamide pretreated mice.

ICAM-1 KO: ICAM-1 knock out mice.

* $p < 0.05$ compared to controls.
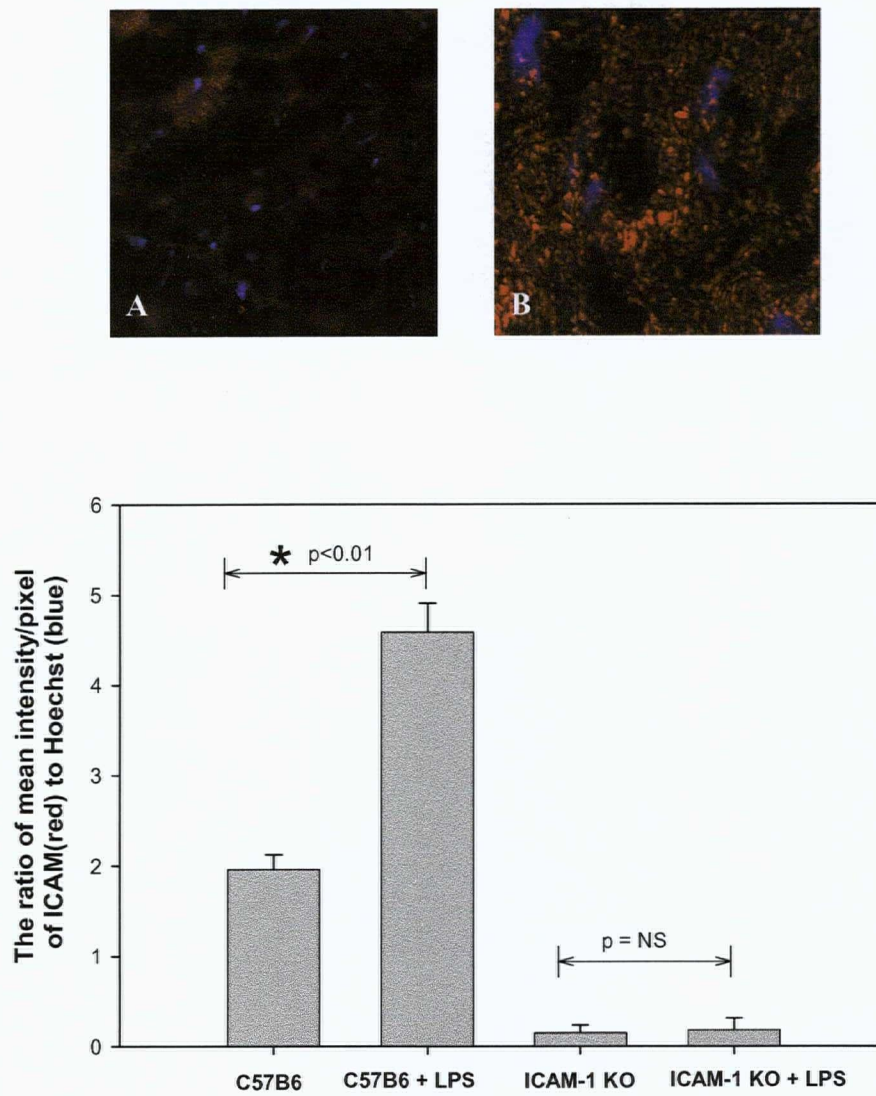
Figure 3.2   Representative immunofluorescent staining of myocardial sections from A) C57B6 saline-treated mice, B) C57B6 LPS-treated mice are shown in the top panel. The ratio of ICAM-1 to nuclear staining is shown for all mice in the above groups in the bottom panel. This ratio is significantly greater in C57B6 LPS-treated mice compared to saline-treated control mice (p<0.01). This ratio is greatly decreased in ICAM-1 knock out mice and is not altered by LPS.

Table 3.2   Peripheral blood cellular components

	C57B6 wild-type Saline	C57B6 wild-type LPS	C57B6 GCSF Saline	C57B6 GCSF LPS	C57B6 CY Saline	C57B6 CY LPS	ICAM-1 KO Saline	ICAM-1 KO LPS
WBC X 10^9/L	3.6 ± 0.2	0.5 ± 0.1	4.3 ± 0.6	1.78 ± 0.3	0.1 ± 0.02	0.02 ± 0.01	4.7 ± 0.8	0.9 ± 0.2
Neutrophil X 10^9/L	0.4 ± 0.04	0.4 ± 0.1	0.7 ± 0.3	1.7 ± 0.3	0.04 ± 0.01	0.004 ± 0.001	1.3 ± 0.3	0.7 ± 0.1
Lymphocyte X 10^9/L	2.9 ± 0.2	0.1 ± 0.06	3.3 ± 0.4	0.1 ± 0.03	0.05 ± 0.01	0.007 ± 0.002	3.1 ± 0.6	0.3 ± 0.1
Red blood cell X 10^{12}/L	8.6 ± 0.1	9.4 ± 0.2	8.4 ± 0.32	8.5 ± 0.52	7.42 ± 0.16	7.51 ± 0.11	8.5 ± 0.2	9.5 ± 0.1
Platelet X 10^9/L	913 ± 21	513 ± 90	354 ± 23	85 ± 5	771 ± 29	306 ± 43	735 ± 48	304 ± 37

C57B6 GCSF: GCSF pretreated mice.

C57B6 CY: cyclophosphamide pretreated mice.

CAM-1 KO: ICAM-1 knock out mice.

3.4.2 Effect of increased and decreased leukocyte count: To test the hypothesis that leukocytes contribute to the early (6 hours) decrease in left ventricular contractility in vivo in this intact whole animal model of sepsis, we increased leukocyte counts using GCSF injection or decreased leukocyte counts using cyclophosphamide injection.

The GCSF injection increased total peripheral leukocyte count by 31 ± 10% and increased peripheral neutrophil count by 20% over untreated control C57B6 wild-type mice (Table 2). The GCSF increased bone marrow leukocyte count 3.5 fold and increased bone marrow neutrophil count 4 fold. In GCSF-treated mice LPS injection resulted in an 59 ± 15% reduction in Ees ($p<0.05$), a 21 ± 19% decrease in $[dP/dt_{max}]/EDV$, and an 36 ± 9% decrease in ejection fraction compared to controls ($p<0.05$; Table 1).

Cyclophosphamide treatment decreased the total leukocyte count by 97 ± 1% to 0.08 ± 0.01 x 10^9/L, and decreased the fraction of neutrophils to 34.7 ± 0.9% (Table 2). Cyclophosphamide pretreatment abolished the effect of LPS, which did not decrease Ees, $[dP/dt_{max}]/EDV$, or ejection fraction (Table 1) in these mice.

3.4.3 Endotoxemic ICAM-1 knock out mice: The ratio of ICAM-1 to nuclear immunofluorescent staining was greatly decreased in ICAM-1 knock out mice (0.15 ± 0.09) compared to C57B6 wild-type mice (1.96 ± 0.16, $p<0.05$) and did not increase with LPS injection (0.18 ± 0.13) (Figure 2). In contrast to C57B6 wild-type mice, left ventricular contractility and function in ICAM-1 knock out mice, as measured by Ees (16.1 ± 3.6), $[dP/dt_{max}]/EDV$ (518 ± 146), and ejection fraction (46 ± 6%), was not

decreased (p=NS; Table 1 and Figure 3B). Similarly, six hours after LPS injection heart rate changed less in ICAM-1 knock out mice (increased 14%) compared to C57B6 wild-type mice (increased 72%) while end-systolic pressure decreased to the same extent in ICAM-1 knock out mice (by 24%) compared to C57B6 wild-type mice (by 23%).

3.4.4 Endotoxemic chimeric mice: LPS injection decreased left ventricular contractility of M+/H+ and M-/H+ chimeric mice. Specifically, Ees decreased by 43 ± 7% (p<0.05) in M+/H+ chimeric mice and Ees decreased by 56 ± 13% (p<0.05) six hours after LPS injection in M-/H+ chimeric mice. These changes in left ventricular contractility in M+/H+ and M-/H+ mice were not different from the effect of LPS injection in C57B6 wild-type mice (Table 1 and Figure 3). In contrast, LPS injection did not decrease left ventricular contractility of M+/H- chimeric mice. Indeed, in M+/H- chimeric mice LPS injection resulted in increases in contractility as measured by Ees (24 ± 3.7 in LPS group vs 13 ± 2.2 in controls), [dP/dt$_{max}$]/EDV (1012 ± 178 in LPS group vs 500 ± 90 in controls) and ejection fraction (54 ± 8% in LPS group vs 45 ± 4% in controls, p=NS, Table 3). Taken together, the lack of LPS-induced myocardial dysfunction in H- mice compared to the significant LPS-induced myocardial dysfunction in both M+ or M-/ H+ mice indicate that cardiac ICAM-1 expression is an important factor leading to decreased left ventricular contractility following LPS injection.

Injection of the bone marrow concentrate into the chimeric recipient mice significantly increased the peripheral blood total leukocyte count compared to non-injected cyclophosphamide-treated mice, confirming successful bone marrow transplantation. In

M+/H- mice the peripheral blood total leukocyte count was 1.2 ± 0.04 x 10^9/L, the fraction of neutrophils was $29.8 \pm 3.7\%$, and the fraction of lymphocytes was $23.3 \pm 3.6\%$. In M+/H+ mice the peripheral blood total leukocyte count was 1.2 ± 0.05 x 10^9/L, the fraction of neutrophils was $46.8 \pm 5.6\%$, and the fraction of lymphocytes was $18.9 \pm 5.3\%$.

Table 3.3   Hemodynamics and ventricular function measures in chimeric mice

	Chimera Saline	Chimera M^+/H^+ LPS	Chimera M^-/H^+ LPS	Chimera M^+/H^- LPS
Number	5	4	6	6
Heart rate (bpm)	290 ± 17	414 ± 12 *	384 ± 27 *	382 ± 18 *
End Systolic Pressure (mmHg)	80 ± 4	61 ± 8.2	52 ± 6.5	73 ± 10
End Diastolic Pressure (mmHg)	4.5 ± 0.8	5.2 ± 0.7	4.9 ± 0.6	2.5 ± 0.9
End Systolic Volume (μL)	6.4 ± 0.8	15.5 ± 2.9	4.2 ± 1.0 *	2 ± 0.4 *
End Diastolic Volume (μL)	11.5 ± 0.8	33 ± 8 *	6.2 ± 1.5 *	4.1 ± 0.6 *
Ejection fraction	45 ± 4	29 ± 8 *	49 ± 8	54 ± 8

M^+: ICAM-1 competent bone marrow cells

M^-: ICAM-1 knock out bone marrow cells

H^+: ICAM-1 competent heart

H^-: ICAM-1 knock out heart

* $p < 0.05$ compared to slaine treated chimera.

Figure 3.3A
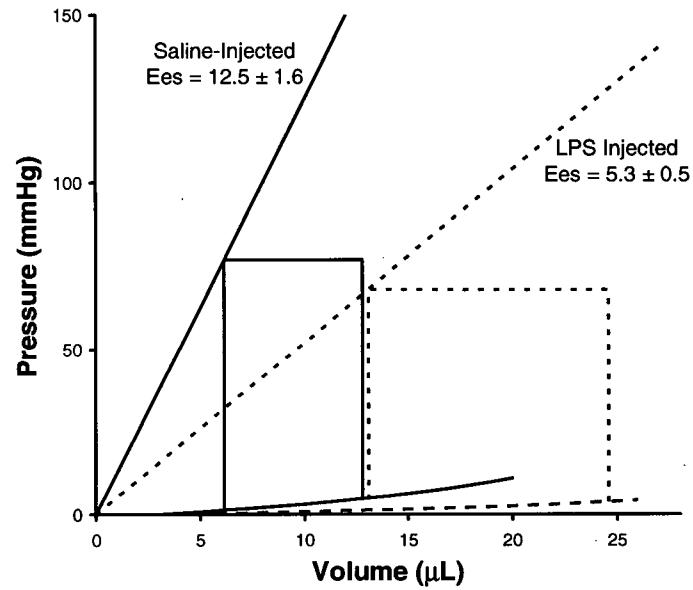
Figure 3   Stylized pressure volume loops drawn using average end-systolic elastance (Ees), end-diastolic volume (EDV), end-diastolic pressure (EDP) and end-systolic pressure (ESP) as reported in Table 1. End-systolic volume (ESV) derived from these plots corresponds closely (but not exactly due to averaging) to the measured ESV values reported in Table 1. A) In C57B6 wild-type mice, LPS results in a significant decrease in left ventricular contractility as measured by Ees. This is accompanied by an increase in ESV and EDV. B) In ICAM-1 knock out mice, LPS does not result in a decrease in left ventricular contractility measured by Ees.

Figure 3.3B
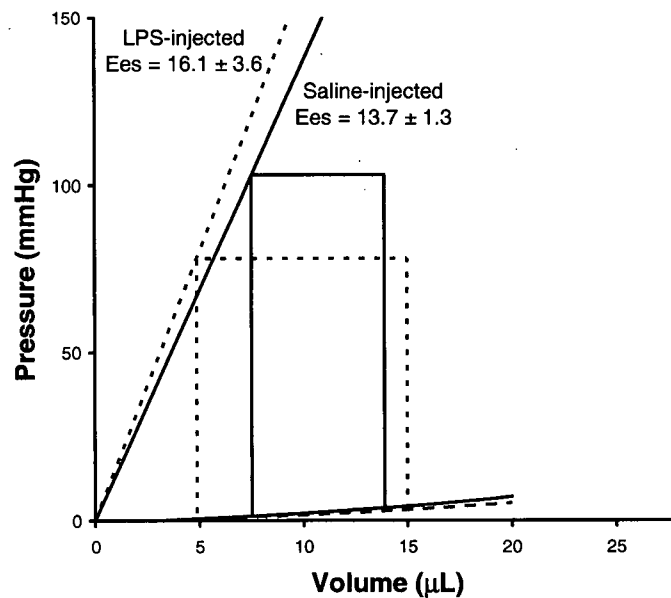
Table 3.4   Peripheral blood cellular components in chimeric mice

	Chimera M^+/H^+ Saline	Chimera M^+/H^+ LPS	Chimera M^+/H^- Saline	Chimera M^+/H^- LPS	Chimera M^-/H^+ LPS
WBC X 10^9/L	1.2 ± 0.1	$0.05 \pm 0.01*$	1.2 ± 0.04	$0.06 \pm 0.01 *$	$0.05 \pm 0.01 *$
Neutrophil X 10^9/L	0.6 ± 0.1	$0.04 \pm 0.01 *$	0.4 ± 0.1	$0.04 \pm 0.001 *$	$0.03 \pm 0.01 *$
Lymphocyte X 10^9/L	0.2 ± 0.07	$0.01 \pm 0.003 *$	0.3 ± 0.1	$0.01 \pm 0.006 *$	$0.01 \pm 0.001 *$
Red blood cell X 10^{12}/L	7.0 ± 0.2	7.4 ± 0.2	7.4 ± 0.2	8.3 ± 0.5	7.9 ± 0.4
Platelet X 10^9/L	405 ± 18	$109 \pm 9 *$	466 ± 79	$157 \pm 64 *$	$131 \pm 16 *$

M^+: ICAM-1 competent bone marrow cells

M^-: ICAM-1 knock out bone marrow cells

H^+: ICAM-1 competent heart

H^-: ICAM-1 knock out heart

* $p<0.05$ compared to all saline treated groups.

3.4.5 Morphometery of coronary vascular space: The LPS injection in C57B6 wild-type mice increased coronary intravascular neutrophil concentration from 2.5 ± 1.9 x $10^{-5}/\mu m^2$ in control to 137 ± 22 x $10^{-5}/\mu m^2$ in septic mice. LPS injection also increases the ratio of adherent neutrophil to endothelial surface from 3.2 ± 2.3 x $10^{-5}/\mu m^2$ in control to 99 ± 18 x $10^{-5}/\mu m^2$ in endotemic mice ($p < 0.05$). However LPS injection did not increase extracellular neutrophil infiltration into the cardiac tissue (Figure 4).
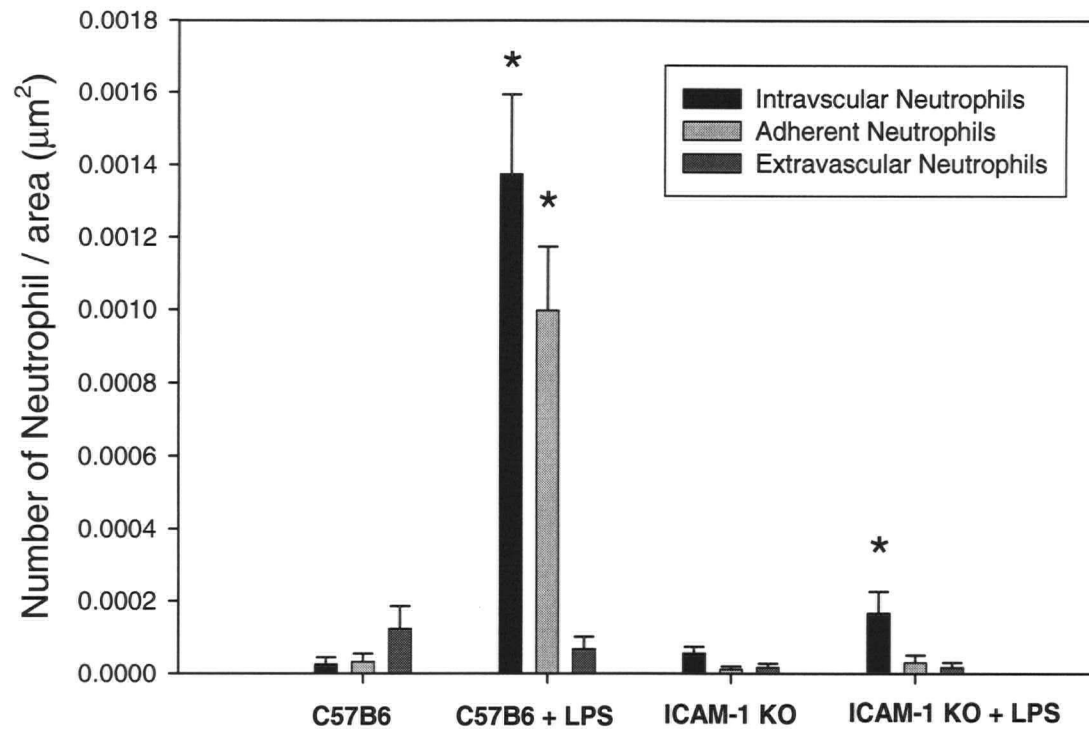
Figure 4   Formalin fixed heart sections were stained with DAB and Hematoxyline & Eosin to measure the ratio of the number of inflammatory cells per surface area of intravascular and perivascular spaces. LPS injection significantly increased this ratio in the intravscular space (*p<0.01 compared to saline treated C57B6). The number of adherent inflammatory cells on endothelial surface is also significantly increased in LPS-treated mice (*p<0.01 compared to saline treated ICAM-1 KO). However this ratio is not significantly different in the perivascular space in LPS-treated mice.

3.5 Discussion

LPS injection reduced left ventricular contractility in this whole animal model of systemic inflammation, similar to previous measurements in a variety of animal models of sepsis, and similar to the decrease in left ventricular function observed during human septic shock. Decreasing leukocyte count using cyclophosphamide abrogated the effect of LPS, confirming previous reports that leukocytes contribute to the development of decreased left ventricular contractility in sepsis. ICAM-1 knock out mice were resistant to the effect of LPS on left ventricular contractility indicating that ICAM-1 plays an important causal role in mediating the effect of LPS. Chimeric mouse constructs further implicate cardiac ICAM-1 expression, versus ICAM-1 expressed on bone marrow-derived cells transiting the heart. Thus, signaling via cardiac ICAM-1 is necessary for the development of leukocyte-dependent decreases of left ventricular contractility in this whole animal model of systemic inflammation.

Many mechanisms contribute to myocardial depression during sepsis [54]. In sepsis, release of pathogenic toxins such as LPS from gram negative bacteria, glycolipid from gram positive bacteria, or mannan from fungal wall initiate a systemic inflammatory response. Pro-inflammatory cytokines trigger increased NO production [184] by NOS III within minutes, and greatly increased NO production by NOS II within hours [204]. NO is an important mediator of myocardial dysfunction in sepsis [71,204,205]. Reactive oxygen intermediates contribute directly and via formation of peroxynitrite radicals, to myocardial damage and dysfunction [163,205]. Coronary capillary endothelial activation, damage and dysfunction also contribute, in part by impaired regulation of coronary

microvascular blood flow, which impairs myocardial oxygen extraction [51]. Leukocytes also contribute. Leukocytes are slowed and retained within the coronary vasculature after endotoxin infusion [203], predominantly within coronary capillaries. Leukocyte retention is associated with myocardial morphometric damage and decreased ventricular contractility [196]. In an ex vivo preparation, filtering leukocytes from coronary blood perfusing the heart prevented the decrease in contractility within the first 6 hours of endotoxin infusion [197]. Activated neutrophils appear to be a particularly important leukocyte subset involved in early myocardial depression [65]. Our current results support these previous observations by demonstrating that the LPS-induced decrease in left ventricular contractility is leukocyte dependent – being abrogated by a decreased peripheral blood leukocyte count.

Part of the leukocyte effect may be due to binding of leukocytes to cardiac ICAM-1. Pro-inflammatory cytokines, including IL-6 generated by the myocardium following ischemia-reperfusion, result in CD18 - ICAM-1 dependent adhesion of PMN to cardiomyocytes [171]. Adhesion of highly (unphysiologically) activated PMN to cardiomyocytes results in cardiomyocyte cell death in vitro, possibly due to reactive oxygen intermediates [59,107,163,164]. Co-culture of macrophages or neutrophils with cardiomyocytes resulted in ICAM-1 dependent adhesion and decreased cardiomyocyte fractional shortening [59,60]. Adhesion alone was a fundamentally important aspect of this interaction because the same effect was reproduced by co-culture with killed and fixed neutrophils or simply by ICAM-1 cross linking antibodies [60].

ICAM-1 is a 76 – 110 kDa glycoprotein from the immunoglobulin gene family [206,207]. ICAM-1 expression by a variety of different cell types, including on cardiomyocytes, increases during inflammation [59,60,107]. Activated coronary endothelial cells in cell culture increase ICAM-1 expression in 2 to 4 hours and maximum ICAM-1 expression is reached in 6 to 8 hours. High levels of ICAM-1 expression are maintained as long as the inflammatory response is active [109]. Activation of ICAM-1 stimulates further production and expression of vascular cellular adhesion molecule-1 (VCAM-1) and ICAM-1 [208]. Activation of isolated cardiomyocytes increases ICAM-1 mRNA production within 1 to 4 hours [60] and expression of ICAM-1 protein within 4-6 hours [59]. Maximum production of ICAM-1 occurs 18 to 24 hours after cytokine stimulation [107]. Ligands for ICAM-1 include CD11/CD18 receptors [206,208,209], fibrinogen [135], rhinovirus receptors [210] and plasmodium falciparum [211].

Our current findings extend these in vitro observations and demonstrate that binding of ICAM-1 expressed on cardiomyocytes reduced left ventricular contractility in a whole animal model of systemic inflammation. Using isolated rat cardiomyocytes we have shown that activation of ICAM-1 using cross-linking antibodies can initiate intracellular signals which cause discoordinate calcium influx leading to reduction in cardimyocyte contractility [60]. This effect of ICAM-1 cross-linking mediated via the cytoskeleton [60]. The presence of cardiac contractile dysfunction after LPS injection in M+/H+, and M-/H+ chimera mice, and absence in M+/H- chimera mice demonstrates the importance of ICAM-1 expression within cardiac tissue. Lack of ICAM-1 on bone marrow-derived inflammatory cells did not prevent the effect of LPS on cardiac contractility.

Several potential ligands may be involved in ICAM-1 binding and activation in this whole animal model of systemic inflammation, which results in decreased left ventricular contractility. Since we [197] and others [196] have demonstrated that the LPS-induced decrease in left ventricular contractility is, in part, leukocyte dependent, it is reasonable to postulate that CD11/CD18, or other leukocyte expressed ICAM-1 ligands, bind and activate ICAM-1 expressed on cardiomyocytes in vivo. However, we did not find many neutrophils or other leukocytes within the cardiac parenchyma in this and other models of sepsis [65]. It is conceivable that leukocytes enter cardiac parenchyma but undergo apoptosis or other forms of cell death quickly and leave CD11/CD18 to bind to ICAM-1 expressed on cardiomyocytes. However, this has not been demonstrated. We propose an alternative mechanistic pathway to account for the observation of leukocyte-dependent decreases in left ventricular contractility mediated by cardiomyocyte expressed ICAM-1 binding and activation. Current and previous observations demonstrate that leukocytes are retained within coronary capillaries in systemic inflammatory states [65]. These leukocytes damage the capillary endothelium [65] leading to interstitial edema. We postulate that the interstitial edema fluid components that are ICAM-1 ligands, including fibrinogen, could then lead to decreased ventricular contractility via the ICAM-1 binding. This postulated pathway is consistent with the observations of Neviere and his colleagues [196].

In summary, we found that LPS injection in mice resulted in a substantial decrease in left ventricular contractility. This decrease was leukocyte dependent and also dependent on cardiac ICAM-1 expression. However, we did not observe a large number of leukocytes

within the cardiac parenchyma at the time of substantially decreased left ventricular contractility. Therefore, we postulate that this leukocyte-dependent decrease in left ventricular contractility involves at least two steps in series – a leukocyte dependent step and an ICAM-1 dependent step. Leukocyte retention leading to endothelial damage and leakage of ICAM-1 ligands, such as fibrinogen, into the cardiac interstitium is one explanation compatible with our findings. We conclude that signaling via cardiac ICAM-1 expression is necessary to mediate leukocyte-dependent decreases of left ventricular contractility in endotoxemic mice.

Chapter-4

The role of fibrinogen and ICAM-1 interaction in decreased cardiac contractility

4.1   Abstracts

Fibrinogen is involved in coagulation and inflammatory responses. Interaction of ICAM-1 and fibrinogen promotes platelet and leukocyte adhesion onto endothelial cells. Cardiomyocyte ICAM-1 activation decreases cardiomyocyte contractility through an increase in heterogeneity of Ca^{2+} release. We hypothesize that during sepsis fibrinogen can infiltrate into the myocardial interstitial space and decrease cardiomyocyte contractility through the activation of ICAM-1.

To investigate whether fibrinogen can infiltrate into the myocardial interstitial space and affect ICAM-1 on cardiomyocyte membranes, C57B6 mice were injected with LPS (40 mg/kg) or normal saline. Six hours later hearts were excised and stained with horse radish peroxidase conjugated anti-mouse fibrinogen antibody or reperfused with fibrinogen-labeled Alexa-488 for 10 minutes using an ex-vivo model and Langendorff system. To test whether the fibrinogen binding to ICAM-1 decreases cardiomyocyte contractility, isolated rat cardiomyocytes were co-cultured with soluble fibrinogen or fibrinogen coated beads for 3 to 4 hours. Cardiomyocyte fractional shortening was measured in the presence or absence of anti-ICAM-1 antibody.

Confocal microscopy of heart sections showed infiltration of the fibrinogen labeled Alexa-488 into myocardial interstitial tissue in septic mice. Immunohistochemistry of

heart sections indicated lack of fibrinogen infiltration into the myocardial tissue of septic ICAM-1 knock out mice. Incubation of activated cardiomyocytes with soluble fibrinogen decreased cardiomyocyte fractional shortening from 17.2 ± 0.8% to 14.4 ± 0.5%. Incubation of cardiomyocyte with fibrinogen coated beads decreased cardiomyocyte contractility 16.8 ± 1.0% to 10.7 ± 1.0%. This effect of fibrinogen was abolished in the presence of anti ICAM-1 antibody (17.7 ± 0.6%) indicating an interaction of fibrinogen and ICAM-1.

We conclude that fibrinogen infiltrates into the myocardial interstitial space during sepsis and decreases cardiac contractility through adhesion to the ICAM-1 receptor on the cardiomyocyte membrane.

4.2   Introduction

Fibrinogen, 340 kDa protein, is involved in coagulation and inflammatory responses. Fibrinogen adhesion to ICAM-1 increases tyrosine phosphorylation. Interaction of ICAM-1 and fibrinogen promotes platelet [147] and leukocyte adhesion [212] onto endothelial cells. Cardiomyocyte ICAM-1 activation decreases cardiomyocyte contractility through an increase in heterogeneity of Ca^{2+} release [60]. We hypothesize that during sepsis fibrinogen can infiltrate into the myocardial interstitial space and decrease cardiomyocyte contractility through the activation of ICAM-1.

Fibrinogen contains α, β and γ chains. It is involved in the pathogenesis of various types of diseases, including ischemia, trauma and neoplasm. Increased plasma fibrinogen level is associated with a higher risk of cardiovascular diseases, increased risk of myocardial infarction, stroke, peripheral arterial disease, atrial fibrillation, heart failure and post angioplasty restenosis [213,214]. Fibrinogen increases vascular permeability by detachment of endothelial cells from the basement membrane [142]. It has been shown that fibrinogen can enhance adhesion of inflammatory cells and facilitates platelet adhesion to the endothelial surface during arteriosclerosis thereby accelerating atherosclerotic plaque formation [215]. Adhesion of fibrinogen on CD11 receptors of PMN reduced caspase activation and apoptosis of PMN [216]. Saito and his colleagues have shown the extravasation of fibrinogen in rat plural cavity after histamine injection. This effect of fibrinogen is associated with increased PMN infiltration into the plural cavity suggesting the close relation between PMN infiltration and fibrinogen exudation [217]. Fibrinogen can increase the expression of ICAM-1 through activation of NFκB on human synovial

fibroblasts [146]. Languino et al. demonstrated that fibrinogen functions as an intermediate protein for adhesion of monocytes to the endothelial cells [136].

Fibrinogen contains two peripheral, one central and three global domains. A specific site of the γ chain of the fibrinogen molecule, between amino acid 117-133, is responsible for adhesion to amino acid 8-22 of the first extracellular domain of ICAM-1.

Our previous findings have indicated that PMN adhesion can decrease cardiomyocyte contractility and that this effect of PMN occurs through interaction of the ICAM-1 receptor on cardiomyocyte membrane and CD11/CD18 receptors on inflammatory cells. We subsequently found that activation of ICAM-1 on cardiomyocytes using cross-linking methods decreased cardiomyocyte contractility (refer to chapter 2). We also found that cardiac contractility of ICAM-1 knock-out mice was preserved after LPS treatment. This was resistant to the effect of LPS because of the absence of ICAM-1 receptors on cardiac tissue (refer to chapter 3). However we did not observe infiltration of PMNs into the cardiac interstitial space after LPS injection, suggesting that, PMNs are not directly involved in ICAM-1 activation in vivo.

We tested whether fibrinogen can infiltrate into the myocardium after LPS injection and if fibrinogen can induce decreased cardiomyocyte contractility.

4.3   Materials and Methods

4.3.1   Induction of sepsis: C57B6 wild-type and ICAM-1 knock out mice (25-30 g, Jackson Laboratory, Bar Harbor, ME) were injected with purified Escherichia Coli lipopolysaccharide (LPS, 40mg/kg, strain 01 II: B4) or normal saline via intraperitoneal injection. Six hours after LPS injection, mice were anesthetized using Isoflurane 3%. Anesthesia was tested by toe-pinch to ensure absence of withdrawal to pain throughout the procedure. The heart was excised, frozen or fixed (10% Formalin) for further immuno-fluorescent or immuno-histochemistry studies.

4.3.2   Immuno-histochemistry and Immuno-fluorescent study: Formalin fixed hearts were embedded and 6 μm sections were prepared. After de-parafinization, sections were treated with rabbit anti-mouse fibrinogen (Inovation Research Southfield, MI) overnight follow by HRP-conjugated anti- rabbit antibody (BD Pharmingen, San Jose, CA) for 2 hours. The slides were then treated with DAB for 30 minutes follow by hematoxylin staining. Images (X400) were captured using spot camera.

4.3.3   Reperfusion of Alexa-488 labeled fibrinogen into the LPS or saline treated mice: In the preliminary experiments using a mixed in-vivo and ex-vivo method, animals were treated with LPS or saline for 6 hours. Hears were excised and cannulated using a 20 G needle and reperfused using a Langendorff apparatus as described in chapter-5 section-3. To test whether fibrinogen can infiltrate into the cardiac interstitial space, cannulated hearts were reperfused with fibrinogen labeled Alexa-488 (Molecular probe) for 15 minutes while monitoring pulse pressure. The hearts were frozen with Isopentane

in liquid nitrogen. Sections (6 μm) from frozen hearts were prepared and stained with anti-von Willebrand factor (BD Pharmingen) overnight at 4 °C to illustrate coronary endothelial surface. Anti nuclear staining (Hoechst) was used to visualize nuclei. Sequential images were captured using confocal microscopy (LEICA DIMRE2, Exton, PA).

4.3.4 Incubation of soluble fibrinogen with isolated rat cardiomyocytes: Male Sprague-Dawley rat cardiomyocytes were isolated and cultured in 96 well plates as previously described in chapter-2, section-3. To increase ICAM-1 presentation on cardiomyocyte membrane, cultured cardiomyocytes were activated with TNFα (20 ng/ml) for 3 to 4 hours. 25000 fibrinogen coated, BSA coated and plain non-coated beads were incubated with 5000 cardiomyocytes in each well (100 μL) for 4 hours. In a separate set of experiments, cardimyocytes were also co-cultured with different concentrations of soluble fibrinogen. Cardiomyocyte fractional shortening was measured as previously described in chapter-2, section-3.

4.3.5 Coating of Fibrinogen to Polystyrene Beads: Polystyrene Beads (Bangs Laboratories; 8 μm in diameters) were washed twice (5 minutes per wash) with acetate buffer (pH 5.4) and mixed with rat fibrinogen (Enzyme Research Laboratories) (300000 beads/μg fibrinogen, 2% solid in buffer) in a 500 μL eppendorf tube. The mixture was gently stirred for 2 hours at room temperature to promote fibrinogen adhesion to the plain beads through hydrophobic interactions. The beads were then washed three times with

fresh acetate buffer. The fibrinogen coated beads were re-suspended by passing them through a syringe with a 27.5G needle and co-cultured with cardiomyocytes.

4.3.6 Blocking of Cardiomyocyte ICAM-1: After TNF-α activation, the cardiomyocytes were incubated with an anti ICAM-1 blocking antibody (BD Biosciences) or control non-specific mouse IgG (DAKO) for 2 hours. They were co-cultured with fibrinogen coated beads as described previously.

4.4   Results

4.4.1   Fibrinogen   infiltration   into   the   interstitial   space   (in-vivo):
Immunohistochemistry (IHC) was used to assess whether plasma fibrinogen infiltrates into the myocardium during endotoxemia. Fibrinogen staining was observed on cardiac sections of LPS treated animals indicating the presence of fibrinogen in the coronary vascular, perivascular and cardiac interstitial space. Fibrinogen staining in control sections was limited to the endothelial and endocardial surface (Figure 4-1). In LPS treated hearts, deposition of fibrinogen was observed in the myocardium immediately surrounding the vascular space, whereas in saline treated hearts, fibrinogen was located at the edge of the blood vessels and coronary endothelial surface (Figure 4-1).

IHC staining did not show infiltration of fibrinogen in the cardiac interstitial space of ICAM-1 KO mice confirming the above observation. However coronary endothelial cells of ICAM-1 KO mice were stained with fibrinogen antibody (Figure 4-2) indicating the presence of fibrinogen in the serum of ICAM-1 KO mice.
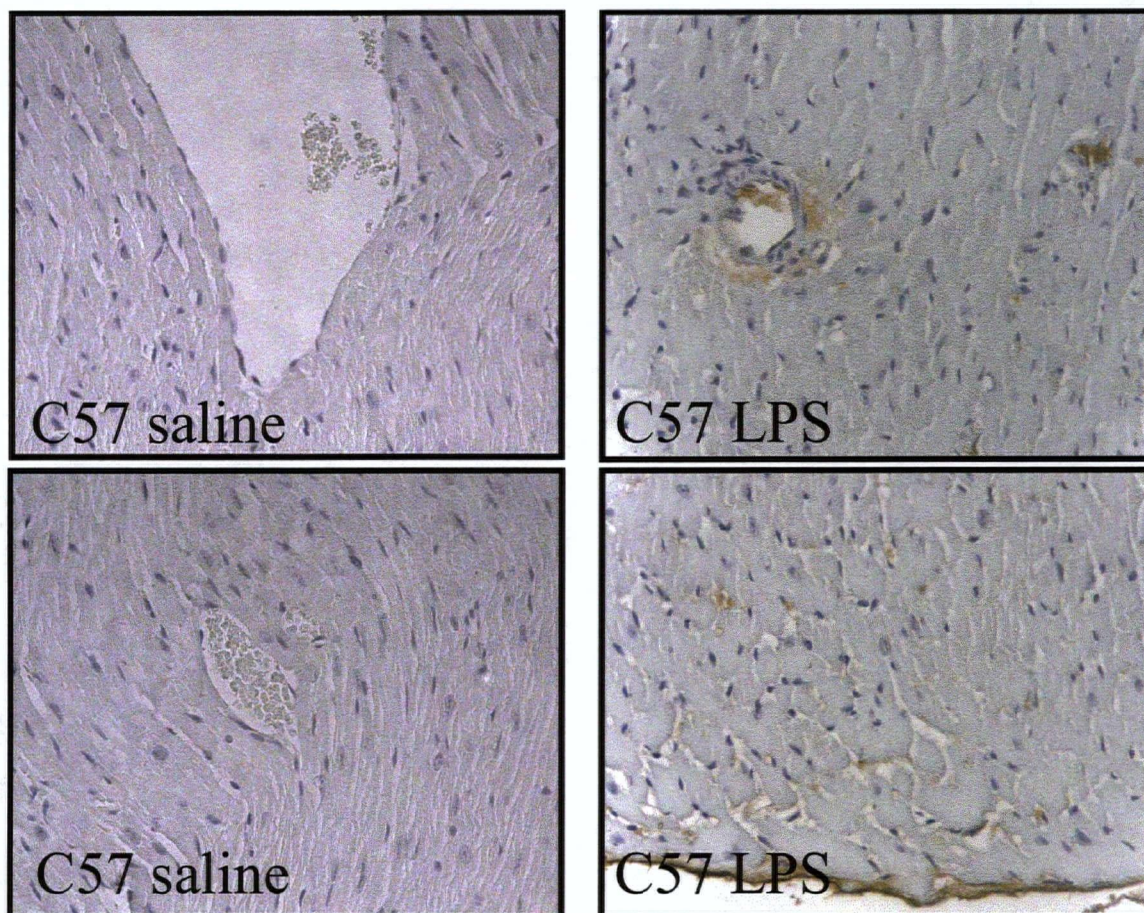
Figure 4.1   Immunohistochemistry of heart sections illustrate the presence of fibrinogen in the myocardial interstitial and perivascular spaces of LPS treated C57. In saline treated mice fibrinogen staining is limited to the vascular space.

ICAM-1 KO saline

ICAM-1 KO LPS
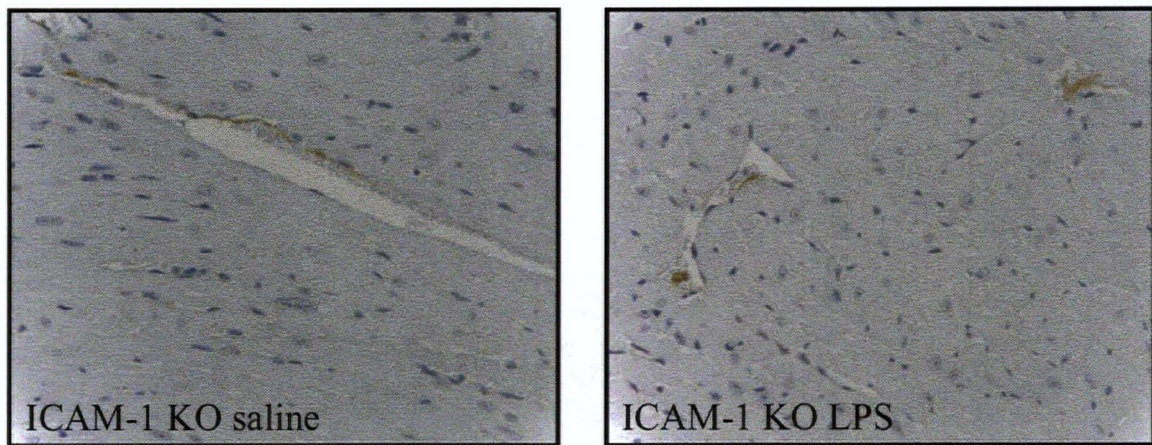
Figure 4.2   IHC of the heart sections of ICAM-1 knock out mice indicate the presence of fibrinogen staining in the vascular space of LPS or saline treated animals. Fibrinogen staining was not observed in the myocardial perivascular and interstitial spaces of ICAM-1 knock out mice indicating the protective effect observed in ICAM-1 knock out mice against infiltration of fibrinogen into the myocardial perivascular or interstitial spaces.

Confocal images of LPS or saline treated hearts (reperfused with Alexa-488 labeled fibrinogen ex-vivo) illustrate the presence of Alexa-488 in the coronary perivascular spaces of LPS treated mice (Figure 4.3A). This shows the presence of a leaky endothelial surface and the feasibility of infiltration of labeled fibrinogen into the cardiac interstitial space of LPS treated mice. In saline treated mice the presence of Alexa-488 is limited to the coronary vascular space (Figure 4.3A). The ratios of fibrinogen to nuclear staining (Fib/Nuc) and of fibrinogen to vonWillebrand factor (Fib/vWf) are higher in LPS treated hearts indicating wide distribution of fluorescent fibrinogen in the cardiac tissue (Figure 4.3B, $p < 0.05$).
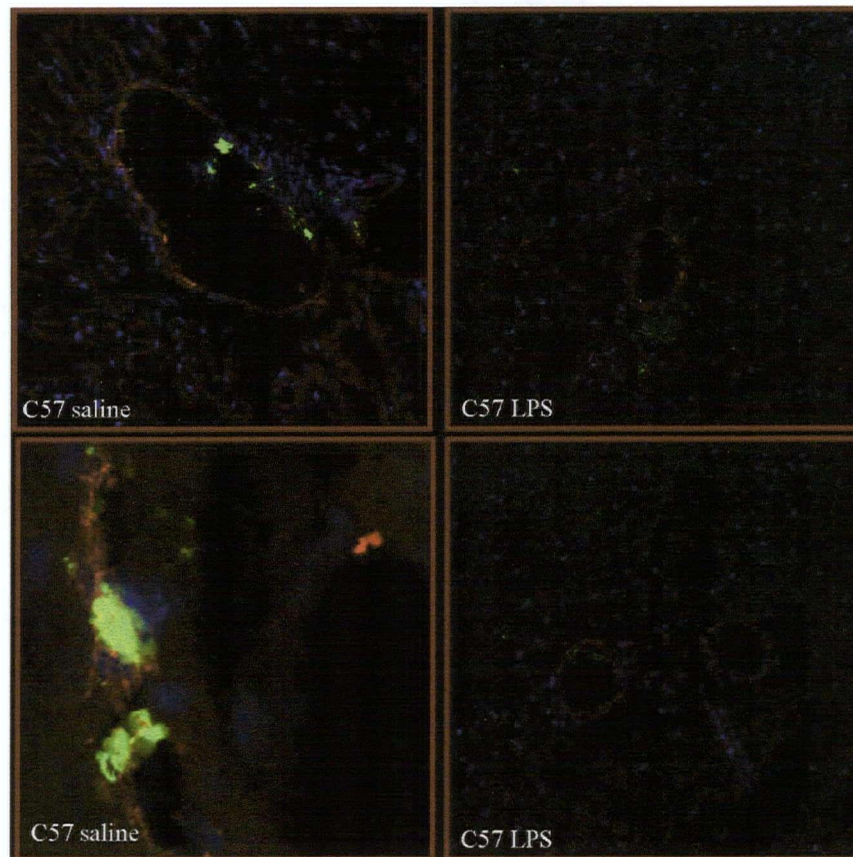
Figure 4.3A   Illustrates the retrograde reperfusion of fluorescent fibrinogen (green) into the coronary arteries of LPS or saline treated mice using an ex-vivo model of reperfusion. Vascular spaces were stained with anti-vonWillebrand factor antibody (red). Confocal images indicate the presence of Alexa-488 fibrinogen in the vascular space of saline treated mice. In the LPS treated mice fibrinogen infiltrates into the myocardial perivascular and interstitial spaces.
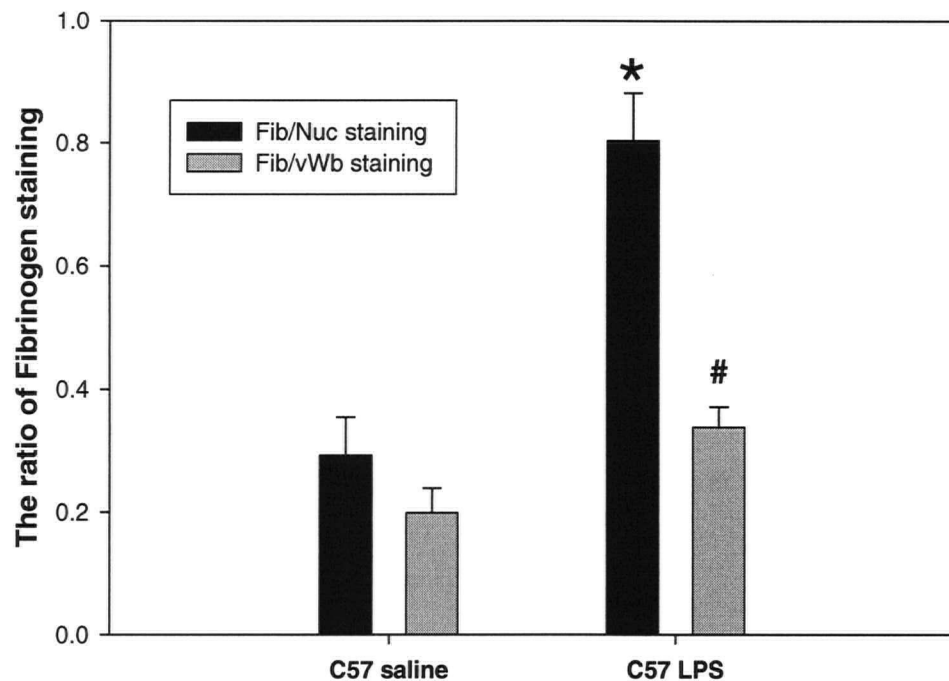
Figure 4.3B   C57B6 mice were treated with saline or LPS. Six hours later the heart was excised and reperfused with fluorescent fibrinogen for 15 minutes using a Langendorff apparatus. The hearts were frozen and stained with anti-nuclear and vonWillebrand factor antibodies. The ratio of fluorescent fibrinogen (green) to the nuclear staining (blue) or vonWillebrand factor (red) were compared between saline or LPS treated groups (*$p<0.01$ and # $p<0.05$).

4.4.2 Fibrinogen effect on cardiomyocyte contractility (in-vitro): Four hour incubation of different concentrations of soluble fibrinogen (0.025, 0.05, 0.1 and 0.2 mg/mL) with activated cardiomyocytes, decreases cardiomyocyte contractility in a dose-response dependant manner (Figure 4.4). The maximum effect of fibrinogen was achieved with a 0.2 mg/mL concentration of fibrinogen ($-26.5\pm7.9\%$, $p<0.004$ vs. control).

To demonstrate that the decrease in cardiomyocyte contractility is due to the effect of fibrinogen, polystyrene beads were coated with fibrinogen and co-cultured with activated cardiomyocytes (Figure 4.5). Confocal microscopy confirmed the deposition of fluorescent labeled fibrinogen onto the beads, indicating the successful adhesion of fibrinogen to the beads (Figure 4.6).
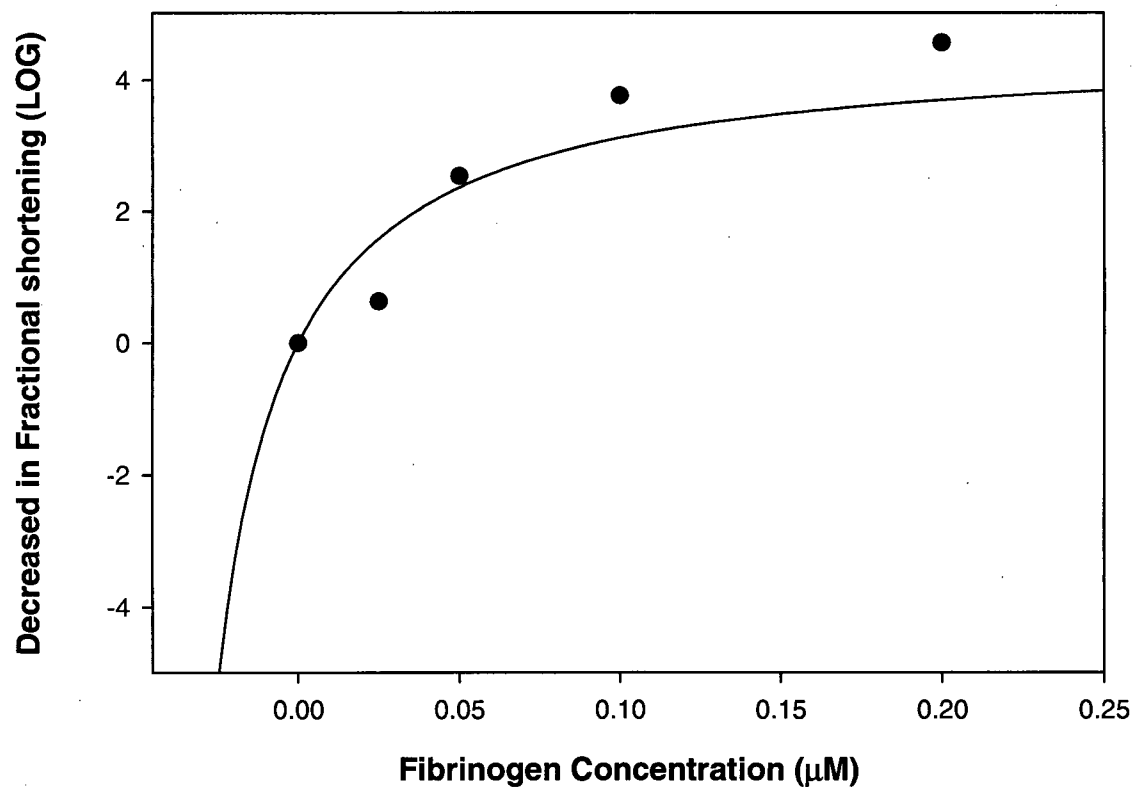
Figure 4.4   Co-incubation of soluble fibrinogen with activated cardiomyocytes decreased fractional

shortening of cardiomyocytes in a dose dependant response manner (EC50 = 0.468, Hill slope = -1.0, Min

= 0.0, and Max = 4.56, p<0.001).
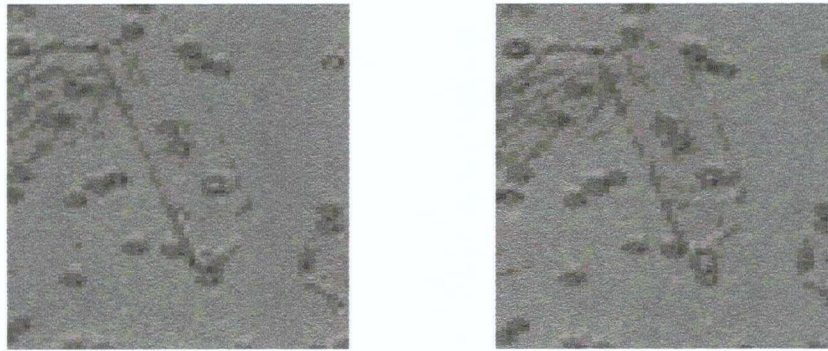
Figure 4.5   Adhesion of Fibrinogen Coated Beads. Fibrinogen coated beads remained adherent to cardiomyocytes during diastole (A) and systole (B).
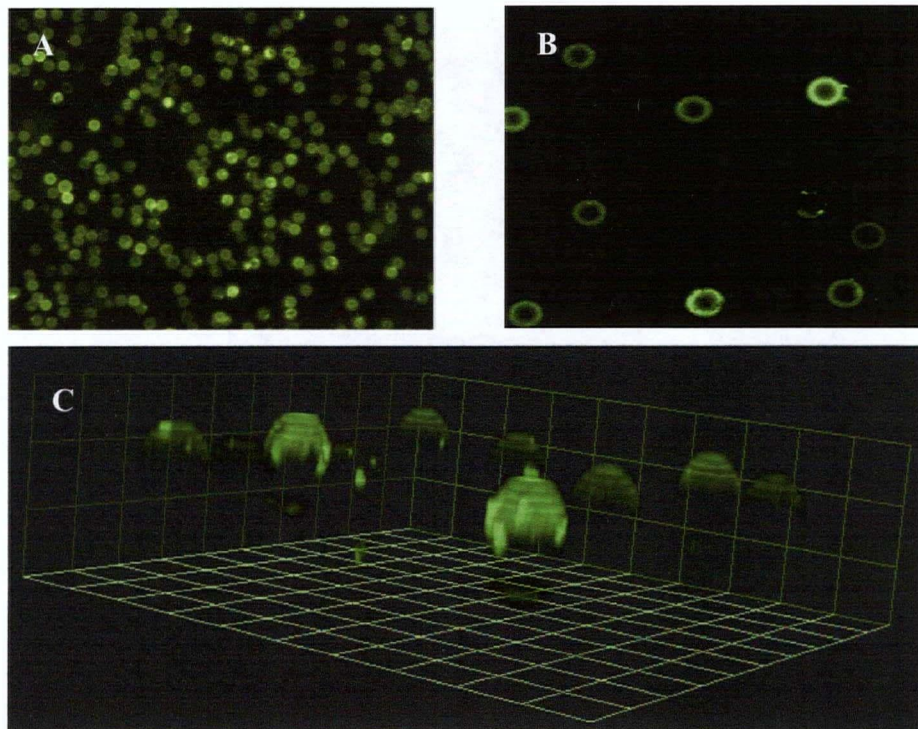
Figure 4.6   Polystyrene beads were coated with Oregon Green labeled fibrinogen and viewed under the fluorescence microscope (A) and confocal microscope (B and C).

Attachment of fibrinogen coated beads to the activated cardiomyocytes decreased cardiomyocyte fraction shortening by 32.0 ± 3.8% (10.7 ± 1.0) compared to control (16.9 ± 0.8, p<0.001). Plain beads and BSA coated beads (negative control) did not decrease the fractional shortening of activated cardiomyocytes (16.8 ± 1.0 and 17.5 ± 0.8 p=NS, Figure 4.7). The adhesion of fibrinogen coated beads to cardiomyocytes also induced a dose dependent decrease in cardiomyocyte fractional shortening, confirming the similar effect of soluble fibrinogen on fractional shortening (Figure 4.7).

4.4.3   Fibrinogen induces decreased cardiomocyte contractility through ICAM-1

ICAM-1 antibody decreases the number of adherent fibrinogen coated beads on the cardiomyocyte membrane. Incubation of activated cardiomyocytes with anti-ICAM-1 abrogates the effect of fibrinogen on cardiomyocyte contractility, indicating that the effect of fibrinogen is mediated by the ICAM-1 signaling cascade. Incubation of activated cardiomyocytes with non-specific IgG did not prevent adhesion of fibrinogen coated beads or the effect of fibrinogen on cardiomyocyte contractility, confirming the interaction between fibrinogen and ICAM-1 in co-culture experiments, and fibrinogen ICAM-1 mediated decreased contractility (Figure 4.7).
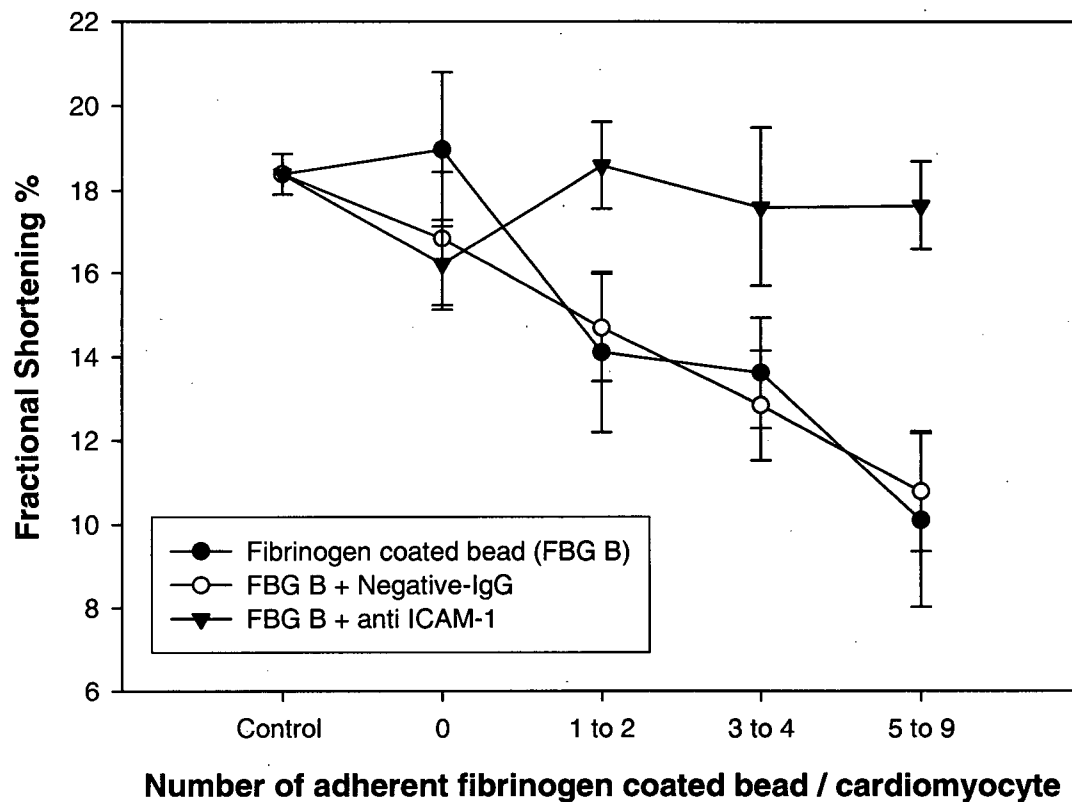
Figure 4.7   The effect of fibrinogen coated beads on cardiomyocyte fractional shortening. Fibrinogen coated beads decrease cardiomyocyte fractional shortening in a dose dependent manner. Incubation of co-culture with anti-ICAM-1 antibody inhibits the above effect of fibrinogen coated beads on cardiomyocyte fractional shortening, indicating the essential interaction of ICAM-1 and fibrinogen for a decrease in fractional shortening. Nonspecific IgG did not prevent the effect of fibrinogen on cardiomyocyte fractional shortening.

4.5 Discussion

Myocardial dysfunction is one of the major causes of death in septic patients. Cardiac inflammation is associated with increased ICAM-1 expression on the endothelial cells and cardiomyocytes [59,60,218]. ICAM-1 is a 114 kDa protein adhesion molecule, activated by binding to various types of ligands including CD11/CD18 receptors of inflammatory cells [182], fibrinogen [134-136], plasmodium falciparum[132] and rhinoviruses. We have shown that ICAM-1 activation on cardiomyocytes initiates a signaling cascade and alters calcium propagation during cardiomyocyte excitation contraction which results in decreased cardiomyocyte contractility [60]. Although the number of cardiac intravascular inflammatory cells is significantly higher in septic animals than control we did not observe infiltration of inflammatory cells into the cardiac interstitial space thereby we concluded that cardiac ICAM-1 can not be activated through binding of CD11/CD18 receptors on inflammatory cells during sepsis. Fibrinogen is a 340 kDa protein involved in coagulation and inflammation. It has been shown that fibrinogen can attach to ICAM-1 and phosphorylates various intracellular tyrosine residues [212,219]. We found that incubation of cardiomyocytes with both soluble fibrinogen and fibrinogen coated beads can decrease fractional shortening. This effect of fibrinogen occurs through the adhesion of fibrinogen to cardiomyocyte membranous ICAM-1. We also found that cardiac sections of LPS treated mice (in-vivo studies) were stained with anti-fibrinogen antibody indicating the availability of fibrinogen in the interstitial space of cardiac tissue for activation of cardiomyocyte ICAM-1. This finding is confirmed by the ex-vivo infusion of fibrinogen labeled Alexa-488 showing infiltration into the cardiac section of LPS treated mice.

The γ chain of fibrinogen binds to domain-1 of ICAM-1 through its 117-133 amino acid sequence [134,135]. Fibrinogen increases endothelial leakiness and enhances angiogenesis on endothelial cells [141-143]. We have reconfirmed the leakiness of the endothelial surface of coronary arteries using fibrinogen labeled Alexa-488 in the ex vivo retrograde reperfusion and immunohistochemistry of in-vivo LPS injection models. Upregulation of ICAM-1 in cardiovascular diseases is also accompanied by high expression of fibrinogen [145,146]. Fibrinogen and ICAM-1 interaction promotes platelet and leukocyte adhesion to endothelial cells [147]. This effect of fibrinogen was inhibited using ICAM-1 knock out mice and a model of ischemia reperfusion injury [148]. Hicks et al. have shown that fibrinogen deposition on endothelial cells induced vasodilation, however when they increased fibrinogen concentration this effect was converted to vasoconstriction [149]. Fibrinogen deposition also upregulated ICAM-1 expression through activation of NFκβ and IL-8 production [146,150].

Regardless of the main cause of myocardial depression during sepsis, we postulated that during sepsis LPS and cytokine release upregulates the expression of ICAM-1 on coronary endothelial cells and cardiomyocytes. Acute phase response during sepsis also increases the level of intravascular fibrinogen, enhancing inflammation and the coagulation cascade. Fibrinogen increases the adhesion of inflammatory cells on coronary endothelial cells which is followed by adhesion of inflammatory cells to endothelial ICAM-1 and VCAM-1. In turn inflammatory cells, including PMNs, release cytotoxic materials onto the coronary endothelial cells which results in the loosening of endothelia cell tight junctions and increased leakiness. This is followed by infiltration of

soluble fibrinogen into the cardiac tissue increasing probability of interaction of ICAM-1 and fibrinogen in the cardiac tissue leading to activation of ICAM-1 and the initiation of intracellular signaling. Activation of ICAM-1 increases the heterogeneity of intracellular Ca^{2+} release which reduces cardiomyocyte contractility. Whether fibrinogen can attach to other inflammatory adhesion molecules such as VCAM-1 remains to be determined. Whether other postulated ICAM-1 ligands such as soluble of CD11/CD18 can infiltrate into the cardiac tissue through the leaky endothelium should also be determined.

Chapter-5

[2]IGF-1 protection of ischemic murine myocardium from ischemia-reperfusion associated injury

5.1   Abstract

Introduction: Ischemia-reperfusion injury occurs in myocardial infarction, cardiac dysfunction during sepsis, cardiac transplantation and coronary artery bypass grafting and results in injury to the myocardium. Although reperfusion injury is related to the nature of ischemia, it is a separate entity that may jeopardize viable cells and ultimately may impair cardiac performance one ischemia is resolved and the organ heals.

Method: The present study was conducted in an ex vivo murine model of myocardial ischemia-reperfusion injury. After 20 minutes of ischemia, isolated hearts were perfused for up to 2 hours with solution (modified Kreb's) only, solution plus insulin growth factor (IGF-1), or solution plus tumor necrosis (TNFα). Cardiac contractility was monitored continuously during this period of reperfusion.

Results: On the basis of histological evidence, IGF-1 prevented reperfusion injury as compared with TNFα; TNFα increased perivascular interstitial edema and disrupted tissue lattice integrity, whereas IGF-1 maintained myocardial cellular integrity and did not increase edema. Also, there was a significant reduction in detectable creatine phosphokinase in the perfusate from IGF-1 treated hearts. By recording transduced pressures generated during the cardiac cycle, reperfusion with IGF-1 was accompanied by markedly improved cardiac performance as compared with reperfusion with TNFα or modified Kreb's solution only. The histological and functional improvement generated

---

by IGF-1 was characterized by maintenance of the ratio of mitochondrial to nuclear DNA within heart tissue.

Conclusion: We conclude that IGF-1 protects ischemic myocardium from further reperfusion injury, and that this may involve mitochondria-dependent mechanisms.

5.2 Introduction

Cardiovascular diseases are among the leading causes of death in North America. The most important presentation of cardiovascular disease is ischemia, which leads to tissue hypoxia, cellular necrosis and apoptosis and in severe situations, organ dysfunction. The main treatment of acute ischemic heart disease is early vascular reperfusion to restore balance to cardiac metabolic demands. Although reperfusion is the foundation of therapy, it may actually initiate further injury to the myocardium. Although the phenomenon of reperfusion injury is related to the duration of ischemia, it is a separate entity and may be more severe than ischemic injury alone [220,221]. Ischemia-reperfusion injury can be generated in various cardiovascular diseases or therapies including myocardial infarction, cardiopulmonary bypass, coronary bypass grafting, heart transplantation and coronary thrombolytic therapy. It has also been speculated that the mechanism of myocardial dysfunction during septic shock is related to segmental ischemia and reperfusion in the left ventricular wall, because the involvement of persistent global ischemia has been disproved [50,222].

Ischemia results from the absence of or sluggish blood flow in coronary vessels. This leads to a mismatch between cardiac metabolic supply and demand. Ischemia of short duration may contribute to stunned myocardium without tissue injury, but prolonged ischemia results in a deficiency in energy supplies and waste removal, with eventual initiation of cellular necrosis and priming of the myocytes for apoptosis [93]. Early restoration of blood flow or reperfusion reduces the extent of myocardium at risk for death from necrosis. However in the presence of prolonged ischemia, reperfusion itself

initiates mechanisms of injury that are fundamentally different and potentially more severe than those of ischemia.

Reperfusion injury is mediated by inflammation and characterized by the production of reactive oxygen species (ROS). Production of ROS may be initiated during the ischemic phase generating "primed" myocardium. ROS activate transcription factors, such as NFκB, both in cardiac myocytes and the endothelium; in turn, this initiates transcription of genes including those encoding adhesion molecules, cytokines, coagulation mediators and proteolytic enzymes [223]. In coordination with the complement cascade, ROS can disrupt the integrity of both cardiac myocyte and endothelial cell membranes [224]. These events can change the intracellular ion homeostasis, resulting in the accumulation of calcium and metabolic by-products. These changes increase the activation of enzymes that are utilized in the processes of necrosis and apoptosis and that alter mitochondrial function [106]. At the tissue level, this is manifested by interstitial edema and disruption of the tissue lattice. Concomitantly, neutrophils and other inflammatory cells migrate into the injured zone using adhesion molecules such as ICAM-1 under the stimulation of secreted cytokines and chemotactic factors. Recruitment and infiltration of neutrophils into the injured tissue is accompanied by neutrophils degranulation and further injury to the border zone of viable cells. These late cellular events in the myocardium only occur after reperfusion [93,103,221,225]. Our previous experiments demonstrated that expression and activation of ICAM-1 is associated with decreased cardiomyocyte contractility and cardiac depression (refer to Chapter 2 and 3) [60].

Sustainable functioning of the myocardium is the central objective of therapeutic intervention in myocardial infarction. Cardiac function and contractility are closely related to cardiac metabolism and energy production. In cardiomyocytes energy production is related to the number of mitochondria, with this organelle occupying up to 40% of the cardiomyocyte cytoplasm. Hence the total number of mitochondria in the myocardial tissue can be used as a measure of cardiomyocyte activity and health [226-228]. In HIV-infected patients with symptomatic hyperlactemia receiving anti retroviral therapy, Cote and co-workers showed that the ratio of mitochondrial DNA (mtDNA) to nuclear DNA (nDNA) can be used as a marker of drug-induced mitochondrial toxicity [229]. During the last century, there have been major improvements in the strategies used to protect myocardial tissue from ischemia and reperfusion injury. These include thrombolytic therapies, percutaneous transluminal angioplasty (PTA), coronary artery bypass grafting (CABG) in the setting of acute occlusion of coronary artery and controlled reperfusion, reperfusion with modified solutions, experimental endothelial gene transcription during cardiac surgery and heart transplantation [230-234]. However, the mechanism of the ischemic-reperfusion injury remains unknown and our abilities to treat or prevent it are therefore limited. Using methods similar to those used by Cote and coworkers, we investigated changes in heart mitDNA:nDNA ratio during myocardial ischemia and reperfusion phases, and compared these levels to additional measures of tissue injury.

New markers of myocardial injury may provide mechanistic insights and reveal therapeutic possibilities in reperfusion injury. Here, we propose a new method, using

IGF-1, of protecting cardiac tissue against ischemia-reperfusion injury in an ex vivo murine model. The mechanism underlying this protective effect remains unclear. However, the level of ICAM-1 protein expression is significantly lower in the presence of IGF-1. The integrity of the myocardial tissue lattice was preserved and the development of interstitial edema in myocardial tissue was inhibited. These effects were correlated with improved perfusion pressure and left ventricular compliance. We also demonstrated that this IGF-1 mediated protection was accompanied by preservation of mtDNA content. It has been shown that mutation in mtDNA promotes apoptosis in the presence of predisposing factors such as ultraviolet [235]. Intragastic administration of ethanol in mice decreases mtDNA level of skeletal muscles, liver, cardiac, and brain tissues. This effect of ethanol can be prevented using antioxidants [227]. The high level of ROS formation is associated with higher level of mutated mtDNA [228].

5.3 Methods and Materials

5.3.1 Ischemia-reperfusion model: C57B6 mice 25-30 g (Jackson Laboratories, Bar Harbor, ME) were anesthetized using 3% isoflurane (Baxter, Toronto, ON, Canada) for one minute and maintained at 1% isoflurane for 3-5 min during cardiac excision. To prevent coagulation in coronary vessels 500 units Heparin-sodium (Organon Teknika Inc. Toronto, ON, Canada) was injected intra-peritoneally 10 min before induction of anesthesia. The heart was excised and assembled on a Langendorff apparatus and perfused with oxygenated (95% O_2 + 5% CO_2) modified Kreb's Henseleit working solution (MK) at 37°C for 3-5 min [236-238] until monitoring reveal that organ was stable. Transduced left ventricle and aortic pressures, and heart rate were monitored continuously using Power lab/8sp detector (AD Instruments Pty Ltd. Castle Hill, Australia). Retrograde perfusion was then stopped for 20 min to model of global ischemia (a period of 20 min of ischemia was found to be optimal for the ischemic phase in this model). The ischemic hearts were then reperfused with MK solution alone, MK solution plus IGF-1 (10 ng/mL), or MK solution plus TNF-α (10 ng/mL) for 1h or 2h. After completion of the reperfusion period, the hearts were divided into symmetrical halves. One half was frozen using 2-methylbutane (Isopentane, MERK KgaA, Darmstadt, Germany) in liquid nitrogen for 80 sec for eventual sectioning and/or DNA isolation. Paraffin embedding of the other half followed fixation of the sample in 10% formalin.

5.3.2 Histologic evaluation: Slides of paraffin embedded tissues from the apex to the basal portion of the hearts were prepared and stained with hematoxylin and eosin (H&E). Serial 400× magnified images were captured using a Nikon E600 microscope and Spot

Advanced software (version 3.4.2 S. Leffler & Silicon Graphics Inc. Mountain view, CA). Image Pro-Plus software (Media Cybernetics, Carlsbad, CA) was used to evaluate the severity of interstitial edema around the perivascular spaces of coronary arteries and veins. Measures were taken in 10 sections from each of 4 hearts for all conditions and time points. The extent of interstitial edema was measured by selecting a circular area with a radius two times greater than the vascular space contained within the drawn circle. The total vascular (V) and perivascular areas (pV) were measured. "Non-tissue" area (NT) was determined by color segmentation images constructed by Image Pro-Plus. Total interstitial edema was determined by subtracting the vascular area from the non-tissue area and expressing this as a percentage of total perivascular area Percentage of edema = [NT-V]/pV × 100.

5.3.3 ICAM-1 expression of cardiac tissue:

Frozen sections of the hearts were fixed and stained with Alexa 594 anti-ICAM-1 antibody, and Hoechst nuclear staining. Using confocal microscopy (400×) images were captured. The mean intensity of ICAM-1 and Hoechst staining were measured using fluo-cytogram software in gray scale (0-255) as previously mentioned in chapter-3 section. The ratio of ICAM-1 to nuclear staining was measured and compared to control groups (refer to chapter 3 section 3). The level of ICAM-1 mRNA was also measured (refer to chapter 2 section 3.3).

5.3.4 Ventricular function assessment:

Heart rate and pressure generated during the cardiac cycle was obtained by transduction of the aortic cannula and recorded

continuously during ischemia and reperfusion using Power lab/8sp detector. Using Powerlab software the difference between *ex vivo* systolic and diastolic pressure ($\Delta P_{Sys/Dia}$) at different time points was calculated to assess ventricular performance. Pressure measured during systole reflected contractility and diastolic pressure drops reflected relaxation of the ventricle. Thus greater $\Delta P_{Sys/Dia}$ values indicate better overall performance of the left ventricle.

5.3.5 Detection of CPK: A 1 mL sample of myocardial perfusate was collected every 15 minutes during the reperfusion phase. The samples were frozen in a mixture of ethanol and dry ice [239,240]. The level of creatine phospho-kinase (CPK) was measured using Vitros CK slides (Ortho-Clinical Diagnostics, Rochester, NY). Briefly 11 µL of perfusate was deposited on the slide and evenly distributed. Samples were incubated for 5 minutes at 37°C. After final interaction, leuco-dye is oxidized by hydrogen peroxide in the presence of peroxidase to form an insoluble dye. Reflection densities are monitored during incubation and the rate of change in reflection density is then converted to enzyme activity by using 670 nm wavelength in the Vitros Chemistry 250 System.

5.3.6 MitDNA:nDNA assay: Frozen hearts initially embedded in opaque tissue-fixation material were thawed, cut into small pieces (~3 mg) and then placed into lysis buffer. DNA was extracted using the Qiagen DNA isolation kit, (Qiagen Canada QIAGEN Inc. Mississauga, Ontario, Canada) in accordance with the manufacturer's protocol. Extracts were then diluted 1/80 with buffer AE before performing the mtDNA assay, as reported in murine tissues as described below [226,229,241].

For each DNA extract, one murine nuclear gene (accessory subunit of the murine mitochondrial DNA polymerase γ (ASPG), Genbank Accession number AF177202) and one murine mitochondrial gene (cytochrome oxidase subunit 1 [COX], Genbank Accession number AB042432) were quantified separately by real-time, quantitative PCR, using the Roche LightCycler (Roche Diagnostics, Indianapolis, IN). For the mitochondrial (COX) gene, the forward primer mCOX1F (5'-TCGTTGATTATTCTCAACCAATCA-3') and the reverse primer mCOX2R (5'-GCCTCCA ATTATTATTGGTATTACTATGA-3') were used. The oligonucleotides 3'-fluorescein-mCOXPR1 (5'-AACCAGGTGCACTTTTAGGAGATGACC-F3') and 5'-LC Red 640 3'-phosphate-blocked-mCOXPR2 (5'-L-AATTTACAATGTTATCGTAACTG CCCATGC-P3') were used as hybridization probes. For the nuclear (ASPG) gene, the forward primer mASPG1F (5'-GGAGGAGGCACTTTCTCAGC-3') and the reverse primer mASPG2R (5'-GAAGACCTGCTCCCTGAACAC-3') were used. The oligonucleotides 5'-flourescein-mASPGPR1 (GCGCTTTGGACCTTTGGGTGTAG-F3') and mASPGPR25'L- GTTACGAAAGAACCTAGCCTCACAGTGGT-P3') were used as hybridization probes. PCR reactions and amplification cycles were performed as described [229].

A standard curve consisting of serially diluted mouse DNA (30 000, 6000, 1200, 240 and 48 nuclear genome equivalents) were included in each run. The same standard curve was used to quantify both the nuclear (ASPG) and the mitochondrial (COX) gene. mtDNA and nDNA genes were assayed in duplicate. Results of the quantitative PCR assay were

expressed as the ratio of the mean value of the duplicate mtDNA measurements to the mean value of duplicate nDNA measurements. As a further quality control, a mouse DNA extract with a mtDNA:nDNA, known to be high and an extract with a mtDNA/nDNA ratio known to be low were included in every run. Repeat sample and intra-sample variations were <5%.

5.4 Results

5.4.1 IGF-1 decreases ICAM-1 expression of cardiac tissue during reperfusion:

Twenty minutes ischemia follow by 2 hours reperfusion with MK increased the expression of ICAM-1 on cardiac tissue compared to control (3.4 ± 0.2 vs 1.5 ± 0.1 $p<0.001$) as determined by the measured ratio of ICAM-1 to nuclear staining. Two hours reperfusion with TNFα significantly increases ICAM-1 expression relative to control, and MK (4.0 ± 0.2, $p<0.05$). Reperfusion in the presence of IGF-1 did not increase ICAM-1 protein expression on cardiac tissue (1.9 ± 0.1 vs 1.5 ± 0.1, $p=NS$). This indicates that suppression of ICAM-1 expression during reperfusion in the presence of IGF-1 (Figure 5.1A) may contribute to better cardiac performance. However reperfusion with IGF-1 did not prevent the increased level of ICAM-1 mRNA suggesting that the inhibition of ICAM-1 is at the level of protein expression during reperfusion (Figure 5.1B).

5.4.2 Perivasular interstitial edema and tissue lattice integrity: The cellular integrity of the myocardium was well preserved in the tissue of hearts reperfused with IGF-1 (Figure 5.2). The area of interstitial edema in IGF-1 treated hearts was $21 \pm 4\%$ compared to $34 \pm 6\%$ and $49 \pm 5\%$ for reperfusions with MK only and MK with TNF-α respectively ($p<0.05$). Representative tissue histology images are presented in Figure 5.2 and were similar throughout the four hearts and in all conditions. Additional histology observations included an increased number of shrunken, contracted myocytes with dense
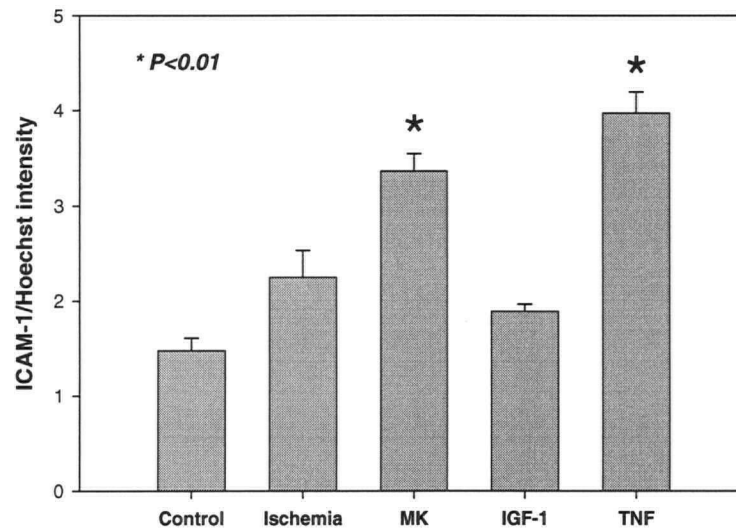
Figure 5.1A   Reperfusion of ischemic hearts with MK only and MK with TNFα increased the expression of ICAM-1 protein on cardiac tissue (p<0.01). This effect can be prevented using IGF-1 in MK.
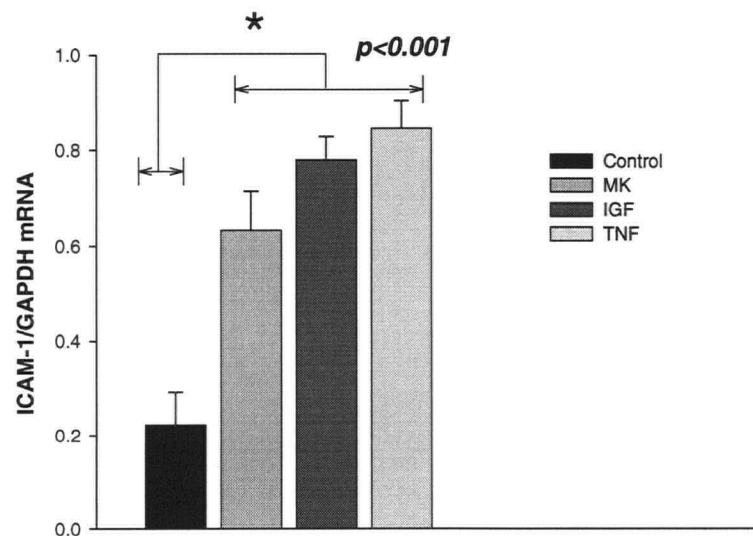
Figure5.1BReperfusion of ischemic hearts with MK only, MK with TNFα, and MK with IGF-1 increased the expression of ICAM-1 mRNA of cardiac tissue compared to control group (p<0.001).
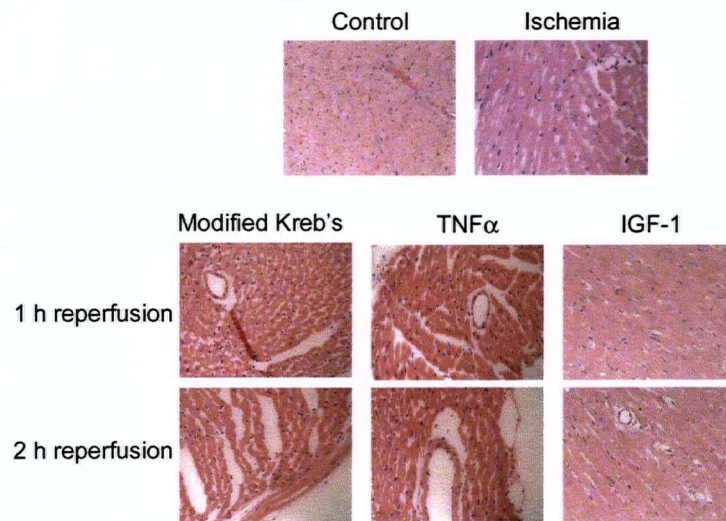
Figure 5.2   Representative images (×400) of hematoxylin and eosin stained sections from murine hearts subjected to ischemia/reperfusion. Images are of control, ischemia without reperfusion, and reperfusion with modified Kreb's Henseleit working solution (MK) alone, MK plus tumor necrosis factor (TNFα), and MK plus insulin-like growth factor (IGF-1), both at 1 and 2 hours. Note the preservation of cellular and structural elements and the lack of interstitial edema in IGF-1 reperfused heart.

pycnotic nuclei with MK plus TNF-α reperfusions as compared with perfusate containing IGF-1.

5.4.3 IGF-1 improvement in myocardial performance during reperfusion: Cardiac performance was determined by calculating the pressure difference between systole and diastole ($\Delta P_{sys/dia}$) at set time points. The systolic and diastolic pressures were determined by taking the average values from a window around the respective time points. Performance is then a measure of both contractility (stroke volume and force of left ventricle contraction manifesting as systolic pressure) and diastolic function, or relaxation of the left ventricle (a reduction in diastolic pressures). Improved performance is manifested then by a widening in $\Delta P_{sys/dia}$. Pressure monitoring demonstrated that cardiac performance increased from 0 to 40 min of reperfusion for all conditions (Figure 5.3). After 40 min of reperfusion, cardiac performance arrived at a plateau and became negative for the remaining minutes for the MK alone or MK plus TNF-α reperfusions. With reperfusion with MK plus TNF-α the $\Delta P_{sys/dia}$ initially increased to 6.8 ± 0.7 mmHg as compared with reperfusion with MK alone (5.1 ± 0.6 mmHg). However, reperfusion with IGF-1 generated a $\Delta P_{sys/dia}$ that was significantly greater (13.8 ± 1.2 mmHg) than with TNF-α (6.8 ± 0.7 mmHg) by 20 min. Heart rate was significantly increased in the presence of IGF-1 (172.4 ± 4.2) compared to MK (58.3 ± 2.8) and TNFα (101.7 ± 3.8). This gain in cardiac performance was maintained up to 120 minutes of reperfusion with IGF-1. The enhanced performance was reflected in improvements in both systolic and diastolic pressures and heart rate. The late descent in slop at 120 minutes of reperfusion with IGF-1 was similar to that occurring with reperfusion with MK alone or MK plus

TNF-α, but may relate to *ex vivo* conditions other than the ischemia time and the reperfusion solution. A paired two sample t-test for means between groups demonstrated a statistically significant difference between IGF-1 and MK alone and MK with TNF-α (p<0.005).

5.4.4 Low creatine phosphokinases level in IGF-1 treated hearts: Collected perfusate from hearts treated with IGF-1, at all reperfusion time points, contained significantly lower quantities of detectable CPK (34.6 U/L) than did perfusate from TNF-α treated hearts (113.6 U/L). This is shown as an average for all time points (Figure 5.4). Single factor ANOVA revealed a significant difference between groups (p<0.005).

5.4.5 Ratio of mitochondrial to nuclear DNA: IGF-1 maintained or improved the mtDNA:nDNA ratio during reperfusion of ischemic myocardium as compared with control reperfusion with MK alone. There was a significant difference between all test groups (baseline, ischemia, MK alone reperfusion, and MK with IGF-1 reperfusion) in the determined mtDNA:nDNA (p<0.05 ANOVA). Based on previous work, it was thought useful to test the utility of mtDNA:nDNA to assess the "cellular health" of ischemic and reperfused myocardium tissues [226,227]. How IGF-1 preserves mtDNA:nDNA and if this also means intact oxidative mitochondrial function that promotes cellular viability remains to be investigated. We found that IGF-1 appeared to protect heart tissue against a reduction in the mtDNA:nDNA, which was accompanied by improved histological grading and improved organ function in terms of contractility. A reduction in this ratio may represent either necrosis of at risk tissue or a reduction in mitochondrial

number after the initial stimulus (ischemia) followed by subsequent reperfusion (Figure 5.5). Such a reduction was noted with reperfusion with MK alone after the initial increase in mtDNA:nDNA that occurred after ischemia alone without reperfusion. Because this model utilized a cell free perfusate the mtDNA:nDNA is not confounded by potential contributions from immune cells, a point that has been raised as a possible explanation for changes in mtDNA:nDNA.
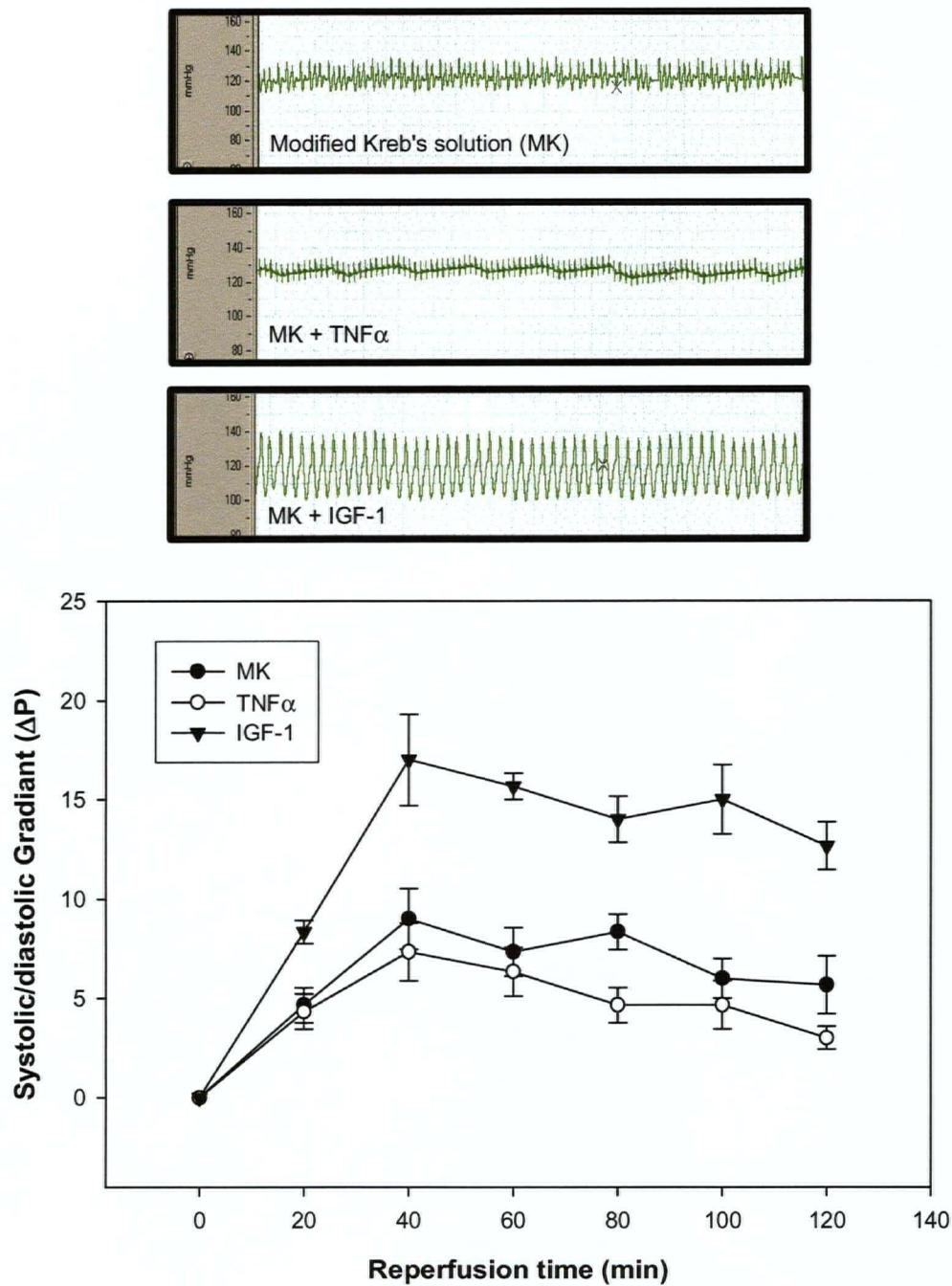
Figure 5.3   Determination of cardiac performance. (A) Tracing from continuous monitor recording obtained during ischemia and reperfusion. (B) Determination of cardiac performance is as described in the methods section and includes calculation of the pressure gradient between systolic and diastolic pressure transductions from the aorta and left ventricle. Reperfusion with IGF-1 generates a significant improvement in cardiac performance at all time points ($p < 0.05$).
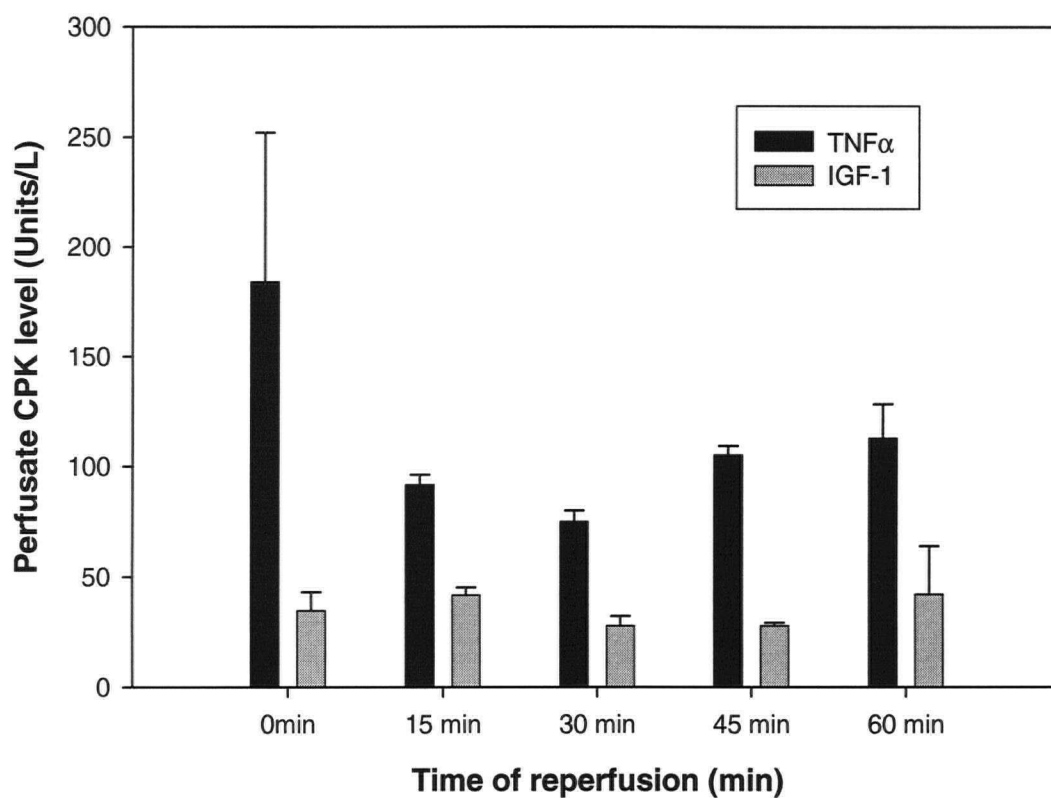
Figure 5.4   Measured creatine phosphokinase (CPK) in perfused murine hearts. Hearts were prepared for ex-vivo reperfusion. Perfusate solution was collected (1 ml/4 min) around each time points. Reperfusion with TNFα generates a significant elevation in the detectable amount of CPK activity relative to that detected with IGF-1 (p<0.005).
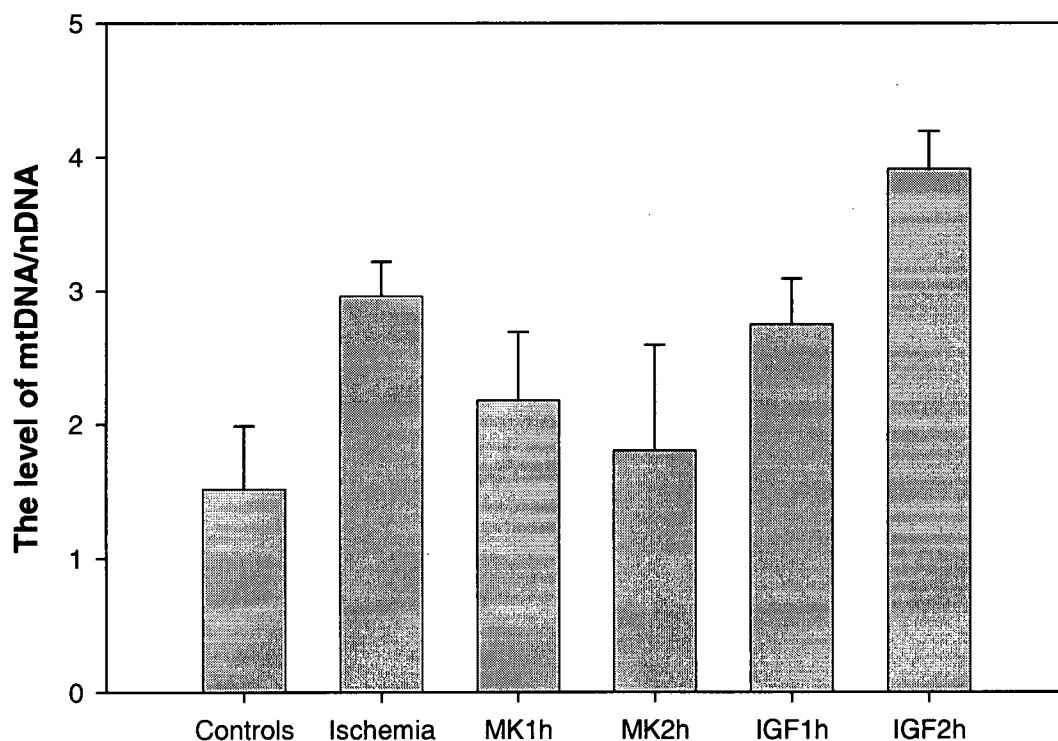
Figure 5.5   Determination of mitochondrial DNA (mtDNA) to nuclear DNA (nDNA) ratio. The mtDNA:nDNA ration was determined for all conditions (p<0.05). The ratio of mtDNA/nDNA was determined for the following conditions: control, ischemia without reperfusion, modified Kreb's alone for 1h (MK 1h), modified Kreb's alone for 2h (MK 2h), modified Kreb's with IGF-1 for 1h (IGF 1h), and modified Kreb's with IGF-1 for 2h (IGF 2h). The number within each histogram represents the number of hearts processed for that condition. The values for mtDNA/nDNA in the controls, ischemic myocardial tissue and either reperfusion group (MK or IGF-1) were significantly different from each other (p<0.05).

5.5   Discussion

Despite a range of clinical interventions, our ability to prevent reperfusion injury after disruption of blood flow to vascular beds remains disappointing. An appreciation of the mechanism of ischemia/reperfusion injury is central to development of better treatments. In the present study we demonstrated that IGF-1 can lessen reperfusion injury following an initial ischemic insult.

The anti-inflammatory effect of IGF-1 on cardiac and other tissues has been shown previously [85,102,242]. We found that IGF-1 inhibits the expression of ICAM-1 protein on myocardial tissue after ischemia and during reperfusion. However IGF-1 cannot inhibit the presence of ICAM-1 mRNA suggesting the effect is on translation or transportation of ICAM-1 during reperfusion. The failure in translation or transportation of ICAM-1 protein to the membrane could be related to the activation of PI3-kinase pathways which is activated by IGF-1 [87,231]. This effect of IGF-1 can be through usage of PIP2 [243] which is also necessary for ICAM-1 dimerization [151,244]. ICAM-1 expression and activation is associated with decreased cardiomyocyte contractility which results in decreased cardiac contractility. IGF-1 decreases ICAM-1 expression on cardiac tissue and improves cardiac performance.

This effect of IGF-1 on the ischemic myocardium was supported by histological evidence of improved tissue and cellular integrity, including markedly less interstitial edema around the perivascular spaces. In this model, ischemic myocardium treated with IGF-1

had significantly lesser amounts of detectable CPK than did myocardium treated with TNF-α, suggesting reduced cellular injury. This is also consistent with the cardiac performance and left ventricular contractility of IGF-1 treated hearts that exhibited a greater $\Delta P_{Sys/Dia}$ and heart rate compared to control and TNFa treated groups. It should be noted that the detectable CPK levels would not be above the normal range as determined for human whole blood samples. However, there was considerable histological evidence of tissue damage in the TNF-α treated hearts, suggesting the relative insensitivity of CPK in detecting lesser myocardial injuries. A more sensitive marker would be valuable not only for studying the mechanism that underlies reperfusion injury but also for evaluating the efficacy of therapeutic interventions. This is particularly true when one considers the segmental and intermittent ischemic/reperfusion zones that characterize dysfunctional myocardium in sepsis. The initial improvement in contractility, observed under all conditions of reperfusion, was probably the result of a new supply of nutrients after the ischemic period, including oxygen. The addition of IGF-1 significantly augmented this improvement in left ventricular pressure generation and relaxation (thus increasing $\Delta P_{Sys/Dia}$). This improvement was maintained throughout the period of reperfusion.

Myocardial performance at the cellular level is associated with the number or functional capacity of mitochondria. To investigate indirectly whether mitochondrial function may represent a maker of this beneficial effect of IGF-1, we determined the mtDNA:nDNA ratio in relation to myocardial function. Although not appreciated clinically, ischemia and reprefusion are two distinct periods [87,98,225,230,232]. The ischemic period has been described as 'priming' cardiac myocytes for either a necrotic or apoptotic death. A marked increase

in mtDNA:nDNA ratio was detected in the ischemic myocardium relative to baseline control levels. Apoptosis has been found to be an event that requires energy [245,246]. This increased mtDNA:nDNA ratio may indicate an increase in the number of mitochondria per cell or an increase in the genome copy number per mitochondria. However the above effect of IGF-1 should be investigated because of the effect of IGF-1 on saving mutant forms of mtDNA [228].

Myocardial reperfusion injury, as a separate event, can increase the extent of injury beyond that caused by ischemia alone. It has been shown that modification of solutions or other conditions during the reperfusion phase can alter the extent of cellular and functional damage to the myocardium. We determined that the nature of the reperfusate can affect mtDNA:nDNA ratio. Reperfusion with MK alone resulted in a reduction, in mtDNA:nDNA ratio toward baseline values. This may reflect either mitochondrial mitoptosis in damaged and 'primed' tissues or the necrotic loss of similar cells that were 'primed', resulting in elevated mtDNA:nDNA ratio after ischemia. The net effect would be that the remaining tissue is spared and should reflect baseline tissue. However, a mtDNA:nDNA ratio that does not differ from baseline does not indicate that the tissue is working normally. In fact, histology and contractility determinations demonstrated that the heart had sustained significant tissue damage and was dysfunctional after MK reperfusion. With IGF-1 reperfusion this reduction in mtDNA:nDNA ratio was prevented, suggesting that the extent of injury is not associated with elevated mtDNA:nDNA ratio alone. In fact, after ischemia reperfusion, it was found a normal mtDNA:nDNA early after reperfusion predicted significant tissue injury. The patterns of

mtDNA:nDNA ratio, as seen in this model, may prove useful in future investigation of possible mitochondrial-related mechanisms of reperfusion injury.

IGF-1 can affect cardiomyocyte contractility through its receptor - a heterotetrameric protein with intracellular tyrosine kinase activity [247]. Downstream signals after receptor activation include Shc, Crk and phospholipase C, and activation of phosphatidylinositol-3 (PI3) kinase. Guse and coworkers [243] demonstrated that IGF-1 can increase IP3 levels in rat cardiomyocytes. Through its action on PI3 kinase, IGF-1 can affect both contractility [85] contractility and apoptosis [248]. The action of IGF-1, as demonstrated in our myocardial ischemia/reperfusion model, may occur via PI3 kinase and/ or effects on mitochondria. Increases in cardiomyocyte calcium levels and cardiomyocyte sensitivity to calcium [249] have been demonstrated to effect cardiac performance. Alteration in calcium metabolism may interfere with the action of calcium because the filamentous network of cardiomyocytes and their contractile properties are extremely sensitive to even small fluctuations in calcium ion concentration [250]. ICAM-1 activation and hemodimerization is dependent on the one of the products of PI3 kinase pathways ie PIP2[151,244]. The decreased expression of ICAM-1 in the presence of IGF-1 can be explained by an increase level of IP3 which need consumption of PIP2. This may show that IGF-1 reduces the level of PIP2 to increase production of IP3 and calcium release from sarcoplasmic reticulum. However in this ex vivo model of ischemia reperfusion injury the protective effect of IGF-1 may not be related to the ICAM-1 activation because of lack of ICAM-1 ligands such as CD11/CD18 receptors on inflammatory cells. Fibrinogen, a ligand for ICAM-1, is present but not at the concentration that may be in the circulation. Thereby the

protective effect of IGF-1 may be more from the indirect effect of IGF-1 on ICAM-1 expression, i.e., PI3K pathway.

Hence it is logical to speculate that IGF-1 can be used as a therapeutic intervention to inhibit ICAM-1 expression in various types of inflammatory responses including sepsis especially when we use it before the initiation of inflammatory responses as a preventive agent. It is important to note that IGF-1 per se can increase the survival of inflammatory cells and increase the degranulation ability of the inflammatory cells thereby using IGF-1 as a therapeutic agents in inflammatory response should be with a very careful assessment and evaluation and it needs more investigations.

A similar result to that presented here for IGF-1 in myocardial ischemia/reperfusion has been demonstrated for vascular endothelial growth factor (VEGF), suggesting that a final common 'protective' pathway may exist [250]. Anwar and coworkers [251] showed that TNF-α decreased IGF-1 mRNA and increased IGF-1 binding protein-3 mRNA expression in vascular smooth muscle cells. These actions of TNF-α effectively reduce free IGF-1 levels and activity, promoted endothelial instability. Infusion of the modified IGF-1 reduced the TNF-α induced apoptosis. An interaction between VEGF and IGF-1 was characterized in retinal neovascularization in diabetic patients [86,252]. The authors of that report described common mitogen kinase 44/42 pathways that may be related to the mitogenic effect of those two molecules. However the short time effect for both IGF-1 and VEGF in myocardial ischemia/reperfusion models is most probable through the Akt pathway [86,252]. Akt activation can improve contractility through PI3 kinase signaling and

is also an initiator of protein kinase C activation upstream. Protein kinase C plays an important role in cardiac function, calcium metabolism, and contractility. Michell and coworkers showed that IGF-1 and VEGF both stimulate nitric oxide production from endothelial cells and that inhibition of PI3 kinase by wortmannin and LY29004 decreases nitric oxide production and reduces cardiac function [86]. Akt signaling has also been demonstrated to prevent apoptosis. Whether this pathway alters the expression of bcl-2 family members by IGF-1 exposure remains unknown.

It has been shown that IGF-1 can protect myocardium and other tissues against apoptosis in various animal models [84,253,254]. IGF-1 may also improve cardiac function in diabetic patients [84,102,254-256] and rat models of myocardial infarction and reperfusion [87]. It has been shown that IGF-1 can protect myocardium by regulating changes in proapoptotic and/or antiapoptotic molecules such as Bcl-2, Bcl-X_L and Bax. These are all related to the mitochondrial apoptotic pathway and mitochondrial energetics [87]. This may also explain, in part, how IGF-1 protects myocardium even in the later phase of reperfusion injury.

In an ex vivo model of myocardial ischemia and reprefusion we demonstrated that IGF-1 protects against the reperfusion-associated injury. It can decrease the level of the inflammatory response by the reduction of membranous ICAM-1 presentation. We found this protective effect of IGF-1 to be correlated with elevated mtDNA:nDNA relative to baseline, and this may represent a marker for the preservation of mitochondrial function. This study provides new insight into ischemia/ reperfusion and possible mechanisms and treatment for the tissue injury and organ dysfunction associated with this process. The

eventual benefit of this to our understanding of myocardial dysfunction in sepsis awaits further study.

Chapter-6

Final conclusion

All cardiac inflammatory diseases including ischemia reperfusion injury, sepsis, transplant rejection, myocarditis and cardiomyopathy contain a common pathway regardless of the main causes of myocardial inflammation. The inflammatory response of the heart is manifested by lowered cardiac pumping function. At the cellular level, myocardial inflammation is associated with increased cytokine release, recruitment and activation of inflammatory cells [59,60,107,108] and activation of coronary endothelial cells [109,110]. The above events increase the level of adhesion molecules on endothelial cells and cardiomyocytes [92,110,160,162] followed by an interaction between receptors of endothelial cells and activated leukocytes. One of the most important receptors in cardiac inflammatory responses is ICAM-1.

ICAM-1 (CD-54), a 76-114 kDa glycoprotein, is expressed in both normal and activated cardiomyocytes [59,60,107,108]. Within 2 to 4 hours cytokines and LPS treatments increase endothelial ICAM-1 expression [109,110]. This upregulation of ICAM-1 facilitates neutrophil binding and migration which has been demonstrated using cultured endothelial cell monolayer in vitro, a process involving the interaction of ICAM-1 with LFA-1 (CD11a/CD18) and Mac-1 (CD11b/CD18) [126-128]. Furthermore, the extracellular domains of the ICAM-1 molecule can interact with various ligands including fibrinogen [129], Rhinoviruses [125], Coxsackie viruses [130,131], and Plasmodium falciparum [132].

Our experiments demonstrate that ICAM-1 is not only a receptor for adhesion of leukocytes or other proteins, but also functions as a regulatory protein, specifically in cardiomyocyte contractility. In vitro we have shown that cardiomyocyte ICAM-1 activation, through the binding of CD11/CD18 receptors of inflammatory cells, or by cross-linking, reduces cardiomyocyte contractility. This effect of ICAM-1 activation is associated with cardiomyocyte cortical cytoskeleton assembly and related proteins such as FAK and RhoA which result in alteration of Ca^{2+} propagation during excitation contraction cycles. Whether this change in calcium influx is due to the alteration in juxtaposition of cardiomyocyte Ca^{2+} ions should be investigated through electron microscopy. Our preliminary experiments, using nanogold labeled antibodies to detect RyR and DHPR juxtaposition, seem promising (Figure 6.1).

Using an in vivo model of sepsis in mice we then demonstrated that LPS injection increases ICAM-1 expression of cardiac tissue and decreases cardiac function. LPS injection in mice changes the peripheral blood cell differentiation showing decreased the leukocyte count, increased the percentage of PMN, and decreased the platelet count. The effect of LPS on cardiac function is related to the number of inflammatory cells as demonstrated by impaired cardiac function in neutrophillic (GCSF treatment) mice and improved cardiac function in neutropenic mice (cyclophosphamide treatment). These findings indicate the importance of inflammatory cells in inducing cardiac dysfunction in the endotoxemia models.

Lack of the ICAM-1 gene (protein) protects murine cardiac function against the effect of LPS. By using a chimeric model we have found that the level of ICAM-1 expression on cardiac tissue is directly associated with lower cardiac function. Although the presence of ICAM-1 on inflammatory cells is an important co-factor for antigen recognition, there is no defect of inflammatory response in our chimeric model demonstrated by the same response of chimeric (H^+/M^-) and wild type mice to the effect of LPS.

Although the above effect of LPS (decreased cardiac function) is associated with recruitment of circulatory inflammatory cells to the left ventricle, which was demonstrated by a higher number of intravascular and adherent inflammatory cells, there is no evidence of the presence of inflammatory cells in the cardiac interstitial space, excluding the role of inflammatory cells in the activation of cardiomyocyte ICAM-1 through the interaction of their ligands (CD11/CD18). Furthermore investigations using BrdU staining of bone marrow did not show the presence of inflammatory cells in the cardiac interstitial space confirming the above results. Therefore CD11/CD18 receptors on inflammatory cells may not be a reason for cardiomyocyte ICAM-1 activation after LPS injection.

Figure 6.1   Preliminary experiment using nanogold beads and electron microscopy to define the juxtaposition of RyR (< 5 nm) and DHPR (6 nm).

We then demonstrated that fibrinogen can decrease cardiomyocyte contractility. This effect of fibrinogen occurs via its activation of ICAM-1. We also observed that after LPS injection fibrinogen infiltrates into the cardiac tissue indicating that fibrinogen can enter into cardiac tissue in the presence of a leaky endothelial surface.

The result of investigation of IGF-1 in the model of ischemia reperfusion injury demonstrated that IGF-1 can inhibit the expression of ICAM-1 in cardiac tissue. The mechanisms of cardiac dysfunction in the model of ischemia reperfusion injury, although is different from those of the sepsis model, have many common intracellular cascades including increased ICAM-1 expression. During ischemia reperfusion injury some part of myocardial dysfunction is irreversible because of myocardial necrosis, while viable and at-risk cardiac tissues accompanies with less injury and reversible dysfunction. The important step to save myocardium from further cardiac damage during reperfusion is to save at-risk and remaining myocardium. I believe that the at-risk area of myocardium has a similar mechanism of myocardial dysfunction to that of sepsis. Whether IGF-1 can be used as a therapeutic intervention to improve cardiac function during sepsis has yet to be investigated. Although the clinical trial of IGF-1 in septic patients failed to show the benefits of IGF-1 treatment in critically ill patients, I believe the decrease in ICAM-1 expression in the presence of IGF-1 should be seen before initiation of the severe inflammatory process as we have also seen in chapter 5. In addition to the other benefits of IGF-1 on cardiac function which were mentioned in chapter 5, it is important to consider that IGF-1 can improve calcium release which may abrogate the final effect of ICAM-1 activation on cardiomyocyte Ca^{2+} influx.

Taken together we have found that one of the most important causes of decreased cardiomyocyte contractility is a result of ICAM-1 activation. ICAM-1 activation changes Ca^{2+} influx during excitation contraction. The expression of ICAM-1 on cardiac tissues was increased after LPS injection and the presence and activation of ICAM-1 on cardiac tissue is necessary and sufficient to induce cardiac dysfunction. LPS injection increases intravascular and adherent inflammatory cells on the coronary endothelium. The number of interstitial inflammatory cells in the LPS treated hearts did not increase thereby excluding the role of CD11/CD18 receptors in ICAM-1 activation. However we speculate that the presence of inflammatory cells increases the leakiness of the endothelial surface, enabling infiltration of fibrinogen into the cardiac tissue after LPS injection. The adhesion of fibrinogen to cardiomyocyte ICAM-1 can decrease cardiomyocyte contractility and consequently cardiac function in our endotoxemic model of sepsis. This experimental conclusion could be extended to describe one of the mechanisms of cardiac inflammatory processes which are involved in reversible cardiac dysfunction in various types of cardiac diseases.

References:

1. Angus DC, Wax RS. Epidemiology of sepsis: an update. *Crit Care Med.* 2001;29:S109-16.

2. Bone RC, Balk RA, Cerra FB, Dellinger RP, Fein AM, Knaus WA, Schein RM, Sibbald WJ. Definitions for sepsis and organ failure and guidelines for the use of innovative therapies in sepsis. The ACCP/SCCM Consensus Conference Committee. American College of Chest Physicians/Society of Critical Care Medicine. *Chest.* 1992;101:1644-55.

3. Slade E, Tamber PS, Vincent JL. The Surviving Sepsis Campaign: raising awareness to reduce mortality. *Crit Care.* 2003;7:1-2.

4. Rivers E, Nguyen B, Havstad S, Ressler J, Muzzin A, Knoblich B, Peterson E, Tomlanovich M. Early goal-directed therapy in the treatment of severe sepsis and septic shock. *N Engl J Med.* 2001;345:1368-77.

5. Fatkin D, Graham RM. Molecular mechanisms of inherited cardiomyopathies. *Physiol Rev.* 2002;82:945-80.

6. Fill M, Copello JA. Ryanodine receptor calcium release channels. *Physiol Rev.* 2002;82:893-922.

7. Fill M. Mechanisms that turn-off intracellular calcium release channels. *Front Biosci.* 2003;1:d46-54.

8.	Ferrier GR, Howlett SE. Cardiac excitation-contraction coupling: role of membrane potential in regulation of contraction. *Am J Physiol Heart Circ Physiol*. 2001;280:H1928-44.

9.	Ramos-Franco J, Fill M, Mignery GA. Isoform-specific function of single inositol 1,4,5-trisphosphate receptor channels. *Biophys J*. 1998;75:834-9.

10.	Fujita K, Matsumura Y, Miyazaki Y, Takaoka M, Morimoto S. Effects of the endothelin ETA-receptor antagonist FR139317 on development of hypertension and cardiovascular hypertrophy in deoxycorticosterone acetate-salt hypertensive rats. *Jpn J Pharmacol*. 1996;70:313-9.

11.	Chandrashekhar Y, Prahash AJ, Sen S, Gupta S, Roy S, Anand IS. The role of arginine vasopressin and its receptors in the normal and failing rat heart. *J Mol Cell Cardiol*. 2003;35:495-504.

12.	Rosales RA, Fill M, Escobar AL. Calcium regulation of single ryanodine receptor channel gating analyzed using HMM/MCMC statistical methods. *J Gen Physiol*. 2004;123:533-53.

13.	Sham JS, Song LS, Chen Y, Deng LH, Stern MD, Lakatta EG, Cheng H. Termination of Ca2+ release by a local inactivation of ryanodine receptors in cardiac myocytes. *Proc Natl Acad Sci U S A*. 1998;95:15096-101.

14.	Tibbits GF, Xu L, Sedarat F. Ontogeny of excitation-contraction coupling in the mammalian heart. *Comp Biochem Physiol A Mol Integr Physiol*. 2002;132:691-8.

15.   Wier WG, Balke CW. Ca(2+) release mechanisms, Ca(2+) sparks, and local control of excitation-contraction coupling in normal heart muscle. *Circ Res.* 1999;85:770-6.

16.   Krishnagopalan S, Kumar A, Parrillo JE. Myocardial dysfunction in the patient with sepsis. *Curr Opin Crit Care.* 2002;8:376-88.

17.   Parker MM. Pathophysiology of cardiovascular dysfunction in septic shock. *New Horiz.* 1998;6:130-8.

18.   Court O, Kumar A, Parrillo JE, Kumar A. Clinical review: Myocardial depression in sepsis and septic shock. *Crit Care.* 2002;6:500-8.

19.   MacKenzie IM. The haemodynamics of human septic shock. *Anaesthesia.* 2001;56:130-44.

20.   Di Giantomasso D, May CN, Bellomo R. Vital organ blood flow during hyperdynamic sepsis. *Chest.* 2003;124:1053-9.

21.   Shoemaker WC, Appel PL, Kram HB, Bishop MH, Abraham E. Temporal hemodynamic and oxygen transport patterns in medical patients. Septic shock. *Chest.* 1993;104:1529-36.

22.   Ruokonen E, Takala J, Kari A, Saxen H, Mertsola J, Hansen EJ. Regional blood flow and oxygen transport in septic shock. *Crit Care Med.* 1993;21:1296-303.

23. Fong YM, Marano MA, Moldawer LL, Wei H, Calvano SE, Kenney JS, Allison AC, Cerami A, Shires GT, Lowry SF. The acute splanchnic and peripheral tissue metabolic response to endotoxin in humans. *J Clin Invest.* 1990;85:1896-904.

24. Silverman HJ, Tuma P. Gastric tonometry in patients with sepsis. Effects of dobutamine infusions and packed red blood cell transfusions. *Chest.* 1992;102:184-8.

25. Wan L, Bellomo R, Di Giantomasso D, Ronco C. The pathogenesis of septic acute renal failure. *Curr Opin Crit Care.* 2003;9:496-502.

26. Smith SM, Padayachee S, Modaresi KB, Smithies MN, Bihari DJ. Cerebral blood flow is proportional to cardiac index in patients with septic shock. *J Crit Care.* 1998;13:104-9.

27. Booke M, Westphal M, Hinder F, Traber LD, Traber DL. Cerebral blood flow is not altered in sheep with Pseudomonas aeruginosa sepsis treated with norepinephrine or nitric oxide synthase inhibition. *Anesth Analg.* 2003;96:1122-8.

28. Berre J, De Backer D, Moraine JJ, Vincent JL, Kahn RJ. Effects of dobutamine and prostacyclin on cerebral blood flow velocity in septic patients. *J Crit Care.* 1994;9:1-6.

29. Neviere R, Mathieu D, Chagnon JL, Lebleu N, Millien JP, Wattel F. Skeletal muscle microvascular blood flow and oxygen transport in patients with severe sepsis. *Am J Respir Crit Care Med.* 1996;153:191-5.

30.   Ognibene FP, Parker MM, Natanson C, Shelhamer JH, Parrillo JE. Depressed left ventricular performance. Response to volume infusion in patients with sepsis and septic shock. *Chest*. 1988;93:903-10.

31.   Raper RF, Sibbald WJ, Hobson J, Neal A, Cheung H. Changes in myocardial blood flow rates during hyperdynamic sepsis with induced changes in arterial perfusing pressures and metabolic need. *Crit Care Med*. 1993;21:1192-9.

32.   Suffredini AF, Fromm RE, Parker MM, Brenner M, Kovacs JA, Wesley RA, Parrillo JE. The cardiovascular response of normal humans to the administration of endotoxin. *N Engl J Med*. 1989;321:280-7.

33.   Stahl TJ, Alden PB, Ring WS, Madoff RC, Cerra FB. Sepsis-induced diastolic dysfunction in chronic canine peritonitis. *Am J Physiol*. 1990;258:H625-33.

34.   Farias S, Powers FM, Law WR. End-diastolic pressure-volume relationship in sepsis: relative contributions of compliance and equilibrium chamber volume differ. *J Surg Res*. 1999;82:172-9.

35.   Ronco JJ, Belzberg A, Phang PT, Walley KR, Dodek PM, Russell JA. No differences in hemodynamics, ventricular function, and oxygen delivery in septic and nonseptic patients with the adult respiratory distress syndrome. *Crit Care Med*. 1994;22:777-82.

36.   Parrillo JE, Parker MM, Natanson C, Suffredini AF, Danner RL, Cunnion RE, Ognibene FP. Septic shock in humans. Advances in the understanding of

pathogenesis, cardiovascular dysfunction, and therapy. *Ann Intern Med.* 1990;113:227-42.

37.   Adams HR, Parker JL, Laughlin MH. Intrinsic myocardial dysfunction during endotoxemia: dependent or independent of myocardial ischemia? *Circ Shock.* 1990;30:63-76.

38.   Parker MM, Shelhamer JH, Bacharach SL, Green MV, Natanson C, Frederick TM, Damske BA, Parrillo JE. Profound but reversible myocardial depression in patients with septic shock. *Ann Intern Med.* 1984;100:483-90.

39.   Russell JA, Ronco JJ, Lockhat D, Belzberg A, Kiess M, Dodek PM. Oxygen delivery and consumption and ventricular preload are greater in survivors than in nonsurvivors of the adult respiratory distress syndrome. *Am Rev Respir Dis.* 1990;141:659-65.

40.   Balk RA. Severe sepsis and septic shock. Definitions, epidemiology, and clinical manifestations. *Crit Care Clin.* 2000;16:179-92.

41.   Hess ML, Hastillo A, Greenfield LJ. Spectrum of cardiovascular function during gram-negative sepsis. *Prog Cardiovasc Dis.* 1981;23:279-98.

42.   Sibbald WJ, Driedger AA, Myers ML, Short AI, Wells GA. Biventricular function in the adult respiratory distress syndrome. *Chest.* 1983;84:126-34.

43.   Sibbald WJ. Myocardial function in the critically ill: factors influencing left and right ventricular performance in patients with sepsis and trauma. *Surg Clin North Am.* 1985;65:867-93.

44.   Parker MM, McCarthy KE, Ognibene FP, Parrillo JE. Right ventricular dysfunction and dilatation, similar to left ventricular changes, characterize the cardiac depression of septic shock in humans. *Chest.* 1990;97:126-31.

45.   Bernardin G, Strosberg AD, Bernard A, Mattei M, Marullo S. Beta-adrenergic receptor-dependent and -independent stimulation of adenylate cyclase is impaired during severe sepsis in humans. *Intensive Care Med.* 1998;24:1315-22.

46.   Silverman HJ, Penaranda R, Orens JB, Lee NH. Impaired beta-adrenergic receptor stimulation of cyclic adenosine monophosphate in human septic shock: association with myocardial hyporesponsiveness to catecholamines. *Crit Care Med.* 1993;21:31-9.

47.   McIntyre RC, Jr., Banerjee A, Bensard DD, Brew EC, Hahn AR, Fullerton DA. Adenosine A1-receptor mechanisms antagonize beta-adrenergic pulmonary vasodilation in hypoxia. *Am J Physiol.* 1994;267:H2179-85.

48.   Bensard DD, Banerjee A, McIntyre RC, Jr., Berens RL, Harken AH. Endotoxin disrupts beta-adrenergic signal transduction in the heart. *Arch Surg.* 1994;129:198-204.

49.   Dhainaut JF, Huyghebaert MF, Monsallier JF, Lefevre G, Dall'Ava-Santucci J, Brunet F, Villemant D, Carli A, Raichvarg D. Coronary hemodynamics and

myocardial metabolism of lactate, free fatty acids, glucose, and ketones in patients with septic shock. *Circulation.* 1987;75:533-41.

50.   Cunnion RE, Schaer GL, Parker MM, Natanson C, Parrillo JE. The coronary circulation in human septic shock. *Circulation.* 1986;73:637-44.

51.   Herbertson MJ, Werner HA, Russell JA, Iversen K, Walley KR. Myocardial oxygen extraction ratio is decreased during endotoxemia in pigs. *J Appl Physiol.* 1995;79:479-86.

52.   Bloos FM, Morisaki HM, Neal AM, Martin CM, Ellis CG, Sibbald WJ, Pitt ML. Sepsis depresses the metabolic oxygen reserve of the coronary circulation in mature sheep. *Am J Respir Crit Care Med.* 1996;153:1577-84.

53.   Groeneveld AB, van Lambalgen AA, van den Bos GC, Bronsveld W, Nauta JJ, Thijs LG. Maldistribution of heterogeneous coronary blood flow during canine endotoxin shock. *Cardiovasc Res.* 1991;25:80-8.

54.   Walley KR. Heterogeneity of oxygen delivery impairs oxygen extraction by peripheral tissues: theory. *J Appl Physiol.* 1996;81:885-94.

55.   Herbertson MJ, Werner HA, Studer W, Russell JA, Walley KR. Decreased left ventricular contractility during porcine endotoxemia is not prevented by ibuprofen. *Crit Care Med.* 1996;24:815-9.

56. Goddard CM, Allard MF, Hogg JC, Walley KR. Myocardial morphometric changes related to decreased contractility after endotoxin. *Am J Physiol.* 1996;270:H1446-52.

57. Shibano T, Vanhoutte PM. Induction of NO production by TNF-alpha and lipopolysaccharide in porcine coronary arteries without endothelium. *Am J Physiol.* 1993;264:H403-7.

58. Hung J, Lew WY. Cellular mechanisms of endotoxin-induced myocardial depression in rabbits. *Circ Res.* 1993;73:125-34.

59. Simms MG, Walley KR. Activated macrophages decrease rat cardiac myocyte contractility: importance of ICAM-1-dependent adhesion. *Am J Physiol.* 1999;277:H253-60.

60. Davani EY, Dorscheid DR, Lee CH, Van Breemen C, Walley KR. Novel Regulatory Mechanism of Cardiomyocyte Contractility Involving Icam-1 and the Cytoskeleton. *Am J Physiol Heart Circ Physiol.* 2004;15:15.

61. Botha AJ, Moore FA, Moore EE, Sauaia A, Banerjee A, Peterson VM. Early neutrophil sequestration after injury: a pathogenic mechanism for multiple organ failure. *J Trauma.* 1995;39:411-7.

62. Chiba Y, Morioka K, Muraoka R, Ihaya A, Kimura T, Uesaka T, Tsuda T, Matsuyama K. Effects of depletion of leukocytes and platelets on cardiac dysfunction after cardiopulmonary bypass. *Ann Thorac Surg.* 1998;65:107-13.

63.   Goode HF, Webster NR. Free radicals and antioxidants in sepsis. *Crit Care Med.* 1993;21:1770-6.

64.   Bhattacharyya J, Biswas S, Datta AG. Mode of action of endotoxin: role of free radicals and antioxidants. *Curr Med Chem.* 2004;11:359-68.

65.   Goddard CM, Poon BY, Klut ME, Wiggs BR, vanEeden SF, Hogg JC, Walley KR. Leukocyte activation does not mediate myocardial leukocyte retention during endotoxemia in rabbits. *Am J Physiol.* 1998;275:H1548-57.

66.   Herbertson MJ, Werner HA, Goddard CM, Russell JA, Wheeler A, Coxon R, Walley KR. Anti-tumor necrosis factor-alpha prevents decreased ventricular contractility in endotoxemic pigs. *Am J Respir Crit Care Med.* 1995;152:480-8.

67.   Vincent JL, Bakker J, Marecaux G, Schandene L, Kahn RJ, Dupont E. Administration of anti-TNF antibody improves left ventricular function in septic shock patients. Results of a pilot study. *Chest.* 1992;101:810-5.

68.   Fisher CJ, Jr., Agosti JM, Opal SM, Lowry SF, Balk RA, Sadoff JC, Abraham E, Schein RM, Benjamin E. Treatment of septic shock with the tumor necrosis factor receptor:Fc fusion protein. The Soluble TNF Receptor Sepsis Study Group. *N Engl J Med.* 1996;334:1697-702.

69.   Kumar A, Krieger A, Symeoneides S, Parrillo JE. Myocardial dysfunction in septic shock: Part II. Role of cytokines and nitric oxide. *J Cardiothorac Vasc Anesth.* 2001;15:485-511.

70. Kinugawa K, Takahashi T, Kohmoto O, Yao A, Aoyagi T, Momomura S, Hirata Y, Serizawa T. Nitric oxide-mediated effects of interleukin-6 on [Ca2+]i and cell contraction in cultured chick ventricular myocytes. *Circ Res*. 1994;75:285-95.

71. Kumar A, Brar R, Wang P, Dee L, Skorupa G, Khadour F, Schulz R, Parrillo JE. Role of nitric oxide and cGMP in human septic serum-induced depression of cardiac myocyte contractility. *Am J Physiol*. 1999;276:R265-76.

72. Toth I, Heard SO. Nitric oxide does not mediate lipopolysaccharide-induced myocardial depression in guinea pigs. *Crit Care Med*. 1997;25:684-8.

73. Vona-Davis L, Wearden P, Hill J, Hill R. Cardiac response to nitric oxide synthase inhibition using aminoguanidine in a rat model of endotoxemia. *Shock*. 2002;17:404-10.

74. Keller RS, Jones JJ, Kim KF, Myers PR, Adams HR, Parker JL, Rubin LJ. Endotoxin-induced myocardial dysfunction: is there a role for nitric oxide? *Shock*. 1995;4:338-44.

75. Klabunde RE, Coston AF. Nitric oxide synthase inhibition does not prevent cardiac depression in endotoxic shock. *Shock*. 1995;3:73-8.

76. Herbertson MJ, Werner HA, Walley KR. Nitric oxide synthase inhibition partially prevents decreased LV contractility during endotoxemia. *Am J Physiol*. 1996;270:H1979-84.

77.   Daemen-Gubbels CR, Groeneveld PH, Groeneveld AB, van Kamp GJ, Bronsveld W, Thijs LG. Methylene blue increases myocardial function in septic shock. *Crit Care Med.* 1995;23:1363-70.

78.   Phillis JW, Song D, O'Regan MH. Mechanisms involved in coronary artery dilatation during respiratory acidosis in the isolated perfused rat heart. *Basic Res Cardiol.* 2000;95:93-7.

79.   Kohmoto O, Spitzer KW, Movsesian MA, Barry WH. Effects of intracellular acidosis on [Ca2+]i transients, transsarcolemmal Ca2+ fluxes, and contraction in ventricular myocytes. *Circ Res.* 1990;66:622-32.

80.   Voerman HJ, Strack van Schijndel RJ, de Boer H, van der Veen EA, Thijs LG. Growth hormone: secretion and administration in catabolic adult patients, with emphasis on the critically ill patient. *Neth J Med.* 1992;41:229-44.

81.   Carroll PV. Treatment with growth hormone and insulin-like growth factor-I in critical illness. *Best Pract Res Clin Endocrinol Metab.* 2001;15:435-51.

82.   Pittas AG, Siegel RD, Lau J. Insulin therapy for critically ill hospitalized patients: a meta-analysis of randomized controlled trials. *Arch Intern Med.* 2004;164:2005-11.

83.   Van den Berghe G. How does blood glucose control with insulin save lives in intensive care? *J Clin Invest.* 2004;114:1187-95.

84. Guan J, Bennet L, George S, Wu D, Waldvogel HJ, Gluckman PD, Faull RL, Crosier PS, Gunn AJ. Insulin-like growth factor-1 reduces postischemic white matter injury in fetal sheep. *J Cereb Blood Flow Metab.* 2001;21:493-502.

85. Cittadini A, Ishiguro Y, Stromer H, Spindler M, Moses AC, Clark R, Douglas PS, Ingwall JS, Morgan JP. Insulin-like growth factor-1 but not growth hormone augments mammalian myocardial contractility by sensitizing the myofilament to Ca2+ through a wortmannin-sensitive pathway: studies in rat and ferret isolated muscles. *Circ Res.* 1998;83:50-9.

86. Michell BJ, Griffiths JE, Mitchelhill KI, Rodriguez-Crespo I, Tiganis T, Bozinovski S, de Montellano PR, Kemp BE, Pearson RB. The Akt kinase signals directly to endothelial nitric oxide synthase. *Curr Biol.* 1999;9:845-8.

87. Yamamura T, Otani H, Nakao Y, Hattori R, Osako M, Imamura H. IGF-I differentially regulates Bcl-xL and Bax and confers myocardial protection in the rat heart. *Am J Physiol Heart Circ Physiol.* 2001;280:H1191-200.

88. Rogiers P, Zhang H, Leeman M, Nagler J, Neels H, Melot C, Vincent JL. Erythropoietin response is blunted in critically ill patients. *Intensive Care Med.* 1997;23:159-62.

89. Shander A. Anemia in the critically ill. *Crit Care Clin.* 2004;20:159-78.

90. Hotchkiss RS, Karl IE. The pathophysiology and treatment of sepsis. *N Engl J Med.* 2003;348:138-50.

91. Gowda RM, Khan IA, Vasavada BC, Sacchi TJ. Reversible myocardial dysfunction: basics and evaluation. *Int J Cardiol.* 2004;97:349-53.

92. Entman ML, Michael L, Rossen RD, Dreyer WJ, Anderson DC, Taylor AA, Smith CW. Inflammation in the course of early myocardial ischemia. *Faseb J.* 1991;5:2529-37.

93. Gross GJ, Kersten JR, Warltier DC. Mechanisms of postischemic contractile dysfunction. *Ann Thorac Surg.* 1999;68:1898-904.

94. Vroom MB, van Wezel HB. Myocardial stunning, hibernation, and ischemic preconditioning. *J Cardiothorac Vasc Anesth.* 1996;10:789-99.

95. Hittinger L, Shannon RP, Kohin S, Manders WT, Kelly P, Vatner SF. Exercise-induced subendocardial dysfunction in dogs with left ventricular hypertrophy. *Circ Res.* 1990;66:329-43.

96. Kim SJ, Kudej RK, Yatani A, Kim YK, Takagi G, Honda R, Colantonio DA, Van Eyk JE, Vatner DE, Rasmusson RL, Vatner SF. A novel mechanism for myocardial stunning involving impaired Ca(2+) handling. *Circ Res.* 2001;89:831-7.

97. Piper HM, Meuter K, Schafer C. Cellular mechanisms of ischemia-reperfusion injury. *Ann Thorac Surg.* 2003;75:S644-8.

98. Flood AJ, Willems L, Headrick JP. Coronary function and adenosine receptor-mediated responses in ischemic-reperfused mouse heart. *Cardiovasc Res.* 2002;55:161-70.

99. Sorescu D, Griendling KK. Reactive oxygen species, mitochondria, and NAD(P)H oxidases in the development and progression of heart failure. *Congest Heart Fail.* 2002;8:132-40.

100. Dhalla NS, Temsah RM, Netticadan T. Role of oxidative stress in cardiovascular diseases. *J Hypertens.* 2000;18:655-73.

101. Droge W. Free radicals in the physiological control of cell function. *Physiol Rev.* 2002;82:47-95.

102. von Lewinski D, Voss K, Hulsmann S, Kogler H, Pieske B. Insulin-like growth factor-1 exerts Ca2+-dependent positive inotropic effects in failing human myocardium. *Circ Res.* 2003;92:169-76.

103. Kukreja RC, Janin Y. Reperfusion Injury: Basic Concepts and Protection Strategies. *J Thromb Thrombolysis.* 1997;4:7-24.

104. Loucks EB, Godin DV, Walley KR, McManus BM, Rahimian R, Granville DJ, Hong JM, Aktary FM, Qayumi AK. Role of platelet activating factor in cardiac dysfunction, apoptosis and nitric oxide synthase mRNA expression in the ischemic-reperfused rabbit heart. *Can J Cardiol.* 2003;19:267-74.

105. Nathan C, Srimal S, Farber C, Sanchez E, Kabbash L, Asch A, Gailit J, Wright SD. Cytokine-induced respiratory burst of human neutrophils: dependence on extracellular matrix proteins and CD11/CD18 integrins. *J Cell Biol.* 1989;109:1341-9.

106. Park JL, Lucchesi BR. Mechanisms of myocardial reperfusion injury. *Ann Thorac Surg.* 1999;68:1905-12.

107. Smith CW, Entman ML, Lane CL, Beaudet AL, Ty TI, Youker K, Hawkins HK, Anderson DC. Adherence of neutrophils to canine cardiac myocytes in vitro is dependent on intercellular adhesion molecule-1. *J Clin Invest.* 1991;88:1216-23.

108. Luscinskas FW, Gimbrone MA, Jr. Endothelial-dependent mechanisms in chronic inflammatory leukocyte recruitment. *Annu Rev Med.* 1996;47:413-21.

109. Bevilacqua MP, Nelson RM, Mannori G, Cecconi O. Endothelial-leukocyte adhesion molecules in human disease. *Annu Rev Med.* 1994;45:361-78.

110. Bevilacqua MP. Endothelial-leukocyte adhesion molecules. *Annu Rev Immunol.* 1993;11:767-804.

111. Rothlein R, Mainolfi EA, Czajkowski M, Marlin SD. A form of circulating ICAM-1 in human serum. *J Immunol.* 1991;147:3788-93.

112. Sultan S, Gosling M, Nagase H, Powell JT. Shear stress-induced shedding of soluble intercellular adhesion molecule-1 from saphenous vein endothelium. *FEBS Lett.* 2004;564:161-5.

113. Szekanecz Z, Shah MR, Pearce WH, Koch AE. Intercellular adhesion molecule-1 (ICAM-1) expression and soluble ICAM-1 (sICAM-1) production by cytokine-activated human aortic endothelial cells: a possible role for ICAM-1 and sICAM-1 in atherosclerotic aortic aneurysms. *Clin Exp Immunol.* 1994;98:337-43.

114. van de Stolpe A, van der Saag PT. Intercellular adhesion molecule-1. *J Mol Med.* 1996;74:13-33.

115. Fiore E, Fusco C, Romero P, Stamenkovic I. Matrix metalloproteinase 9 (MMP-9/gelatinase B) proteolytically cleaves ICAM-1 and participates in tumor cell resistance to natural killer cell-mediated cytotoxicity. *Oncogene.* 2002;21:5213-23.

116. Justicia C, Panes J, Sole S, Cervera A, Deulofeu R, Chamorro A, Planas AM. Neutrophil infiltration increases matrix metalloproteinase-9 in the ischemic brain after occlusion/reperfusion of the middle cerebral artery in rats. *J Cereb Blood Flow Metab.* 2003;23:1430-40.

117. Lawson C, Ainsworth ME, McCormack AM, Yacoub M, Rose ML. Effects of cross-linking ICAM-1 on the surface of human vascular smooth muscle cells: induction of VCAM-1 but no proliferation. *Cardiovasc Res.* 2001;50:547-55.

118. Haught WH, Mansour M, Rothlein R, Kishimoto TK, Mainolfi EA, Hendricks JB, Hendricks C, Mehta JL. Alterations in circulating intercellular adhesion molecule-1 and L-selectin: further evidence for chronic inflammation in ischemic heart disease. *Am Heart J.* 1996;132:1-8.

119. Roche Y, Pasquier D, Rambeaud JJ, Seigneurin D, Duperray A. Fibrinogen mediates bladder cancer cell migration in an ICAM-1-dependent pathway. *Thromb Haemost*. 2003;89:1089-97.

120. Dustin ML, Springer TA. Lymphocyte function-associated antigen-1 (LFA-1) interaction with intercellular adhesion molecule-1 (ICAM-1) is one of at least three mechanisms for lymphocyte adhesion to cultured endothelial cells. *J Cell Biol*. 1988;107:321-31.

121. Lawson C, Ainsworth M, Yacoub M, Rose M. Ligation of ICAM-1 on endothelial cells leads to expression of VCAM-1 via a nuclear factor-kappaB-independent mechanism. *J Immunol*. 1999;162:2990-6.

122. Dustin ML, Singer KH, Tuck DT, Springer TA. Adhesion of T lymphoblasts to epidermal keratinocytes is regulated by interferon gamma and is mediated by intercellular adhesion molecule 1 (ICAM-1). *J Exp Med*. 1988;167:1323-40.

123. Barton WW, Wilcoxen SE, Christensen PJ, Paine R, 3rd. Association of ICAM-1 with the cytoskeleton in rat alveolar epithelial cells in primary culture. *Am J Physiol*. 1996;271:L707-18.

124. Wissink S, van de Stolpe A, Caldenhoven E, Koenderman L, van der Saag PT. NF-kappa B/Rel family members regulating the ICAM-1 promoter in monocytic THP-1 cells. *Immunobiology*. 1997;198:50-64.

125. Staunton DE, Merluzzi VJ, Rothlein R, Barton R, Marlin SD, Springer TA. A cell adhesion molecule, ICAM-1, is the major surface receptor for rhinoviruses. *Cell.* 1989;56:849-53.

126. Driessens MH, van Hulten P, Zuurbier A, La Riviere G, Roos E. Inhibition and stimulation of LFA-1 and Mac-1 functions by antibodies against murine CD18. Evidence that the LFA-1 binding sites for ICAM-1, -2, and -3 are distinct. *J Leukoc Biol.* 1996;60:758-65.

127. Lo SK, Van Seventer GA, Levin SM, Wright SD. Two leukocyte receptors (CD11a/CD18 and CD11b/CD18) mediate transient adhesion to endothelium by binding to different ligands. *J Immunol.* 1989;143:3325-9.

128. Smith CW, Marlin SD, Rothlein R, Toman C, Anderson DC. Cooperative interactions of LFA-1 and Mac-1 with intercellular adhesion molecule-1 in facilitating adherence and transendothelial migration of human neutrophils in vitro. *J Clin Invest.* 1989;83:2008-17.

129. Pluskota E, D'Souza SE. Fibrinogen interactions with ICAM-1 (CD54) regulate endothelial cell survival. *Eur J Biochem.* 2000;267:4693-704.

130. Shafren DR, Dorahy DJ, Ingham RA, Burns GF, Barry RD. Coxsackievirus A21 binds to decay-accelerating factor but requires intercellular adhesion molecule 1 for cell entry. *J Virol.* 1997;71:4736-43.

131.   Xiao C, Bator CM, Bowman VD, Rieder E, He Y, Hebert B, Bella J, Baker TS, Wimmer E, Kuhn RJ, Rossmann MG. Interaction of coxsackievirus A21 with its cellular receptor, ICAM-1. *J Virol.* 2001;75:2444-51.

132.   Ockenhouse CF, Betageri R, Springer TA, Staunton DE. Plasmodium falciparum-infected erythrocytes bind ICAM-1 at a site distinct from LFA-1, Mac-1, and human rhinovirus. *Cell.* 1992;68:63-9.

133.   Wang J, Springer TA. Structural specializations of immunoglobulin superfamily members for adhesion to integrins and viruses. *Immunol Rev.* 1998;163:197-215.

134.   Altieri DC, Duperray A, Plescia J, Thornton GB, Languino LR. Structural recognition of a novel fibrinogen gamma chain sequence (117-133) by intercellular adhesion molecule-1 mediates leukocyte-endothelium interaction. *J Biol Chem.* 1995;270:696-9.

135.   Duperray A, Languino LR, Plescia J, McDowall A, Hogg N, Craig AG, Berendt AR, Altieri DC. Molecular identification of a novel fibrinogen binding site on the first domain of ICAM-1 regulating leukocyte-endothelium bridging. *J Biol Chem.* 1997;272:435-41.

136.   Languino LR, Plescia J, Duperray A, Brian AA, Plow EF, Geltosky JE, Altieri DC. Fibrinogen mediates leukocyte adhesion to vascular endothelium through an ICAM-1-dependent pathway. *Cell.* 1993;73:1423-34.

137.   Ernst E, Koenig W. Fibrinogen and cardiovascular risk. *Vasc Med.* 1997;2:115-25.

138. Mosesson MW. Fibrin polymerization and its regulatory role in hemostasis. *J Lab Clin Med*. 1990;116:8-17.

139. Reganon E, Aznar J, Vila V. Degradation of human fibrinogen by plasmin: isolation and partial characterization of an early degradation product. *Haemostasis*. 1978;7:26-34.

140. Lominadze D, Tsakadze N, Sen U, Falcone JC, D'Souza SE. Fibrinogen and fragment D-induced vascular constriction. *Am J Physiol Heart Circ Physiol*. 2005;288:H1257-64.

141. Kurose I, Miura S, Fukumura D, Tsuchiya M. Mechanisms of endothelin-induced macromolecular leakage in microvascular beds of rat mesentery. *Eur J Pharmacol*. 1993;250:85-94.

142. Ge M, Tang G, Ryan TJ, Malik AB. Fibrinogen degradation product fragment D induces endothelial cell detachment by activation of cell-mediated fibrinolysis. *J Clin Invest*. 1992;90:2508-16.

143. Lo SK, Del Vecchio PJ, Lum H, Malik AB. Fibrin contact increases endothelial permeability to albumin. *J Cell Physiol*. 1992;151:63-70.

144. D'Souza SE, Byers-Ward VJ, Gardiner EE, Wang H, Sung SS. Identification of an active sequence within the first immunoglobulin domain of intercellular cell adhesion molecule-1 (ICAM-1) that interacts with fibrinogen. *J Biol Chem*. 1996;271:24270-7.

145. Harley SL, Sturge J, Powell JT. Regulation by fibrinogen and its products of intercellular adhesion molecule-1 expression in human saphenous vein endothelial cells. *Arterioscler Thromb Vasc Biol.* 2000;20:652-8.

146. Liu X, Piela-Smith TH. Fibrin(ogen)-induced expression of ICAM-1 and chemokines in human synovial fibroblasts. *J Immunol.* 2000;165:5255-61.

147. Massberg S, Enders G, Matos FC, Tomic LI, Leiderer R, Eisenmenger S, Messmer K, Krombach F. Fibrinogen deposition at the postischemic vessel wall promotes platelet adhesion during ischemia-reperfusion in vivo. *Blood.* 1999;94:3829-38.

148. Schoots IG, Levi M, van Vliet AK, Maas AM, Roossink EH, van Gulik TM. Inhibition of coagulation and inflammation by activated protein C or antithrombin reduces intestinal ischemia/reperfusion injury in rats. *Crit Care Med.* 2004;32:1375-83.

149. Hicks RC, Golledge J, Mir-Hasseine R, Powell JT. Vasoactive effects of fibrinogen on saphenous vein. *Nature.* 1996;379:818-20.

150. Gawaz M, Neumann FJ, Dickfeld T, Koch W, Laugwitz KL, Adelsberger H, Langenbrink K, Page S, Neumeier D, Schomig A, Brand K. Activated platelets induce monocyte chemotactic protein-1 secretion and surface expression of intercellular adhesion molecule-1 on endothelial cells. *Circulation.* 1998;98:1164-71.

151. Carpen O, Pallai P, Staunton DE, Springer TA. Association of intercellular adhesion molecule-1 (ICAM-1) with actin-containing cytoskeleton and alpha-actinin. *J Cell Biol.* 1992;118:1223-34.

152. Vogetseder W, Dierich MP. Intercellular adhesion molecule-1 (ICAM-1, CD 54) is associated with actin-filaments. *Immunobiology.* 1991;182:143-51.

153. Koyama Y, Tanaka Y, Saito K, Abe M, Nakatsuka K, Morimoto I, Auron PE, Eto S. Cross-linking of intercellular adhesion molecule 1 (CD54) induces AP-1 activation and IL-1beta transcription. *J Immunol.* 1996;157:5097-103.

154. Rothlein R, Dustin ML, Marlin SD, Springer TA. A human intercellular adhesion molecule (ICAM-1) distinct from LFA-1. *J Immunol.* 1986;137:1270-4.

155. Durieu-Trautmann O, Chaverot N, Cazaubon S, Strosberg AD, Couraud PO. Intercellular adhesion molecule 1 activation induces tyrosine phosphorylation of the cytoskeleton-associated protein cortactin in brain microvessel endothelial cells. *J Biol Chem.* 1994;269:12536-40.

156. van Horssen M, Loman S, Rijkers GT, Boom SE, Bloem AC. Co-ligation of ICAM-1 (CD54) and membrane IgM negatively affects B cell receptor signaling. *Eur J Immunol.* 1995;25:154-8.

157. Etienne S, Adamson P, Greenwood J, Strosberg AD, Cazaubon S, Couraud PO. ICAM-1 signaling pathways associated with Rho activation in microvascular brain endothelial cells. *J Immunol.* 1998;161:5755-61.

158. Pluskota E, Chen Y, D'Souza SE. Src homology domain 2-containing tyrosine phosphatase 2 associates with intercellular adhesion molecule 1 to regulate cell survival. *J Biol Chem.* 2000;275:30029-36.

159. Holland J, Owens T. Signaling through intercellular adhesion molecule 1 (ICAM-1) in a B cell lymphoma line. The activation of Lyn tyrosine kinase and the mitogen-activated protein kinase pathway. *J Biol Chem.* 1997;272:9108-12.

160. Raeburn CD, Calkins CM, Zimmerman MA, Song Y, Ao L, Banerjee A, Harken AH, Meng X. ICAM-1 and VCAM-1 mediate endotoxemic myocardial dysfunction independent of neutrophil accumulation. *Am J Physiol Regul Integr Comp Physiol.* 2002;283:R477-86.

161. Lucchesi BR, Werns SW, Fantone JC. The role of the neutrophil and free radicals in ischemic myocardial injury. *J Mol Cell Cardiol.* 1989;21:1241-51.

162. Hansen PR, Stawski G. Neutrophil mediated damage to isolated myocytes after anoxia and reoxygenation. *Cardiovasc Res.* 1994;28:565-9.

163. Poon BY, Ward CA, Cooper CB, Giles WR, Burns AR, Kubes P. alpha(4)-integrin mediates neutrophil-induced free radical injury to cardiac myocytes. *J Cell Biol.* 2001;152:857-66.

164. Entman ML, Youker K, Shoji T, Kukielka G, Shappell SB, Taylor AA, Smith CW. Neutrophil induced oxidative injury of cardiac myocytes. A compartmented system requiring CD11b/CD18-ICAM-1 adherence. *J Clin Invest.* 1992;90:1335-45.

165. Norgauer J, Bartels F, Gohring U, Schopf E, Gebicke-Haerter P, Kownatzki E, Krutmann J. Expression of intercellular adhesion molecule-1 is regulated by the actin network in epidermoid carcinoma cells. *Exp Cell Res*. 1995;219:15-20.

166. Amos C, Romero IA, Schultze C, Rousell J, Pearson JD, Greenwood J, Adamson P. Cross-linking of brain endothelial intercellular adhesion molecule (ICAM)-1 induces association of ICAM-1 with detergent-insoluble cytoskeletal fraction. *Arterioscler Thromb Vasc Biol*. 2001;21:810-6.

167. Casey LC, Balk RA, Bone RC. Plasma cytokine and endotoxin levels correlate with survival in patients with the sepsis syndrome. *Ann Intern Med*. 1993;119:771-8.

168. Natanson C, Hoffman WD, Suffredini AF, Eichacker PQ, Danner RL. Selected treatment strategies for septic shock based on proposed mechanisms of pathogenesis. *Ann Intern Med*. 1994;120:771-83.

169. Lancel S, Tissier S, Mordon S, Marechal X, Depontieu F, Scherpereel A, Chopin C, Neviere R. Peroxynitrite decomposition catalysts prevent myocardial dysfunction and inflammation in endotoxemic rats. *J Am Coll Cardiol*. 2004;43:2348-58.

170. Krishnagopalan S, Kumar A, Parrillo JE, Kumar A. Myocardial dysfunction in the patient with sepsis. *Curr Opin Crit Care*. 2002;8:376-88.

171. Youker K, Smith CW, Anderson DC, Miller D, Michael LH, Rossen RD, Entman ML. Neutrophil adherence to isolated adult cardiac myocytes. Induction by

cardiac lymph collected during ischemia and reperfusion. *J Clin Invest.* 1992;89:602-9.

172. Hasslen SR, Burns AR, Simon SI, Smith CW, Starr K, Barclay AN, Michie SA, Nelson RD, Erlandsen SL. Preservation of spatial organization and antigenicity of leukocyte surface molecules by aldehyde fixation: flow cytometry and high-resolution FESEM studies of CD62L, CD11b, and Thy-1. *J Histochem Cytochem.* 1996;44:1115-22.

173. Wang Q, Doerschuk CM. Neutrophil-induced changes in the biomechanical properties of endothelial cells: roles of ICAM-1 and reactive oxygen species. *J Immunol.* 2000;164:6487-94.

174. Etienne-Manneville S, Manneville JB, Adamson P, Wilbourn B, Greenwood J, Couraud PO. ICAM-1-coupled cytoskeletal rearrangements and transendothelial lymphocyte migration involve intracellular calcium signaling in brain endothelial cell lines. *J Immunol.* 2000;165:3375-83.

175. Conchello JA. Superresolution and convergence properties of the expectation-maximization algorithm for maximum-likelihood deconvolution of incoherent images. *J Opt Soc Am A Opt Image Sci Vis.* 1998;15:2609-19.

176. Calaghan SC, White E, Bedut S, Le Guennec JY. Cytochalasin D reduces Ca2+ sensitivity and maximum tension via interactions with myofilaments in skinned rat cardiac myocytes. *J Physiol.* 2000;529:405-11.

177.   Stamenovic D, Fredberg JJ, Wang N, Butler JP, Ingber DE. A microstructural approach to cytoskeletal mechanics based on tensegrity. *J Theor Biol.* 1996;181:125-36.

178.   Wear MA, Schafer DA, Cooper JA. Actin dynamics: assembly and disassembly of actin networks. *Curr Biol.* 2000;10:R891-5.

179.   Seko Y, Takahashi N, Sabe H, Tobe K, Kadowaki T, Nagai R. Hypoxia induces activation and subcellular translocation of focal adhesion kinase (p125(FAK)) in cultured rat cardiac myocytes. *Biochem Biophys Res Commun.* 1999;262:290-6.

180.   Kacimi R, Karliner JS, Koudssi F, Long CS. Expression and regulation of adhesion molecules in cardiac cells by cytokines: response to acute hypoxia. *Circ Res.* 1998;82:576-86.

181.   Dreyer WJ, Smith CW, Michael LH, Rossen RD, Hughes BJ, Entman ML, Anderson DC. Canine neutrophil activation by cardiac lymph obtained during reperfusion of ischemic myocardium. *Circ Res.* 1989;65:1751-62.

182.   Issekutz AC, Rowter D, Springer TA. Role of ICAM-1 and ICAM-2 and alternate CD11/CD18 ligands in neutrophil transendothelial migration. *J Leukoc Biol.* 1999;65:117-26.

183.   Palazzo AJ, Jones SP, Girod WG, Anderson DC, Granger DN, Lefer DJ. Myocardial ischemia-reperfusion injury in CD18- and ICAM-1-deficient mice. *Am J Physiol.* 1998;275:H2300-7.

184. Schulz R, Ehring T, Heusch G. Stunned myocardium: inotropic reserve and pharmacological attenuation. *Basic Res Cardiol*. 1995;90:294-6.

185. Parrillo JE, Burch C, Shelhamer JH, Parker MM, Natanson C, Schuette W. A circulating myocardial depressant substance in humans with septic shock. Septic shock patients with a reduced ejection fraction have a circulating factor that depresses in vitro myocardial cell performance. *J Clin Invest*. 1985;76:1539-53.

186. Okayama N, Ichikawa H, Coe L, Itoh M, Alexander JS. Exogenous NO enhances hydrogen peroxide-mediated neutrophil adherence to cultured endothelial cells. *Am J Physiol*. 1998;274:L820-6.

187. Saito H, Minamiya Y, Kitamura M, Saito S, Enomoto K, Terada K, Ogawa J. Endothelial myosin light chain kinase regulates neutrophil migration across human umbilical vein endothelial cell monolayer. *J Immunol*. 1998;161:1533-40.

188. Bers DM, Weber CR. Na/Ca exchange function in intact ventricular myocytes. *Ann N Y Acad Sci*. 2002;976:500-12.

189. Katoh H, Schlotthauer K, Bers DM. Transmission of information from cardiac dihydropyridine receptor to ryanodine receptor: evidence from BayK 8644 effects on resting Ca(2+) sparks. *Circ Res*. 2000;87:106-11.

190. Marvin KW, Keelan JA, Sato TA, Coleman MA, McCowan LM, Mitchell MD. Expression of intercellular adhesion molecule-1 (ICAM-1) in choriodecidua with labour and delivery at term and preterm. *Reprod Fertil Dev*. 1999;11:255-62.

191. Dye JF, Jablenska R, Donnelly JL, Lawrence L, Leach L, Clark P, Firth JA. Phenotype of the endothelium in the human term placenta. *Placenta*. 2001;22:32-43.

192. Sedarat F, Xu L, Moore ED, Tibbits GF. Colocalization of dihydropyridine and ryanodine receptors in neonate rabbit heart using confocal microscopy. *Am J Physiol Heart Circ Physiol*. 2000;279:H202-9.

193. McDonald TE, Grinman MN, Carthy CM, Walley KR. Endotoxin infusion in rats induces apoptotic and survival pathways in hearts. *Am J Physiol Heart Circ Physiol*. 2000;279:H2053-61.

194. Hubbard AK, Rothlein R. Intercellular adhesion molecule-1 (ICAM-1) expression and cell signaling cascades. *Free Radic Biol Med*. 2000;28:1379-86.

195. Court O, Kumar A, Parrillo JE. Clinical review: Myocardial depression in sepsis and septic shock. *Crit Care*. 2002;6:500-8.

196. Neviere R, Guery B, Mordon S, Zerimech F, Charre S, Wattel F, Chopin C. Inhaled NO reduces leukocyte-endothelial cell interactions and myocardial dysfunction in endotoxemic rats. *Am J Physiol Heart Circ Physiol*. 2000;278:H1783-90.

197. Granton JT, Goddard CM, Allard MF, van Eeden S, Walley KR. Leukocytes and decreased left-ventricular contractility during endotoxemia in rabbits. *Am J Respir Crit Care Med*. 1997;155:1977-83.

198. Nozawa T, Yasumura Y, Futaki S, Tanaka N, Uenishi M, Suga H. Efficiency of energy transfer from pressure-volume area to external mechanical work increases with contractile state and decreases with afterload in the left ventricle of the anesthetized closed-chest dog. *Circulation*. 1988;77:1116-24.

199. Kass DA, Maughan WL, Guo ZM, Kono A, Sunagawa K, Sagawa K. Comparative influence of load versus inotropic states on indexes of ventricular contractility: experimental and theoretical analysis based on pressure-volume relationships. *Circulation*. 1987;76:1422-36.

200. Anton E. Ultrastructural changes of stromal cells of bone marrow and liver after cyclophosphamide treatment in mice. *Tissue Cell*. 1997;29:1-9.

201. Siegal A, Kopel S, Bar-Sela S, Davidai G, Yavetz H, Leibovici J. Bone marrow and peripheral blood modifications in C57BL mice administered with cyclophosphamide and levan. *In Vivo*. 1988;2:349-59.

202. Wierda D, Pazdernik TL. Effects of cyclophosphamide on hemic precursor cells in mouse bone marrow and spleen. *J Immunopharmacol*. 1979;1:357-76.

203. Goddard CM, Allard MF, Hogg JC, Herbertson MJ, Walley KR. Prolonged leukocyte transit time in coronary microcirculation of endotoxemic pigs. *Am J Physiol*. 1995;269:H1389-97.

204. Bateson AN, Jakiwczyk OM, Schulz R. Rapid increase in inducible nitric oxide synthase gene expression in the heart during endotoxemia. *Eur J Pharmacol*. 1996;303:141-4.

205.   Schulz R, Dodge KL, Lopaschuk GD, Clanachan AS. Peroxynitrite impairs cardiac contractile function by decreasing cardiac efficiency. *Am J Physiol.* 1997;272:H1212-9.

206.   Staunton DE, Marlin SD, Stratowa C, Dustin ML, Springer TA. Primary structure of ICAM-1 demonstrates interaction between members of the immunoglobulin and integrin supergene families. *Cell.* 1988;52:925-33.

207.   Springer TA. Traffic signals for lymphocyte recirculation and leukocyte emigration: the multistep paradigm. *Cell.* 1994;76:301-14.

208.   Clayton A, Evans RA, Pettit E, Hallett M, Williams JD, Steadman R. Cellular activation through the ligation of intercellular adhesion molecule-1. *J Cell Sci.* 1998;111:443-53.

209.   Landis RC, McDowall A, Holness CL, Littler AJ, Simmons DL, Hogg N. Involvement of the "I" domain of LFA-1 in selective binding to ligands ICAM-1 and ICAM-3. *J Cell Biol.* 1994;126:529-37.

210.   Yamaya M, Sasaki H. Rhinovirus and asthma. *Viral Immunol.* 2003;16:99-109.

211.   Gray C, McCormick C, Turner G, Craig A. ICAM-1 can play a major role in mediating P. falciparum adhesion to endothelium under flow. *Mol Biochem Parasitol.* 2003;128:187-93.

212.   Sriramarao P, Languino LR, Altieri DC. Fibrinogen mediates leukocyte-endothelium bridging in vivo at low shear forces. *Blood.* 1996;88:3416-23.

213. Ernst E, Resch KL. Fibrinogen as a cardiovascular risk factor: a meta-analysis and review of the literature. *Ann Intern Med.* 1993;118:956-63.

214. Lowe GD, Lee AJ, Rumley A, Price JF, Fowkes FG. Blood viscosity and risk of cardiovascular events: the Edinburgh Artery Study. *Br J Haematol.* 1997;96:168-73.

215. Koscielny J, Jung EM, Mrowietz C, Kiesewetter H, Latza R. Blood fluidity, fibrinogen, and cardiovascular risk factors of occlusive arterial disease: Results of the Aachen study. *Clin Hemorheol Microcirc.* 2004;31:185-95.

216. Yan SR, Sapru K, Issekutz AC. The CD11/CD18 (beta) integrins modulate neutrophil caspase activation and survival following TNF-alpha or endotoxin induced transendothelial migration. *Immunol Cell Biol.* 2004;82:435-46.

217. Saito M, Shima C, Takagi M, Ogino M, Katori M, Majima M. Enhanced exudation of fibrinogen into the perivascular space in acute inflammation triggered by neutrophil migration. *Inflamm Res.* 2002;51:324-31.

218. Adamson P, Etienne S, Couraud PO, Calder V, Greenwood J. Lymphocyte migration through brain endothelial cell monolayers involves signaling through endothelial ICAM-1 via a rho-dependent pathway. *J Immunol.* 1999;162:2964-73.

219. van de Stolpe A, Jacobs N, Hage WJ, Tertoolen L, van Kooyk Y, Novakova IR, de Witte T. Fibrinogen binding to ICAM-1 on EA.hy 926 endothelial cells is dependent on an intact cytoskeleton. *Thromb Haemost.* 1996;75:182-9.

220.   Ganz W. Direct Demonstration in Dogs of the Absence of Lethal Reperfusion Injury. *J Thromb Thrombolysis*. 1997;4:105-107.

221.   Schaper W, Schaper J. Reperfusion Injury: An Opinionated View. *J Thromb Thrombolysis*. 1997;4:113-116.

222.   Dhainaut JF, Huyghebaert MF. [Coronary circulation and myocardial metabolism in septic shock. Effects of a dobutamine-dopamine combination]. *Rev Med Suisse Romande*. 1987;107:477-83.

223.   Kis A, Yellon DM, Baxter GF. Role of nuclear factor-kappaB activation in acute ischaemia-reperfusion injury in myocardium. *Br J Pharmacol*. 2003;138:894-900.

224.   Pietri S, Mercier A, Mathieu C, Caffaratti S, Culcasi M. Hemodynamic and metabolic effects of the beta-phosphorylated nitroxide 2-diethoxyphosphoryl-2,5,5-trimethylpyrrolidinoxyl during myocardial ischemia and reperfusion. *Free Radic Biol Med*. 2003;34:1167-77.

225.   Laude K, Thuillez C, Richard V. [Coronary endothelial dysfunction after ischemia-reperfusion: mechanisms and possibilities for protection]. *Therapie*. 2001;56:589-93.

226.   Benbrik E, Chariot P, Bonavaud S, Ammi-Said M, Frisdal E, Rey C, Gherardi R, Barlovatz-Meimon G. Cellular and mitochondrial toxicity of zidovudine (AZT), didanosine (ddI) and zalcitabine (ddC) on cultured human muscle cells. *J Neurol Sci*. 1997;149:19-25.

227.   Mansouri A, Demeilliers C, Amsellem S, Pessayre D, Fromenty B. Acute ethanol administration oxidatively damages and depletes mitochondrial dna in mouse liver, brain, heart, and skeletal muscles: protective effects of antioxidants. *J Pharmacol Exp Ther*. 2001;298:737-43.

228.   Gu Y, Wang C, Cohen A. Effect of IGF-1 on the balance between autophagy of dysfunctional mitochondria and apoptosis. *FEBS Lett*. 2004;577:357-60.

229.   Cote HC, Brumme ZL, Craib KJ, Alexander CS, Wynhoven B, Ting L, Wong H, Harris M, Harrigan PR, O'Shaughnessy MV, Montaner JS. Changes in mitochondrial DNA as a marker of nucleoside toxicity in HIV-infected patients. *N Engl J Med*. 2002;346:811-20.

230.   Boyle EM, Jr., Canty TG, Jr., Morgan EN, Yun W, Pohlman TH, Verrier ED. Treating myocardial ischemia-reperfusion injury by targeting endothelial cell transcription. *Ann Thorac Surg*. 1999;68:1949-53.

231.   Condorelli G, Drusco A, Stassi G, Bellacosa A, Roncarati R, Iaccarino G, Russo MA, Gu Y, Dalton N, Chung C, Latronico MV, Napoli C, Sadoshima J, Croce CM, Ross J, Jr. Akt induces enhanced myocardial contractility and cell size in vivo in transgenic mice. *Proc Natl Acad Sci U S A*. 2002;99:12333-8.

232.   Lozza G, Conti A, Ongini E, Monopoli A. Cardioprotective effects of adenosine A1 and A2A receptor agonists in the isolated rat heart. *Pharmacol Res*. 1997;35:57-64.

233. Schlensak C, Doenst T, Kobba J, Beyersdorf F. Protection of acutely ischemic myocardium by controlled reperfusion. *Ann Thorac Surg*. 1999;68:1967-70.

234. Todd J, Zhao ZQ, Williams MW, Sato H, Van Wylen DG, Vinten-Johansen J. Intravascular adenosine at reperfusion reduces infarct size and neutrophil adherence. *Ann Thorac Surg*. 1996;62:1364-72.

235. Liu CY, Lee CF, Hong CH, Wei YH. Mitochondrial DNA mutation and depletion increase the susceptibility of human cells to apoptosis. *Ann N Y Acad Sci*. 2004:133-45.

236. Headrick JP, Peart J, Hack B, Flood A, Matherne GP. Functional properties and responses to ischaemia-reperfusion in Langendorff perfused mouse heart. *Exp Physiol*. 2001;86:703-16.

237. Sumeray MS, Yellon DM. Characterisation and validation of a murine model of global ischaemia-reperfusion injury. *Mol Cell Biochem*. 1998;186:61-8.

238. Wang QD, Swardh A, Sjoquist PO. Relationship between ischaemic time and ischaemia/reperfusion injury in isolated Langendorff-perfused mouse hearts. *Acta Physiol Scand*. 2001;171:123-8.

239. O'Brien PJ, Dameron GW, Beck ML, Kang YJ, Erickson BK, Di Battista TH, Miller KE, Jackson KN, Mittelstadt S. Cardiac troponin T is a sensitive, specific biomarker of cardiac injury in laboratory animals. *Lab Anim Sci*. 1997;47:486-95.

240. Apple FS. The specificity of biochemical markers of cardiac damage: a problem solved. *Clin Chem Lab Med*. 1999;37:1085-9.

241. Birkus G, Hitchcock MJ, Cihlar T. Assessment of mitochondrial toxicity in human cells treated with tenofovir: comparison with other nucleoside reverse transcriptase inhibitors. *Antimicrob Agents Chemother*. 2002;46:716-23.

242. Galderisi M, Caso P, Cicala S, De Simone L, Barbieri M, Vitale G, de Divitiis O, Paolisso G. Positive association between circulating free insulin-like growth factor-1 levels and coronary flow reserve in arterial systemic hypertension. *Am J Hypertens*. 2002;15:766-72.

243. Guse AH, Kiess W, Funk B, Kessler U, Berg I, Gercken G. Identification and characterization of insulin-like growth factor receptors on adult rat cardiac myocytes: linkage to inositol 1,4,5-trisphosphate formation. *Endocrinology*. 1992;130:145-51.

244. Heiska L, Alfthan K, Gronholm M, Vilja P, Vaheri A, Carpen O. Association of ezrin with intercellular adhesion molecule-1 and -2 (ICAM-1 and ICAM-2). Regulation by phosphatidylinositol 4, 5-bisphosphate. *J Biol Chem*. 1998;273:21893-900.

245. Kerr JF, Wyllie AH, Currie AR. Apoptosis: a basic biological phenomenon with wide-ranging implications in tissue kinetics. *Br J Cancer*. 1972;26:239-57.

246. Kang PM, Haunstetter A, Aoki H, Usheva A, Izumo S. Morphological and molecular characterization of adult cardiomyocyte apoptosis during hypoxia and reoxygenation. *Circ Res*. 2000;87:118-25.

247. Wang L, Ma W, Markovich R, Chen JW, Wang PH. Regulation of cardiomyocyte apoptotic signaling by insulin-like growth factor I. *Circ Res*. 1998;83:516-22.

248. Datta SR, Dudek H, Tao X, Masters S, Fu H, Gotoh Y, Greenberg ME. Akt phosphorylation of BAD couples survival signals to the cell-intrinsic death machinery. *Cell*. 1997;91:231-41.

249. Ren J, Walsh MF, Hamaty M, Sowers JR, Brown RA. Altered inotropic response to IGF-I in diabetic rat heart: influence of intracellular Ca2+ and NO. *Am J Physiol*. 1998;275:H823-30.

250. Brandes R, Bers DM. Intracellular Ca2+ increases the mitochondrial NADH concentration during elevated work in intact cardiac muscle. *Circ Res*. 1997;80:82-7.

251. Anwar A, Zahid AA, Scheidegger KJ, Brink M, Delafontaine P. Tumor necrosis factor-alpha regulates insulin-like growth factor-1 and insulin-like growth factor binding protein-3 expression in vascular smooth muscle. *Circulation*. 2002;105:1220-5.

252. Fulton D, Gratton JP, McCabe TJ, Fontana J, Fujio Y, Walsh K, Franke TF, Papapetropoulos A, Sessa WC. Regulation of endothelium-derived nitric oxide production by the protein kinase Akt. *Nature*. 1999;399:597-601.

253.   Reeves I, Abribat T, Laramee P, Jasmin G, Brazeau P. Age-related serum levels
        of insulin-like growth factor-I, -II and IGF-binding protein-3 following
        myocardial infarction. *Growth Horm IGF Res*. 2000;10:78-84.

254.   Norby FL, Wold LE, Duan J, Hintz KK, Ren J. IGF-I attenuates diabetes-induced
        cardiac contractile dysfunction in ventricular myocytes. *Am J Physiol Endocrinol
        Metab*. 2002;283:E658-66.

255.   Boes M, Dake BL, Booth BA, Sandra A, Bateman M, Knudtson KL, Bar RS.
        IGF-I and IGFBP-3 transport in the rat heart. *Am J Physiol Endocrinol Metab*.
        2003;284:E237-9.

256.   Nakao Y, Otani H, Yamamura T, Hattori R, Osako M, Imamura H. Insulin-like
        growth factor 1 prevents neuronal cell death and paraplegia in the rabbit model of
        spinal cord ischemia. *J Thorac Cardiovasc Surg*. 2001;122:136-43.

Appendix:

Copyright permission